Strathmore UNIVERSITY

SU+ @ Strathmore University Library

Electronic Theses and Dissertations

2025

Renewable Energy-Based Hybrid Power Systems for off-grid Base Transceiver Stations - a case study of BTS site in Kajiado County.

Kiarie, Andrew Benson
School of Computing and Engineering Sciences
Strathmore University

Recommended Citation

Kiarie, A. B. (2025). *Renewable Energy-Based Hybrid Power Systems for off-grid Base Transceiver Stations—A case study of BTS site in Kajiado County* [Strathmore University]. http://hdl.handle.net/11071/15970

Follow this and additional works at: http://hdl.handle.net/11071/15970

This work is availed for free and open access by Strathmore University Library.
It has been accepted for digital distribution by an authorized administrator of SU+ @Strathmore University.
For more information, please contact library@strathmore.edu

Renewable Energy-Based Hybrid Power Systems for off-grid Base Transceiver Stations

(A case study of BTS site in Kajiado county)

Andrew Benson Kiarie

152852

A Dissertation Submitted to School of Computing Engineering Sciences, Strathmore University for the Award of Master of Science in Sustainable Energy Transitions

STRATHMORE UNIVERSITY

NAIROBI, KENYA

March 2025

Declaration

I, Andrew Benson Kiarie, S/N 152852, I therefore declare that this project is the outcome of my individual endeavor, solely dependent on my personal research. I have properly recognized all the resources used in its development, including but not limited to books, papers, reports, lecture notes, and any other types of documents, whether in electronic or personal communication.

I thus affirm that this project has not been previously presented for assessment in any academic setting, and that I have not committed any act of replication, whether in part or in whole, or any other type of intellectual theft of others' work.

I hereby affirm that I have thoroughly discovered and disclosed all potential conflicts that I may possess.

Candidate ID: Sign:

152852 _____

Date 3rd April 2025

This dissertation has been submitted with our endorsement as university supervisors.

Signed:

_____

Date: 3 April 2025

Dr Vitalis Oziany, PhD

Strathmore University, Kenya

AKNOWLEDGEMENT

I would like to thank God for endowing me with fortitude and guidance in this dissertation right from the beginning.

Special thanks to my supervisor Dr. Vitalis Ozianyi, together with Dr. Fenwicks Musonye and Strathmore University staff especially those at Strathmore Energy research centre for the great support I got from them and good relation throughout the time I've been a student at this great university.

I wish to acknowledge my parents, Charles Nganga and Jane Kabura, for their constant support financially, morally and in any other form. I also wish to thank my siblings for their support and patience during my time in the university. Special thanks to Yvonne Muhingi, Kennedy Mukuha and Teccy Wanja for their continued support. I am grateful and pray that God blesses each of you.

VT OMNES VNVM SINT

Abstract

This study explores the technical and economic feasibility of deploying a renewable hybrid power system comprising solar photovoltaic (PV), battery storage, and hydrogen fuel cells for powering off-grid Base Transceiver Stations (BTS) in Kenya. Motivated by the environmental impact and high operational costs of diesel generators currently used as backup power sources in telecommunications infrastructure, the research proposes an alternative energy solution aligned with Kenya's carbon reduction targets under the Nationally Determined Contributions (NDC). A case study of a BTS site in Kajiado County was used to evaluate the proposed hybrid configuration. The system was modelled and simulated using MATLAB/Simulink to assess power flow, fuel cell activation, battery state of charge, and solar irradiance behaviour. HOMER software was used for system optimization and economic analysis, incorporating real load data, solar resource inputs, and cost parameters. Results indicate that the hybrid system meets energy demands reliably, with solar PV supplying most of the energy, batteries stabilizing supply, and the proton exchange membrane fuel cell (PEMFC) acting as a backup. The proposed system achieves an annual electricity output of approximately 67.43 MWh, with a Levelized Cost of Electricity (LCOE) of $0.351/kWh and a Net Present Cost (NPC) of $87,404 lower than the $102,253 NPC of a diesel-based system. Additionally, the system significantly reduces carbon emissions and fuel dependency. The findings demonstrate that integrating hydrogen fuel cells with solar and battery systems can provide a sustainable, cost-effective power solution for off-grid telecom sites. The study supports broader adoption of clean energy in Kenya's telecommunications sector and contributes to climate action and energy access goals.

VT OMNES VNVM SINT

Table of Contents

Contents

List of figures

List of Tables

VT OMNES VNVM SINT

List of Equations

VT OMNES VNVM SINT

List of Abbreviations

AC	Alternating Current
ATC	American Tower Corporation
BTS	Base Transceiver Station
CEOs	Chief Executive Officers
CO_2	Carbon Dioxide
COE	Cost of Energy
DC	Direct Current
DG	Diesel Generators
eV	Electron Volts
FCG	Fuel Cell Generator
GHGs	greenhouse gases
GSMA	Global System for Mobile Communications Association
H3PO4	Phosphoric Acid
ICT	Information and Communications Technology
Kwh	Kilowatt-Hours
LCOE	Levelized Cost of Electricity
NPC	Net Present Cost
MEA	Membrane Electrode Assembly
Mwh	Megawatt-Hours
NPV	Net Present Value
PAFC	Phosphoric Acid Fuel Cell
PEM	Polymer Electrolyte Membrane
PEMFC	Proton Exchange Membrane Fuel Cell
PV	Photovoltaic
RRU	Radio Remote Units
SOC	Status of Charge
SOFC	Solid Oxide Fuel Cell
OPEX	Operational Expenses
CAPEX	Capital Expenditure
RHFC	Regenerative Hydrogen Fuel cell

Chapter 1: Introduction

1.1 Background of Study

The global energy problems are caused by the fact that there isn't enough energy to meet everyone's needs. The expanding global population has led to an amplified demand for energy. Unfortunately, the majority of the energy consumed come from fossil fuels, which are getting depleted on a daily basis and contribute to environmental degradation. Greenhouse gases released by burning fossil fuels help to explain the phenomena of world climate change. Due to these changes, severe weather and environmental degradation is evidently experienced in several parts of the world. (Licker et al., 2019).

According to the analyses conducted by Bowmans (2021), the Kenyan telecommunications sector has experienced significant growth, as evidenced by the increase in mobile connectivity from 37% to 49.6% between 2014 and 2019. According to GSMA's rankings, Kenya has made the most progress in connectivity growth as compared to other African nations. The report underscores that connectivity in the African continent have improved because of the growth of consumer market and infrastructure coverage.

The telecom industry consumes considerable amounts of energy because it constitutes of infrastructure which includes towers, BTS, and data switching centres. For best performance to be achieved, these sectors need a steady and reliable source of electricity (Spagnuolo et al., 2015). Diesel generators and energy from the utility grid have often been used to meet this demand even though they are expensive, unreliable, and emit greenhouse gas emissions. In the past few years, the telecoms business has put more emphasis on renewable energy.

According to Wang and others (2021) suggest that the telecom sector accounts for about 4% of the global CO_2 emissions. This is almost twice as much as is released by civil aviation. The numbers are projected to grow at least 60% each year because of the increasing demand for data traffic around the world. Renewable energy methods need to be put in place to reduce the degradation of the environment.

Currently, solar photovoltaic (PV), wind, battery storage, and diesel engines are used to power both grid-connected and off-grid telecommunication towers. The major goal is to use renewable energy sources like wind and solar PV as much as possible. Renewable energy sources are less secure because they can't always be relied on. More and more people are using hybrid configuration systems that use both green energy and DGs to deal with this problem. Most of the time, battery storage systems are added to these systems to make them more reliable. A hybrid power system with green sources, battery storage, and DGs is used to make sure that telecommunication towers have a steady and long-term supply of energy (Deevela et al., 2023).

A study by Bartolucci et al. (2019) performed an extensive examination of hybrid renewable energy systems utilising fuel cells for off-grid telecommunications installations. They thought about how to get rid of diesel engines, cut down on costs, and lower carbon emissions. The result they came to showed that the fuel cell could, in fact, be used instead of the diesel generator. In the same way, this fits with the worldwide shift towards renewable energy sources.

DGs are used as a major backup power source in the telecommunications industry could be harmful for the environment and the economy as a whole. This shows how important it is to switch to other energy sources. The hydrogen fuel cell can lower operating costs, protect the environment, and lower greenhouse gas emissions.(Odoi-Yorke & Woenagnon, 2021).

These studies evidently show that renewable energy technologies are becoming more popular and effective for both off-grid and grid-connected telecom BTS. They also lay the foundation for more research on the performance viability and optimization of the hybrid power systems in the telecommunications industry.

1.2 Problem Statement

The telecommunication sector has seen notable growth in energy demand over the past decade. The growth can be attributed to the expansion of Base Transceiver Stations, which consume a substantial amount of energy (Bowmans-Guide-EA-Data_2021). Diesel generators are the primary backup power source for the BTS. Diesel combustion has emissions that potentially harm the environment. Concerns have been raised about the escalating carbon footprint in several industries of the economy including the telecommunication sector.

Recently, there have been efforts to decrease carbon emissions through adoption of renewable energy sources, which include solar PV and Wind in the BTS. However, these renewable energy sources have intermittency challenges thus reducing their reliability as the dependable sources of energy. These challenges have posed significant obstacles for the Mobile Network Operators to deliver uninterrupted customer services (Deevela et al., 2023).

There have been suggestions to incorporate Fuel cell as a potential solution to address the variable nature of renewable energy sources in powering BTS (Gupta et al., 2024). However, the feasibility and implementation of this solution remain undocumented. In this context, the research aims to design and optimize the existing hybrid energy configuration of an existing BTS by substituting diesel generators with hydrogen fuel cells.

In addition, the research will perform an economic evaluation to identify the most efficient and affordable option through technical design, simulation and optimization, while also considering the environmental benefits of implementing such a system in an off-grid BTS.

The research aims to examine the feasibility of implementing renewable energy systems within Kenya's telecommunication sector.

1.3 Project Aim and Objectives

1.3.1 Main Objective

This study aims to assess the viability of implementing a solar PV - Battery- fuel cell hybrid system for a BTS.

1.3.2 Specific Objectives

i) To analyse load demand of an off-grid BTS.

ii) Analysis of requirements for hydrogen fuel cell in an off-grid BTS.

iii) To conduct a technical assessment for the incorporation of a hydrogen fuel cell system to an existing BTS hybrid power system.

iv) To conduct a financial assessment of the proposed solution and the existing diesel generator of the BTS.

1.4 Research Questions

i. What is the current energy consumption of an off-grid BTS in Kenya?
ii. What are the key technical components that are required for deploying a hydrogen fuel cell system to power an off-grid BTS?
iii. How can the proposed hybrid energy system be designed and optimized to attain the energy demands of an off-grid BTS?
iv. What are the cost implications of the proposed hybrid power system as compared to the existing diesel generator in the hybrid system of the BTS?

1.5 Justification

The growth of the telecommunication industry in Kenya have resulted to a substantial rise in the number of mobile users in the country over the years. Furthermore, the expansion of the telecom sector, especially in the suburban and remote regions with the deployment of advanced technologies such as 4G and 5G could lead to an increased energy demand in the BTS infrastructure (Bowmans, 2021). In most cases in a BTS set-up, diesel generators serve as the major back-up source of power for both off-grid and grid connected BTS, in which during their operation pose potential risk of emission of GHG, hence, resulting in environmental degradation.

Kenya has dedicated to decreasing greenhouse gas emissions by 32% by 2030 in accordance with its Nationally Determined Contribution (NDC) (KENYA NDC report, 2020). Kenya's commitment aligns with the global initiatives aimed at addressing climate change issue and fulfilling the sustainable development goals (SDGs). This research aligns with sustainable development goals 7 (Affordable and clean energy) and 13 (Climate Action), hence, the replacement of diesel-powered generators with hydrogen fuel cells will aid in contributing to

the Kenya's commitment of reaching its NDC goals. Moreover, this will assist in mitigating climate change efforts (UNDP-Kenya-Annual-Report-2021).

The research will enhance knowledge through conducting a viability assessment of deploying hydrogen fuel cells in the telecommunication sector. Thus, it will provide insights on the economy of scale of implementation and evaluate the environmental benefits that will result into reduction of carbon footprint in the telecom industry.

1.6 Significance of the Study

This study aims to enhance the reliability and the cost of electricity of off-grid telecom base stations in Kenya by increasing the renewable energy penetration in the BTS sites. This will reduce the dependency on fossil fuels, thus mitigating GHG emissions resulting from diesel generators. The study will examine environmental benefits, technical design, economic impact, and applicability of the hydrogen fuel cell as a replacement of diesel generators.

In order for Kenya to achieve the 2050 target for net zero carbon emissions, they will require to increase the proportion of renewables in its energy mix. This research lays a foundation for further research in adoption of hydrogen fuel cells across the various sectors including commercial, industrial and residential.

1.7 Scope of Study

The research will mainly look into investigating the feasibility of implementing a solar PV/fuel cell hybrid power systems at an off-grid BTS site owned by American Towers Corporation or Airtel Kenya. One of the main objectives will be to monitor the energy consumption of the BTS and use the load data to design and optimize the hybrid system that will include solar PV, battery, and fuel cell system. The energy consumption data will be gathered for a period of 6 to 12 months. The research will focus mainly on the hydrogen fuel cell part and will not conduct an in-depth study on the electrolysis part of it.

The research will conduct an economic analysis to compare the existing diesel generator in the hybrid system with the proposed hybrid power system. Moreover, the site will assess the positive environmental impacts of implementing the suggested power system aiming on the reduction on the dependency of fossil fuels.

Chapter 2: Literature Review

2.1 Introduction

This section explores the core theories and models that provide the basis for design optimization of a solar PV, battery and hydrogen fuel cell specifically for an off-grid BTS. The subsequent section examines previous research efforts on renewable energy sources in BTS, focusing specifically on solar PV and hydrogen fuel cell systems. The chapter concludes by identifying the existing literature gap and establishing a structured framework essential for this study.

2.2 Theoretical Literature Review

2.2.1 Solar Photovoltaic System

This research focuses on utilizing Solar Photovoltaic systems as a primary means of generating electricity to to facilitate hydrogen production via electrolysis. Solar sizing is conducted to ensure the BTS have enough energy.

Photovoltaics is a semiconductor-based technology that converts photons into direct current DC electricity, which is recorded in Watts (W) or kilowatts. The ability of a solar cell to produce energy is conditional on its exposure to sunshine (Luque & Hegedus, 2003).

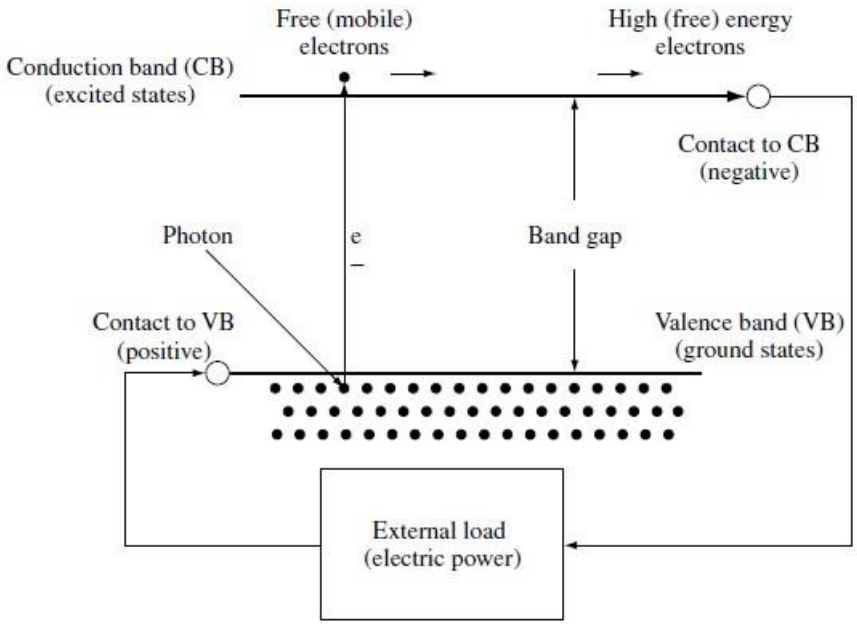

Figure 2.1: Schematic Diagram of a solar cell.

Figure 2.1 illustrates the process of photon-induced electron excitation from the valence band to the conduction band. The electrons are retrieved from the conduction band, an n-doped semiconductor, and are transferred to the external environment through wires to perform useful

tasks. Afterward, they are returned to the valence band, which is a p-type semiconductor, at a lower energy level.

Photons from the sun are absorbed by a semiconductor in a solar cell, creating electron-hole pairs. A photon's energy (Eph = hv) must be equal to or greater than the bandgap energy (Eg) of a semiconductor for absorption to take place. The energy difference between the lowest level of the conduction band (EC) and the highest level of the valence band (EV) is called the bandgap energy (Shah, 2020).

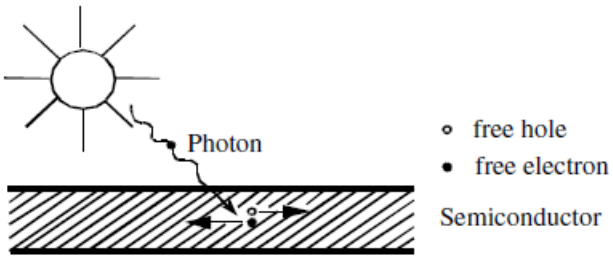

Figure 2.2: E_{ph} = hv phenomenon.

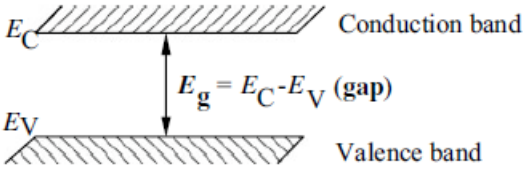

Figure 2.3: E_g of a semiconductor.

Depending on the photon's energy and the semiconductor's bandgap, three scenarios emerge:

1. If Eph equals Eg, the photon is absorbed, creating an electron-hole pair without energy loss.
2. If Eph exceeds Eg, the photon is absorbed, generating an electron-hole pair, with excess energy (Eph - Eg) converted to heat.
3. If Eph is less than Eg, the photon lacks sufficient energy for absorption, leading to reflection or absorption elsewhere, resulting in energy loss.

The efficiency of solar cells in converting the sunlight into electricity is determined by how closely the photon energy (Eph) meets or exceeds the bandgap energy (Eg). Therefore, from these interactions it is essential for improving solar cell efficiency.

2.2.2 Hydrogen and Fuel Cell Technologies

This work examines the green hydrogen industry, which is a fundamental sector in the shift to sustainable energy systems. Green hydrogen is hydrogen generated by use of an electrolyzer through a process called electrolysis. Electrolysis is the process that use electricity derived from renewable energy source, such as Solar PV, to separate water into hydrogen and oxygen. As compared to the traditional hydrogen generation technologies that depend on fossil fuels, green hydrogen provides a clean and environmentally friendly alternative.

2.2.2.1 Proton Exchange Membrane Water Electrolysis

A membrane electrode assembly (MEA) is made by compressing two electrodes against a polymer electrolyte that conducts protons. The MEA is immersed in distilled water. Protons in a mobile state are confined within the polymer membrane.

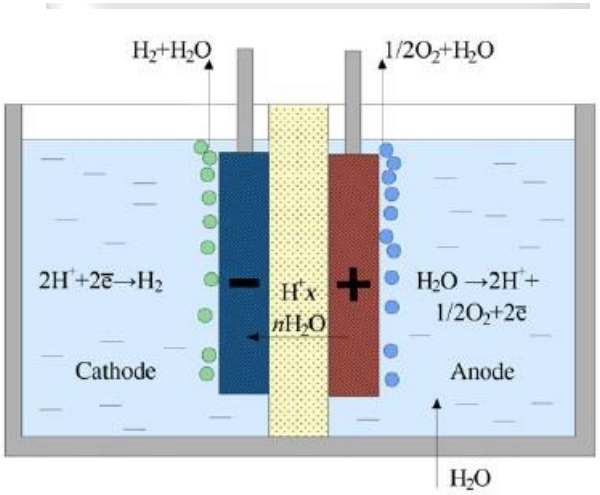

Figure 2.4: Schematic diagram of PEM electrolysis cell.

The electrolyte in a polymer electrolyte membrane (PEM) electrolyser is a solid material composed of a specialised plastic. During the process at the anode, water is converted into oxygen and positively charged hydrogen ions, commonly referred to as protons. Electrons traverse an external circuit, while hydrogen ions swiftly move across the Proton Exchange Membrane towards the cathode. Hydrogen ions at the cathode interact with electrons from the external circuit, leading to the production of hydrogen gas (Millet & Grigoriev, 2013). The electrodes facilitate the occurrence of the following electrochemical reactions. The equation 2.1 below shows the half-cell reactions in an electrochemical cell.

Anode Reaction: $H_2O \rightarrow 1/2\ O_2 + 2H^+ + 2e^-$ ($E^0 = 1.229$ V at 25^0C)

Cathode Reaction: $4H^+ + 4e^- \rightarrow 2H_2$ ($E^0 = 0$V at 25^0C)

2.1

2.2.3 Hydrogen Fuel Cells

A fuel cell efficiently and ecologically produces electricity by utilising the chemical energy of hydrogen. There are just three byproducts produced by hydrogen fuel: heat, water, and energy. They possess a diverse array of possible uses, extending from powering big utility power stations to small laptop computers (Zohuri, 2018).

Fuel cells are increasingly recognised as a promising source of power for various industries and electricity generation due to their cleanliness, economic viability, and technical feasibility. The main focus of this study will be on how hydrogen fuel cells can be utilised in telecommunications base stations.

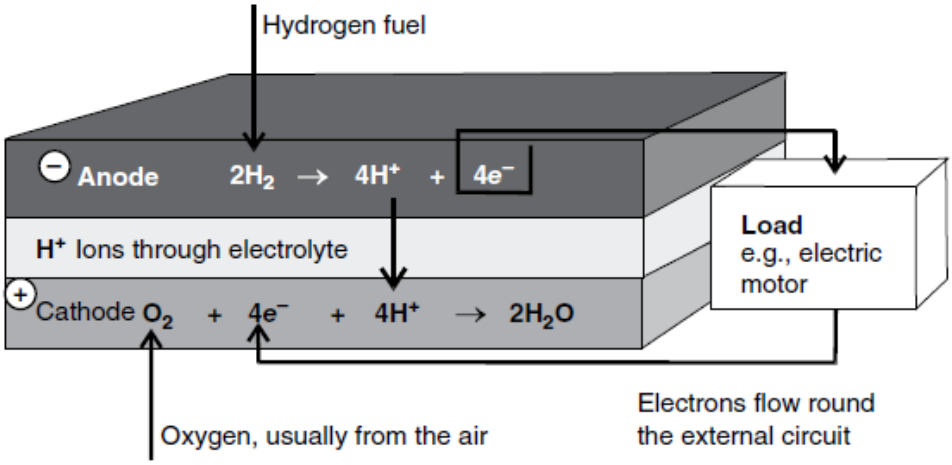

Figure 2.5: Schematic diagram of an individual Fuel Cell

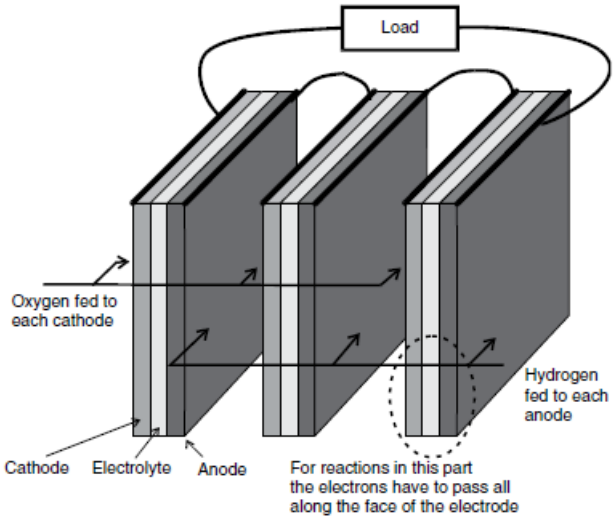

Figure 2.6: Configuration of 3 planar fuel cells connected in series at the edges.

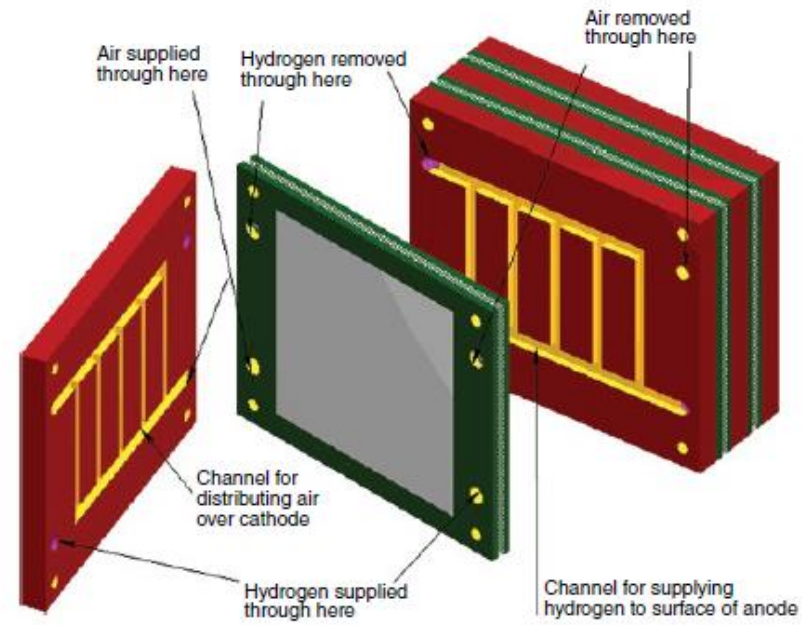

Figure 2.7: Internal manifold design featuring a sophisticated bipolar plate that channels reactant gases to the electrodes via internal tubing (Source: Courtesy of Ballard Power Systems).

Fuel cells are electrochemical systems which effectively transform the chemical energy stored in fuel into electrical power. There is a notable distinction between batteries and fuel cells when it comes to energy storage. Batteries store energy, but fuel cells generate electricity continuously provided that fuel and air are accessible. Fuel cells utilize electrochemical reactions to combine a fuel, typically hydrogen, with an oxidant, all without the need for combustion (Larminie & Dicks, 2003).

Larminie & Dicks (2003) further state that a fuel cell comprises an anode and a cathode, separated by an electrolyte. Hydrogen fuel undergoes a process of electrolysis at the anode, separating protons (H+) and electrons (e^-). The electrolyte allows protons and facilitates their transport to the cathode, while electrons are excluded and must look for an alternative route. Engineers utilize this phenomenon by controlling the flow of electrons through a load. Electrons transfer energy to the load. Electrons, upon exiting the load, possess sufficient energy to react with the incoming oxygen at the cathode and the protons exiting the electrolyte. Water is generated as a byproduct of the electrochemical reaction. The water is subsequently mixed with atmospheric nitrogen to produce the fuel cell's exhaust.

This is a PEMFC that operates at moderate temperatures, typically around 90°C.

2.2.4 Types Of Fuel Cells

The choice of electrolyte material is a feature that can be used to differentiate several fuel cell designs. This work specifically examined the four primary types of fuel cells that are widely used and commercially accessible among the numerous variations available.

According to (Dicks & Rand, 2018) state and describe the primary category of fuel cells as shown in table 2.1:

Table 2.1: Principal types of fuel cell

Fuel Cell Type	Mobile Ion	Operating Temperature (°C)	Fuel Type
Alkaline Fuel Cell (AFC)	OH^-	50–200	Pure H_2
Proton Exchange Membrane (PEMFC)	H^+	30–100 (up to higher values)	Pure H_2
Direct Methanol Fuel Cell (DMFC)	H^+	20–90	Methanol
Phosphoric Acid Fuel Cell (PAFC)	H^+	~220	Hydrogen (H_2)
Molten Carbonate Fuel Cell (MCFC)	CO_3^{2-}	~650	Hydrogen (H_2)
Solid Oxide Fuel Cell (SOFC)	O_2^{2-}	500–1000	Impure H_2

2.2.5 Proton Exchange Membrane Fuel Cell

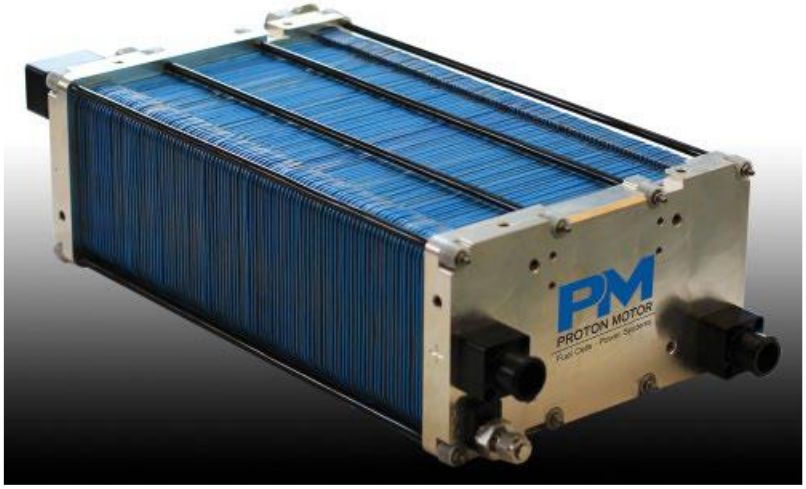

Figure 2.8: A 96-cell PEMFC stack, which is water-cooled and capable of generating up to 8.4 kW while weighing 1.4 kg. (Source: Proton Motor GmbH)

The PEMFC uses a solid polymer or electrolyte. A PEMFC consists of an electrolyte, typically a sulfonic acid polymer known as NafionTM, which facilitates the transfer of protons between

two surfaces. PEMFCs necessitate the utilization of hydrogen and oxygen as inputs, with the possibility of ambient air as the oxidant. It is essential to humidify these gases. PEMFCs exhibit lower operating temperatures than other fuel cells due to the thermal properties of the membrane. The operating temperatures typically reach approximately 90°C. CO contamination in the PEMFC can lead to performance degradation and harm the catalytic materials present in the cell. A PEMFC necessitates cooling together with management of exhaust water for optimal operation (Dicks & Rand, 2018).

2.2.6 Battery

This research focuses on utilizing Battery systems as a source of power back-up for generating electricity to power the BTS when there is no electricity supplied by the solar PV panels.

A battery transforms chemical energy into electrical energy through a series of chemical reactions. There are different kinds of batteries, each with unique chemical compositions. In a battery cell, two chemicals with different loads connect to a -ve (cathode) and +ve electrode (anode). When connected to a device, the -ve electrode releases electrons that pass through the appliance and are collected by the +ve electrode (Zohuri, 2018).

There are two types of batteries:

i. Lead Acid
ii. Lithium-ion batteries

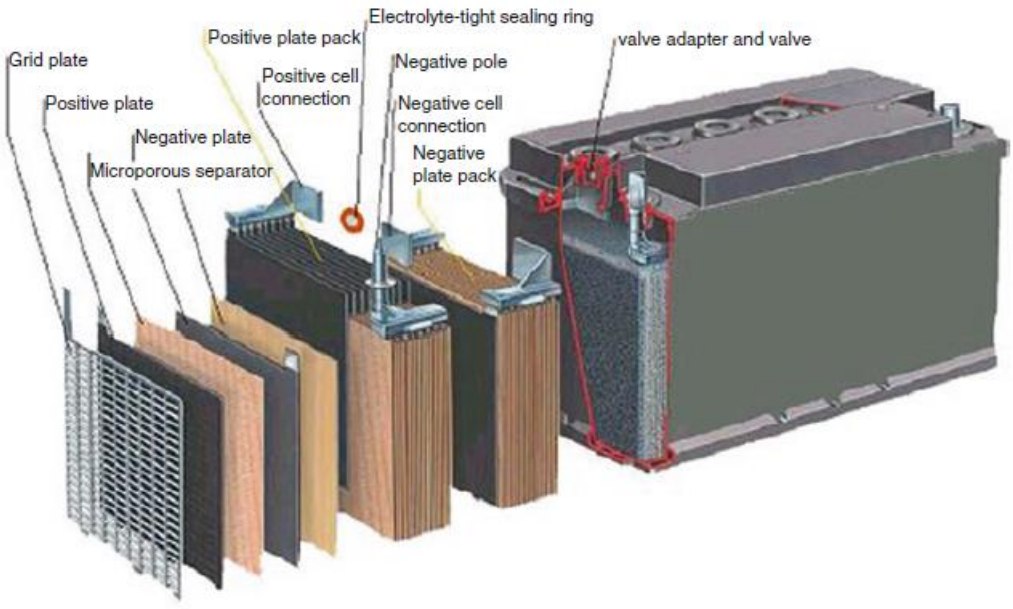

Fig 2.9: Lead Acid battery

A Lead Acid battery utilises lead and lead oxide electrodes with sulfuric acid as the electrolyte in an electrochemical process. Lead-acid batteries are frequently utilised together with solar

(PV) and other alternative energy systems due to their affordable price and widespread availability (Zohuri, 2018).

2.2.6.1 Lithium Battery

Different types of lithium batteries are grouped by the anode material they use, which can be either lithium metal or intercalated lithium, and the type of electrolyte system, which can be either liquid or polymer based. Lithium-ion batteries have become the main source of power for mobile gadgets because of their good performance. They provide notable performance thereby resulting into the realization of benefits for automotive and auxiliary power applications (Moseley & Garche, 2015).

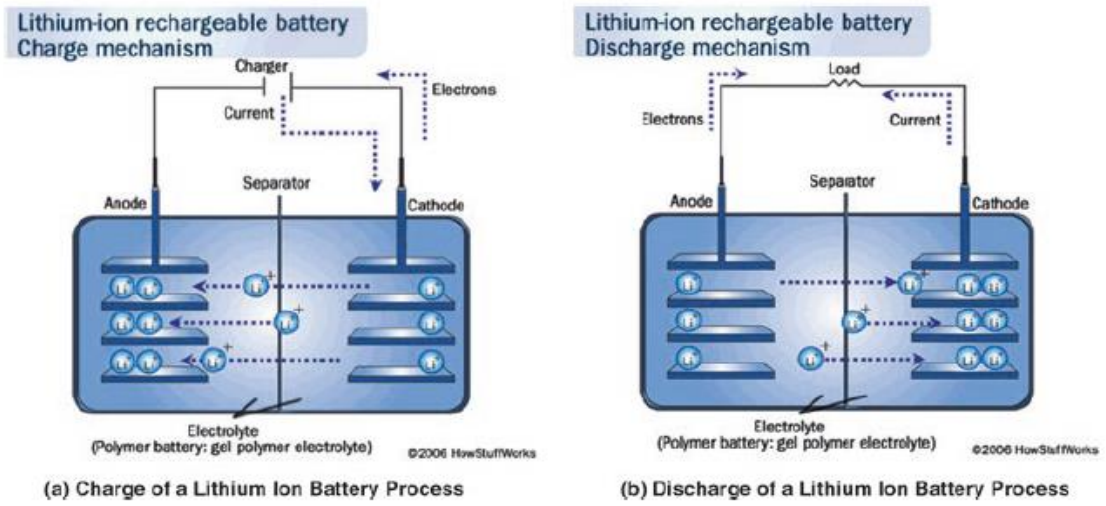

Figure 2.10: Charging and discharging operations in a lithium-ion battery.

During charging, lithium ions move through the microporous separator into the gaps between the graphite layers, facilitated by the external power source supplying electrons. As a result, lithium ions are absorbed into the graphite.

During discharge, lithium atoms in the graphite give off electrons that reach the anode through the external connection generating current. The lithium ions migrate back to the anode alongside the electrons they release (Zohuri, 2018).

2.2.7 Battery and Fuel Cells comparison

Batteries and fuel cells transform chemical energy into electrical energy through redox reactions at the anode and cathode. The anode, which usually has a lower electrode potential, is known as the negative electrode, whereas the cathode, with a higher potential, is known as positive. Batteries are enclosed systems in which the anode and cathode enable redox

processes, acting as active materials for both energy storage and conversion within a single compartment.

Fuel cells operate as open systems. The anode and cathode facilitate the transfer of charges, whereas the active substances participating in redox reactions are derived from external sources, such as oxygen from the atmosphere or hydrogen from a storage container. The spatial separation of energy storage and conversion allows for the independent operation of both processes. (Whittingham et al., 2004).

2.3 Empirical Review

Scholars have shown significant interest in the assessment of different perspectives and methodologies in reference to the utilization of renewable energy in BTS. The key motivation behind these investigations is the need for a reliable and cost-effective hybrid power solution in the telecom base stations. Additionally, the renewable energy adoption in the BTS reduces the environmental degradation, thus aligning to the transition towards an environmentally sustainable energy option.

According to a study conducted by Odoi-Yorke & Woenagnon (2021), the authors examined the feasibility of utilizing a solar PV and a fuel cell power hybrid system to supply electricity to the BTS in Ghana. The authors narrowed down to do a comparison of the parameters technical, economic, and environmental performance of Solar PV and fuel cell hybrid system as compared to stand alone diesel power systems. Their proposed hybrid power system had benefits as compared to the conventional method in terms of lower levelized cost of electricity, increased system resilience and reduced green house gas emission. The study's findings determined that the proposed solar PV and fuel cell hybrid system is a feasible alternative to both Solar PV/diesel and stand-alone diesel power systems in Ghana's BTS.

However, the study assumes a fixed energy demand for the BTS, which may not accurately represent the fluctuating energy demand at a particular time or instance. Even though this work comprehensively discusses the technical parameter, it does not consider the environmental and economic impact of the proposed hybrid system compared to the existing power system at Bududuram BTS in Ghana.

(Bartolucci et al., 2019) conducted research to design a hybrid renewable energy system for specifically off-grid BTS stations. Furthermore, the authors expand on the hybrid renewables, which integrates multiple renewable energy sources for example solar, wind and fuel cells to provide a more reliable and reasonably priced source of power. The authors demonstrated the effectiveness of their methodology by presenting a case study of an Italian BTS. The researchers utilized MATLAB/SIMULINK models to appropriately determine the accurate

sizes of the components of the system by analysing the local weather conditions of the BTS and the load profile. The findings showed that the proposed approach have more benefits in the terms of lower costs and reduced GHG's as compared to the conventional systems that are dependent on diesel generators.

A potential limitation of this study is the missing assessment of the performance and cost incurred by the diesel generators and the proposed hybrid renewable energy sources that is the fuel cell, solar and wind. The study primarily investigates the feasibility of utilizing a fuel cell hybrid system to power an off-grid BTS in Italy. However, the economic comparison of the fuel cell hybrid system compared to the existing energy sources of the BTS is not discussed comprehensively. The authors mainly focused on sizing the fuel cell hybrid system by use of a multi-objective optimal sizing approach.

In their study, (Jansen et al., 2021)) put forward a hybrid energy storage system merging RHFC, solid-state hydrogen storage, Li-ion battery energy storage, and solar PV integration. The utilization of MATLAB/Simulink and Levenburg-Marquardt least square algorithm were utilized for the purposes of modelling energy balances, performing cost-effective sizing of the renewables and assessment the technical viability of the proposed system. The study's findings suggested that the proposed design provides a cost-effective energy solution by reducing the OPEX, increased power reliability and a positive environmental impact for off-grid BTS in the remote areas of the sub-Saharan parts of Africa. The research study further evaluated the LCOE of the system where it reduced to 17.16 ¢/kWh as initially compared to 73.40 ¢/kWh, whereas the IRR of the system achieved 15.15% for the RHFC energy storage system. This illustrates the affordability of the system and the financial viability for the off-grid BTS.

The research study has a notable gap concerning the energy consumption of the BTS. The authors present a 24-hour load data that is insufficient to estimate the energy consumption of the BTS over time since it does not account for fluctuations in network congestion, or seasonal variations in communication patterns. Moreover, the authors have extensively relied on models and simulations without a specific case study of a BTS which could give more insights in a real-world performance. These could have a negative impact in the context of their practicability in real-world scenarios and the dependability of their findings.

In a research done by (Hossain et al., 2021) incorporated a techno-economic feasibility of hybrid solar PV/hydrogen/fuel cell-powered BTS. The primary objective of the research was to create a green mobile communication system in order to mitigate the fossil fuel crisis and minimize the GHG's emissions from the BTS back up power sources. The authors utilized HOMER to examine the optimal size of the renewables, energy production and monitor the

carbon footprint of the system. MATLAB based Monte-Carlo simulations was utilized for the assessment of transmission power, system bandwidth, and inter-cell interference of the cellular base station. Their findings show that the proposed hybrid system have surplus electricity of 17% and have a backup storage of 48.1 h. The research underscores the effectiveness of the proposed hybrid power system through reducing GHG emissions, increasing power reliability and improving the BTS's overall performance.

However, this study is limited to off-grid BTS located in Bangladesh, which limits the global applicability of the findings. In addition, the authors assumed the load demand data relative to the traffic demand data of the cellular base station. Without accounting for the seasonal variations in communication patterns and presenting a specific case study, the results may introduce ambiguities in the real-world application. The economic assessment lacks specificity and does not include a comparison of the proposed system's economic impact with that of an existing system.

(Martinho et al., 2022) provides a potential solution by coming up with a reliable backup power solution for the telecommunications sector. The research study highlights the increasing energy demand in this industry, especially with the emergence of technologies such as 5G, which are expected to greatly increase power consumption levels. The authors suggested a hybrid system that constitutes a reformed methanol fuel cell and a battery, together with an energy management system (EMS) that includes twelve different operating conditions. By utilizing MATLAB/Simulink, simulation was performed while considering the real-world scenarios which involve power outages and varying loads. One of the notable strengths of the research study is the integration of the EMS with the 12 operating conditions which accounts for the SOC of the battery, load requirements, and grid power availability. Hence this exhibits a refined methodology for managing and enhancing the system performance.

However, despite its strengths, the research has limitations of potential carbon emissions related to the process of methanol reformation for hydrogen production in fuel cells. Furthermore, the author acknowledges that the process of getting hydrogen from methanol may lead to carbon dioxide emissions posing environmental challenges even though fuel cells are well known for their clean and efficient performance. In addition, the research primarily emphasizes the technical aspect and environmental benefits of the system thus leaving out on detailed economic assessment of implementing the suggested hybrid system while comparing with the hybrid traditional systems.

The research study by Ayodele et al., (2023) highlight the challenges faced by Mobile Network Operators in Nigeria due to the maintenance schedules of the BTS sites. The authors recognize

that there is high dependence on the conventional DGs and battery systems in both the grid connected and off-grid BTS sites, thus, it results in high OPEX, and greenhouse gas emissions. To mitigate this challenge, the authors did a case study for powering a BTS in Okuku village in Nigeria where they suggested a hybrid renewable energy system adding solar PV, hydro, and fuel cell technology with a hydrogen tank for the storage of hydrogen. The research study revealed that the proposed system achieved a lower net present cost (NPC), LCOE and operational costs as compared diesel generators thereby reducing significantly the GHG. It is worth noting that the research conducts a comprehensive economic and environmental assessment, evaluating the cost benefits and reduction in environmental degradation.

However, the study has limitations, which includes the absence of a comparative economic analysis with energy sources of renewables and the conventional sources of energy in the existing BTS, which could have an impact on the applicability of the proposed system. Additionally, the dependence on hydro-electric power generation from river streams is only limited to the BTS sites that are located near the river streams. The reliance of hydro power generation limits the BTS sites that are not located near the river streams, thus, limiting the applicability of the proposed system.

In the study by (Luta & Raji, 2019), provides a possible solution to the challenge of powering a remote BTS sustainably and cost-effectively. They underscore the high reliance on the diesel generators which significantly contribute to environmental degradation and high operational costs attributed the global varying cost of fuel. The authors propose a renewable hydrogen-based energy system adding solar PV, electrolysis system for hydrogen generation, fuel cell for energy conversion and a battery storage system. According to the study's results, out of the three scenarios that is solar PV and battery, Solar PV, fuel cell and battery, and diesel stand alone system, the Solar PV and battery emerged to be the cost-effective solution followed by solar PV, Fuel cell and battery and lastly the DG. The proposed system was more reliable than the other two scenarios due to availability of three energy sources, thus, demonstrating a promising technical performance and financial benefits as compared to the DG system.

However, the study has limitations whereby the load profiles of the BTS are assumed to have a fixed energy demand which may not represent the actual energy consumption of the BTS site in a real-world application. Additionally, the research do not sufficiently provide for the assessment of the positive environmental impacts of the suggested system since the mainly focus on the technical and economic feasibility aspects of the suggested system as compared to the traditional diesel generators.

In the research done by (Ma et al., 2019), the authors primarily focused on utilizing the fuel cell not only as the back up power solution for the cell towers during emergency but also provide grid services for example the ancillary and demand response services. The study explored other revenue streams and applications for fuel cell technologies in the cell towers such as participating in the energy markets and in microgrid set up for a collection of fuel cells as distributed energy sources aiming to demonstrate their viability and advantages when integrated with the grid. The research study revealed that the fuel cell systems have additional benefits when they are integrated with the grid to provide ancillary services when the energy market prices are high. This will be able to offset the operational expenses of the BTS because of generating revenue from providing grid services.

However, the study has notable limitations. There is insufficient case studies or real-world examples of fuel cell back-up power installations in the telecom industry, thus, prohibiting understanding of practical implementation. The decentralized energy market system is limited also to countries with decentralized electricity markets where bidding is done, and the participants get the offers. Additionally, the study focuses on other revenue streams of the fuel cell technology, hence, a comparative analysis with other energy sources such as the battery and diesel generator is missing to provide more insights and the positive benefits of the fuel cell system in this context as compared to other sources of energy.

In a study by Hossain et al., (2020), put forward a possible remedy to address the challenge of increasing energy demand in the off-grid BTS. They proposed a hybrid renewable energy system that included solar PV and biomass energy sources to produce stable and environmentally friendly energy for BTS. The authors achieved the results by utilization of MATLAB where monte Carlo simulation was performed to assess the network performance through monitoring data throughput, quality of service and the overall efficiency. Additionally, HOMER was utilized to optimize the system performance by considering the appropriate sizing and cost-effectiveness of the system. The study's finding revealed that the suggested hybrid renewable energy BTS provides an environmentally friendly scenario in the telecom industry, thus delivering high quality services.

However, despite the notable contributions, the study acknowledges the limitations related to the energy produced by biomass which may result in the release of CO_2 and other GHGs which affects the quality of air and poses risk for climate change during the combustion process. Moreover, the authors discuss the emissions produced by various sources of energy such as coal, natural gas, bitumen, and biomass to compare their environmental effects. In addition, the

study does not perform an economic analysis to evaluate the advantages of the proposed hybrid renewable energy system in comparison to conventional energy systems.

2.4 Conceptual Framework

This research shall be undertaken under the conceptual framework shown below:

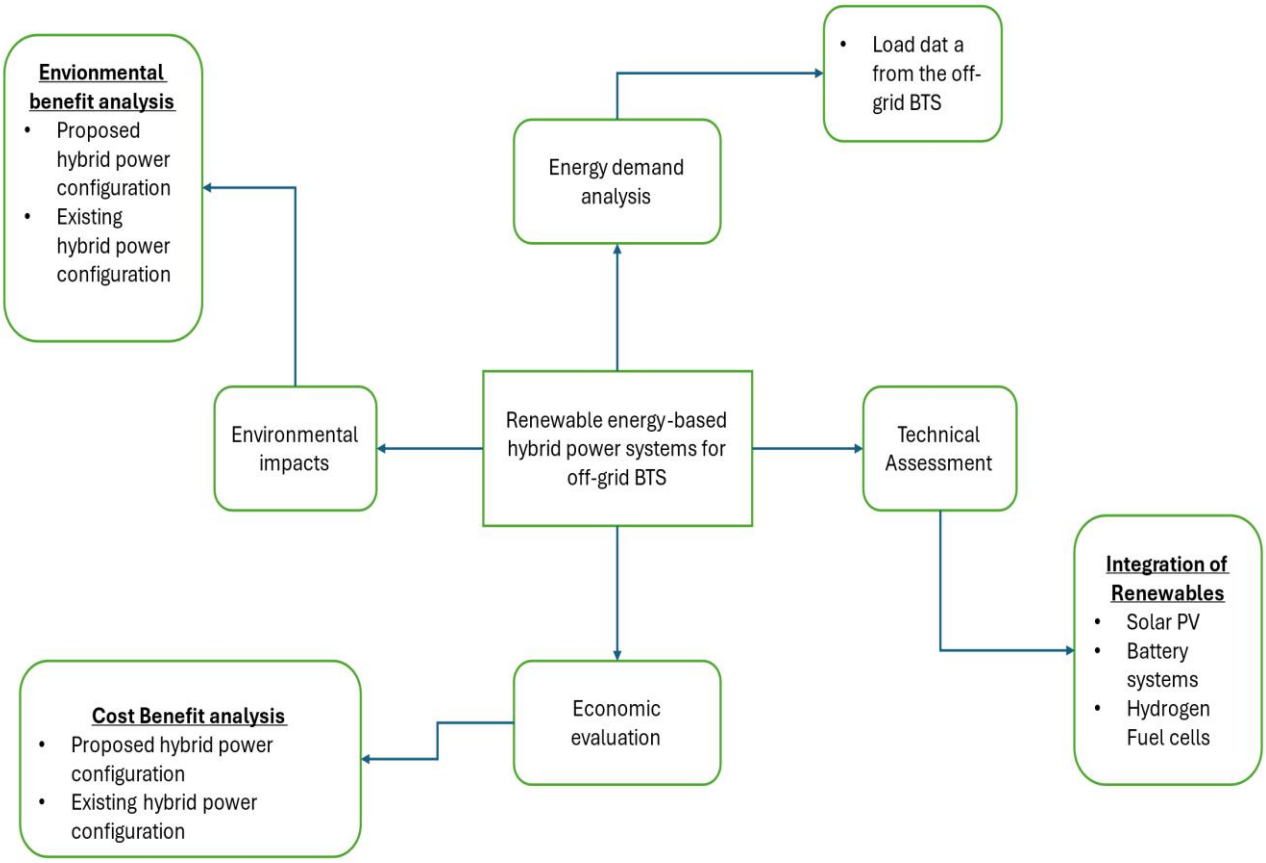

Figure 2.11: Conceptual Framework

Chapter 3: Methodology

3.1 Introduction

This section focused on the approach that was implemented in order to satisfy the objectives stated in this study. It involved using MATLAB to design and model and simulate a fuel cell, solar PV and battery system and HOMER software to size and optimize a solar PV/ fuel cell hybrid system for an off-grid BTS site. In view of this, the chapter outlined the achievements of objectives and the utilization of MATLAB and HOMER software.

Study Area

3.2 Research Design

This work primarily employed the quantitative approach type of research design. The quantitative data was collected from a database system which included the energy consumption of an off-grid BTS located in Kenya. The energy consumption data was analysed to provide insights to the appropriate design and sizing of energy sources. The load data collected aided in the development of a model that simulated the hybrid renewable energy system.

MATLAB and HOMER software's was used to model, design and optimize the hybrid power system configuration of the off-grid BTS site. A comparative cost analysis was conducted to evaluate the financial viability of the hybrid power system in comparison to the hybrid system running on DGs. Furthermore, environmental benefits were highlighted to indicate the advantages of the system.

3.3 Achievement of objectives

3.3.1 Objective 1: To analyze load consumption data of an off-grid BTS.

This work collected load data from an off-grid BTS. The load data was derived from remote monitoring systems for a period of 6 months. Load data assisted in accurately sizing the optimal combination of the proposed renewable energy resources i.e., hydrogen fuel cell, electrolysis plant, solar PV, Battery, and hydrogen tank. HOMER software tool was utilized in performing the design and optimization of the hybrid power system.

Time usage data of each energy resource present at the off-grid site was collected. On the BTS site, we had DG, Solar PV, and Battery as the energy sources of the off-grid BTS, thus, this were to give insights on the level of dependence in supply of energy of the BTS site.

3.3.2 Objective 2: To analyse the requirements for hydrogen fuel cell in an off-grid BTS.

Analysing the requirements for incorporating a hydrogen fuel cell into a stand-alone BTS requires a comprehensive methodology, and MATLAB's computational capabilities enable the simulation of electrochemical phenomena within the fuel cell stack. The fuel cell stack consists of multiple components such as proton exchange membranes, electrodes, hydrogen tank and

catalyst. The average load consumption data aided in sizing the fuel cell system. MATLAB/SIMULINK employed control algorithms to regulate and optimize the power output while considering the fluctuating energy demand patterns.

3.3.3 Objective 3: To conduct a technical assessment for integration of a hydrogen fuel cell system to an existing BTS hybrid power system.

This study utilized MATLAB/Simulink to model and simulate the proposed renewable hybrid system that comprises of solar PV/battery/fuel cell hybrid system. The size of the fuel cell and solar PV system was be determined by the size of the load and the battery size due to the charging and discharging cycles. The hybrid power system was set to operate such that the fuel cell operates only when we do not have enough solar PV power and Battery power. The fuel cell remains OFF if there is enough power to meet the load from the solar PV and the battery.

HOMER examined the load consumption data alongside geographically specific Global Horizontal Irradiance (GHI) data of the existing BTS site and ran several iterations to find the best size of the renewable energy sources configuration while considering the financial implication of the system. The results from the software gave clear picture of the viability of implementing the hydrogen fuel cell into the existing off-grid BTS and the actual cost of implementing the system.

3.3.4 Objective 4: To conduct a financial assessment of the proposed solution and the existing diesel generator of the BTS.

The economic assessment for this study was important because of the financial impact of deploying the modeled hybrid system. HOMER software analyzed several economic parameters in each source of energy, such as CAPEX, OPEX, maintenance cost, discounting rate, and project lifetime. The economic analysis of the designed hybrid system compared to the existing Solar PV, battery and DG system was examined, with a specific focus on the O&M and the NPC of the DG, to determine the energy configuration that was the most cost-effective. Additionally, the cost of producing electricity is important in the suggested hybrid system, hence, the factors such as LCOE, NPC and inflation rate were determined to evaluate the long-term viability of the system.

3.5 Population and Sampling

The target population for this research were the telecommunication companies. There are three major mobile network operators (MNO) that is Safaricom, Airtel and Telkom. The focus of this research was on American towers company, which is one of the telecom companies, where they build telecom towers and rent out to the mentioned MNOs.

This research utilized purposive sampling approach where it narrowed down to a specific telecommunication company, that is ATC, which owns approximately 4,000 BTS sites for both grid-connected and off-grid sites. A specific off-grid BTS site managed by ATC was selected as the case study. This work focused on a single off-grid BTS site where the findings and performance characteristics could be applied to a site with similar characteristics as the site in this case study.

3.6 Data collection and analysis

This study collected data from a BTS in Kajiado County from a database monitoring system. The BTS site was an off-grid site and energy consumption data was collected for a period of 6 months. Additionally, data on the consumption of fuel and time of utilization of the available energy resources on the site were collected to give insights on the current performance of the BTS site.

The data collected was analysed by the Microsoft Excel tool which presented the graphical representation of the varying load data and the time utilization of the energy sources of the BTS.

3.7 Ethical Consideration

The study followed the ethical guidelines provided by Strathmore University and adhered to the regulations set by the National Commission for Science Technology and Innovation (NACOSTI). This study sought ethical approval from the university's ethical board to proceed to data collection. The research ensured the transparency of each step that was undertaken in the methodology section. Additionally, the research-maintained trust with the stakeholders and sought approval before sharing the collected data. The research upheld the trust and confidence of the academic community and society at large by adhering to these ethical norms and assuring the integrity and validity of its findings.

Chapter 4: Results and Discussion

This chapter presents the results of the model and discusses the findings of the simulations and the performance of the hybrid renewable energy system for the BTS. The data obtained from MATLAB/Simulink and HOMER simulations, which included solar, battery, and fuel cell performance, were analysed to assess the viability and the economic feasibility of the proposed system. This study examined the advantages that came with the integration of hydrogen fuel cell with other renewable energy sources in an off-grid BTS such as the technical performance, environmental impact and financial impact. The outcomes were compared with similar previous studies underscoring the benefits and drawbacks linked to the proposed hybrid approach.

4.1 Data Presentation

4.1.1 Base Station Electrical Load Profile Assessment

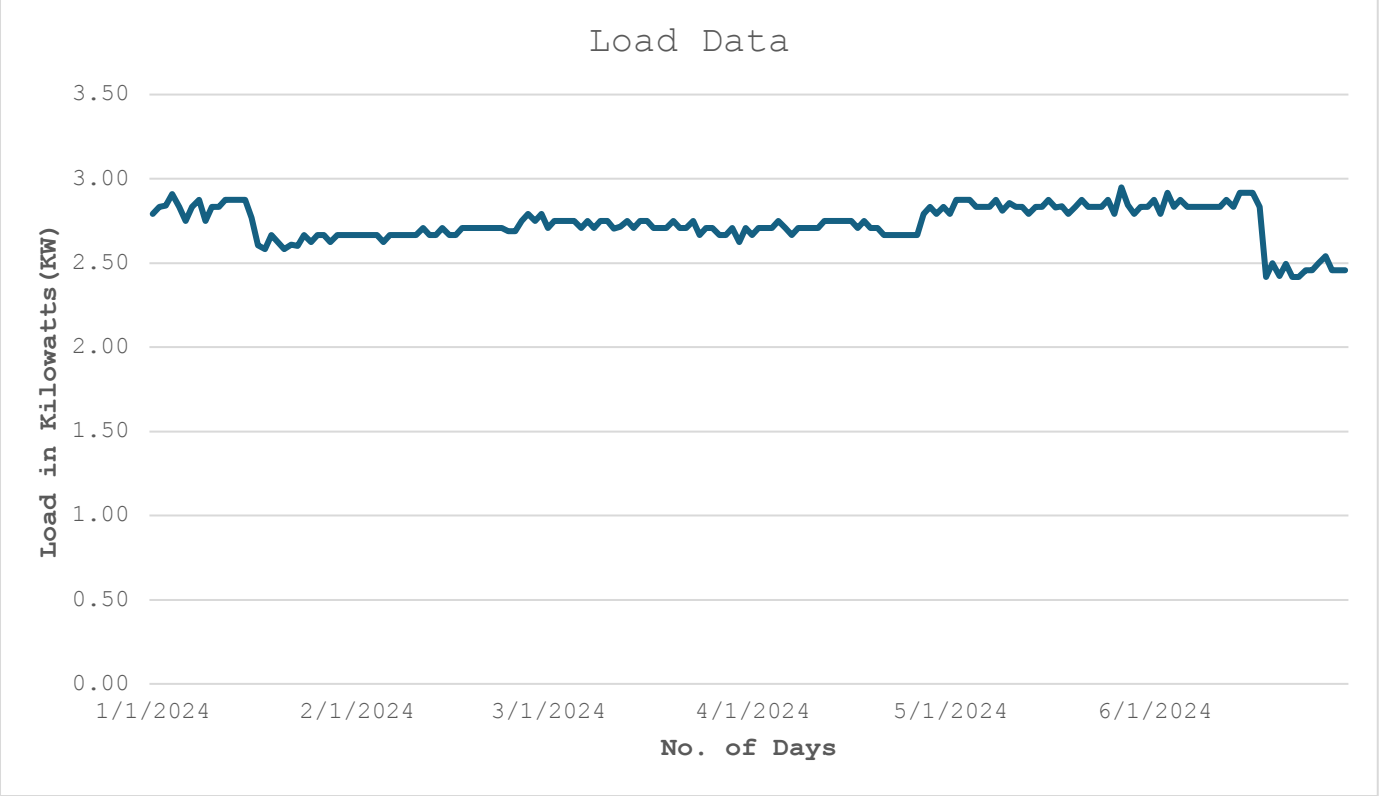

Figure 4.1: BTS Load Profile For Six Months

Figure 4.1 shows the demand for a six-month period. The load is as a result of the telecommunication equipment that provide network frequencies to mobile devices. In most cases the equipment comprises Radio Remote Units (RRU), Base Band Unit (BBU) and the Antennae.

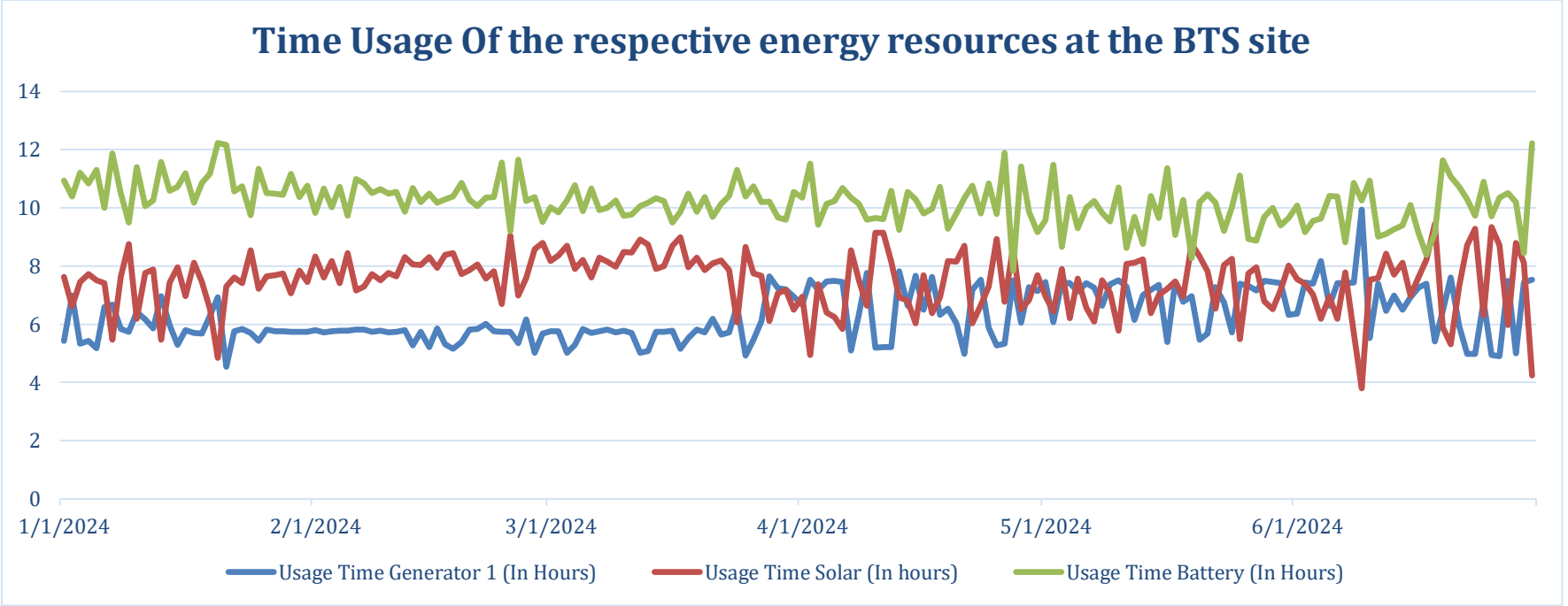

Figure 4.2: Time Usage of Respective Energy Resources at The BTS Site

Figure 4.2 depicts the recorded time usage of each energy source at the BTS for a six-month period. The data indicates that the battery supplies power to the load for an average of 10.2 hours per day. Hence, the solar PV system follows providing power for an average of 7.5 hours per day, and finally, the DG supplies the load for an average of 6.3 hours per day.

4.1.1.3 Modelling With MATLAB/Simulink

This study utilized Matlab/Simulink to design and simulate the solar PV, battery and fuel cell system. Simulink provides an intuitive graphical interface for simulating dynamic systems, enabling precise simulation of power generation, energy storage, and control strategies. The model that was developed integrates the hydrogen fuel cell into the Solar PV and battery configuration, hence the fuel cell was designed to activate only when there is insufficient power to meet the load from both the Solar and the battery energy sources.

4.1.1.3 Overall Design

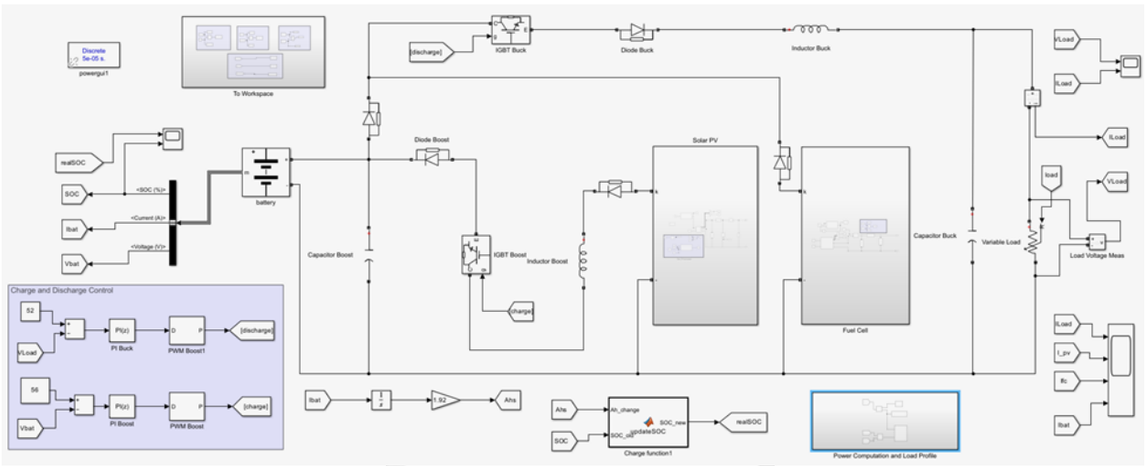

Figure 4.3: General design of solar PV, Fuel Cell, and Battery in MATLAB/Simulink

4.1.1.4 Power Consumption and the load profile

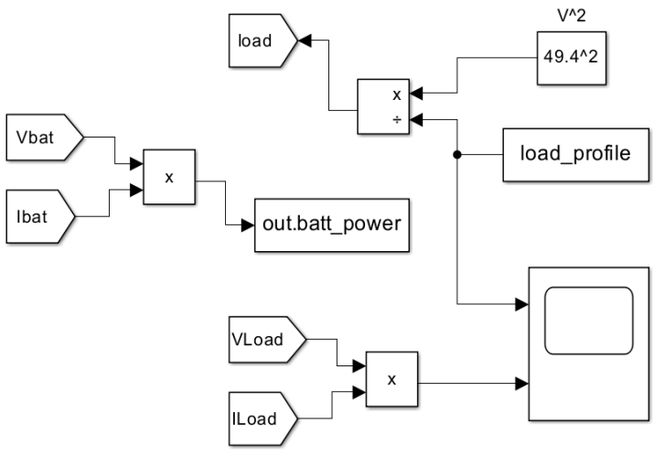

Figure 4.4: Design for Power Consumption and Load Profile

Figure 4.4 illustrates the MATLAB/Simulink model replicates the power consumption and load profile of a Battery Energy Storage System (BESS) for a Base Transceiver Station (BTS), with the bus voltage configured at 49.4V to reflect standard BTS operations. It imports the monthly load demand data from an Excel file into the workspace, illustrating the fluctuations in power requirements of the BTS equipment over time. The model does this by dividing the square of the bus voltage by the load demand to get a varying resistance value. The model computes battery and load power by multiplying voltage and current values, continuously modulating the battery's power output to satisfy the load's fluctuating requirements while overseeing the battery's state of charge.

The simulation guarantees efficient management of the battery's power by matching its output with the load's demands.

4.1.2 PEM Fuel Cell Design

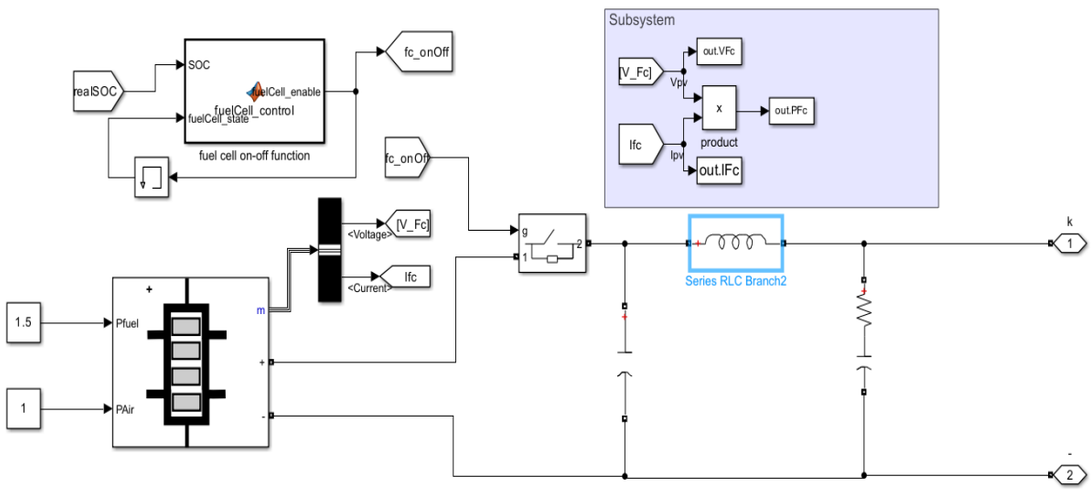

Figure 4.5: Fuel Cell Design

Figure 4.5 illustrates a fuel Simulink model which is essential for providing dependable power supply when solar and battery resources are inadequate. The model comprises the fuel cell stack, activation control circuitry, and power conversion components. The fuel cell activates when the battery's State of Charge (SOC) drops below a certain threshold and solar energy is inadequate. The Simulink model above consists of the following key components:

4.1.2.1 Fuel Cell Stack

In this model type of fuel cell utilized is the PEM fuel cell. It is a preset fuel stack which comprises of the following properties in Figure:

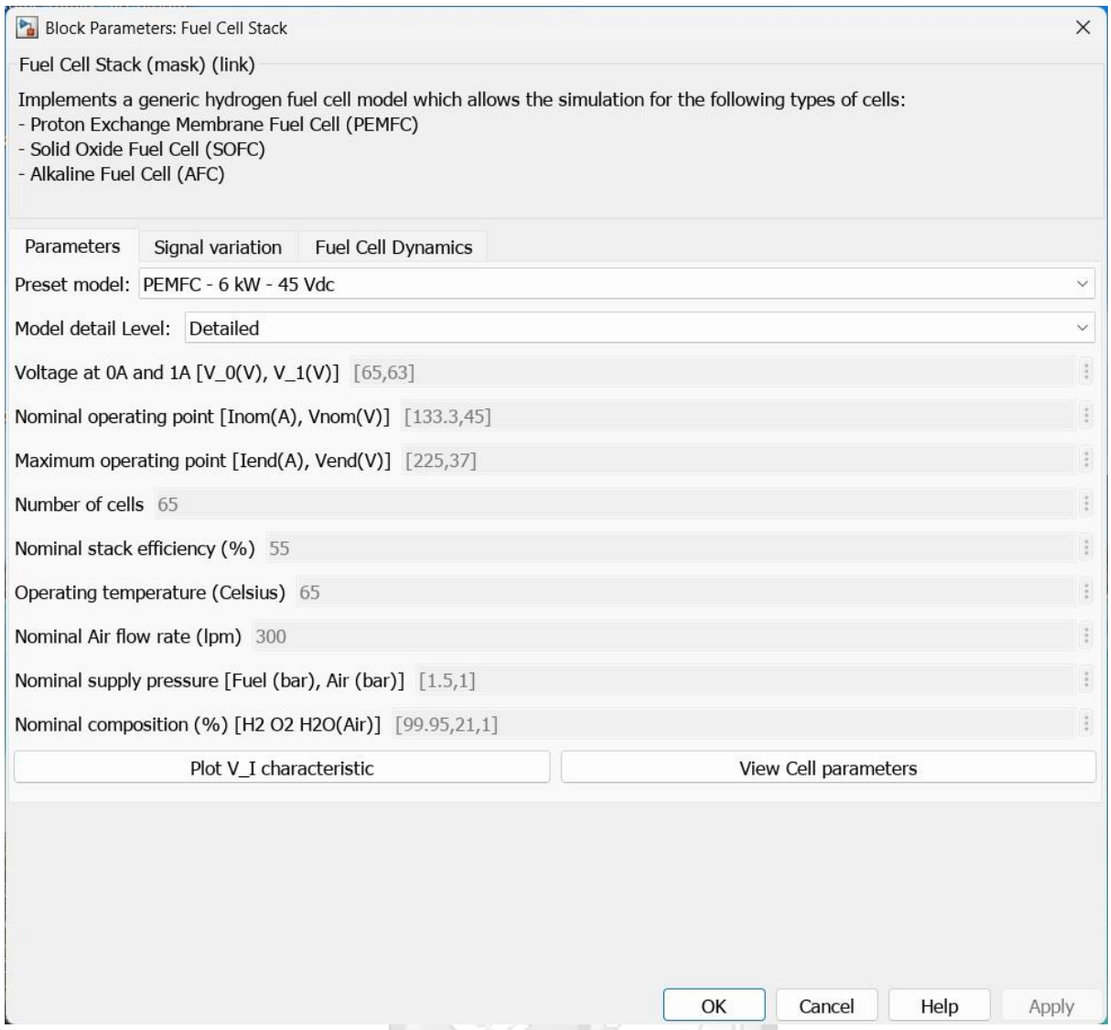

Figure 4.6: Fuel Cell Parameters

In times of reduced or absent sunlight, the system activates a fuel cell to generate electricity, ensuring a continuous and reliable power supply. The model utilises the PEMFC technology, recognised for its great efficiency and minimal emissions. Hydrogen is generally generated via electrolysis utilising excess solar energy during peak sunlight hours, subsequently stored and employed in the fuel cell. Hydrogen reacts with oxygen from the air at the fuel cell's anode and cathode to generate electricity, water, and heat as byproducts.

$$\boldsymbol{E = N(E^{o} + \frac{RT}{2F} \ln\left(\frac{PH_2\sqrt{PO_2}}{PH_2O}\right))}$$

4.1

$$\boldsymbol{V_{FC} = E - V_{act} - V_{conc} - V_{ohm}}$$

4.2

Equation 4.1 and 4.2 represents Nernst Equation of the fuel Cell and final output voltage across the Fuel Cell. Where V_{FC} is calculated as the difference between E and the sum of V_{act}, V_{conc}, and V_{ohm}. E_o denotes the standard reversible cell potential (in V), N indicates the number of cells in the stack, R represents the universal gas constant (in J/K/mol), and F signifies the Faraday constant. The variables PH_2, PO_2, and PH_2O refer to the partial pressures of the reactants (in Pa). V_{act}, V_{conc}, and V_{ohm} signify the voltage drop (in V) attributed to activation, concentration, and ohmic losses, respectively.

V, I and Power Characteristics

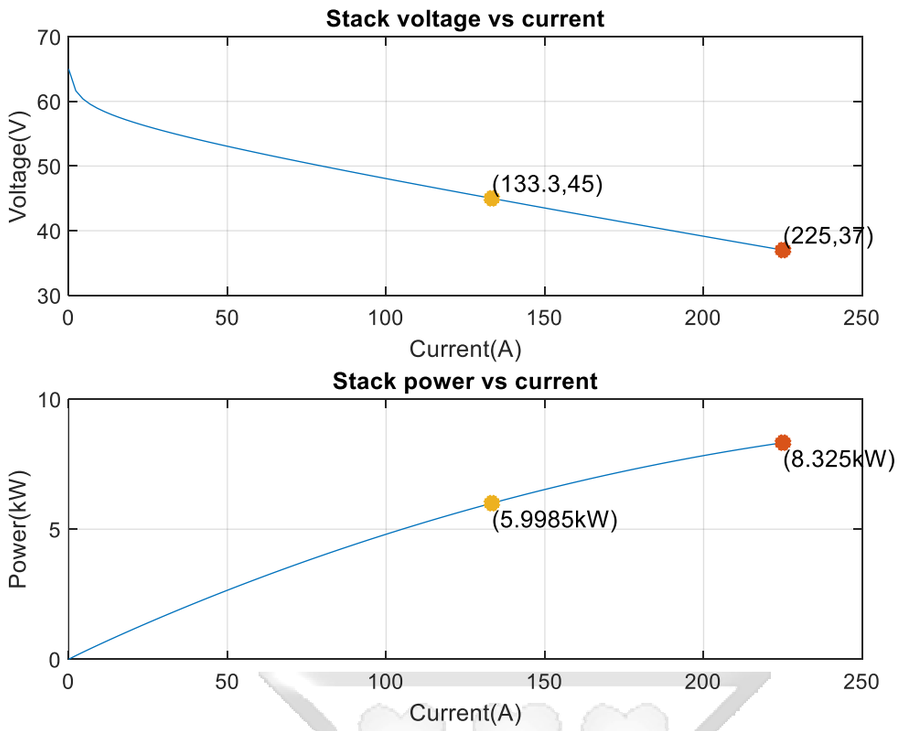

Figure 4.7: V, I and Power Characteristics

From the above figure 4.7, V-I graph demonstrates the correlation between output voltage and current. The observed data indicates a consistent decline in voltage corresponding to an increase in current. At the start, when current levels are low, the voltage tends to stay quite elevated because of the limited resistive and activation losses involved. As the current rises, there is a gradual decline in voltage attributed to the internal resistance present within the fuel cell.

The power-current (P-I) graph, in conjunction with voltage characteristics, provides critical information regarding the energy output of the fuel cell under varying current loads. The power output initially increases with the rise in current, attaining a peak before stabilising. The data presented in the graph shows that at a current of 133.3 A, the fuel cell produces an output of 5.9985 kW. Alternatively, at a current of 225 A, the maximum power output observed is 8.325 kW.

4.1.2.2 Fuel Cell Control Block

The fuel cell control block is designed to control the hybrid model through the management of the fuel cell output power in reference to the battery state of charge. The control logic consists of a threshold of 31% battery state of charge where the fuel cell remains OFF if the state of charge is above the threshold value or else the fuel cell is switched ON if the Battery SOC falls below the threshold value thus conserving fuel and safeguarding the battery from severe depletion. This threshold-based activation mitigates excessive fuel cell utilisation, prolongs its lifespan, and improves overall system efficiency by adaptively responding to energy requirements.

4.1.2.3 Input Signal Variation (Fuel Pressure and Air Pressure)

In the model, the PEMFC fuel cell signal variation inputs are determined by the pressure of the fuel that is the hydrogen and the pressure of air. These inputs are set to constant values, assuming that we have constant supply of the fuel and air. the fuel pressure and air pressure are set to 1.5 and 1 bar respectively, which are the nominal parameters for the selected type of fuel cell. The constant pressure values ensure the fuel cell operates under standard conditions as described in the

properties of the fuel stack. By sustaining these constant pressures, the system presumes a stable and optimal environment, wherein the pressures remain unvarying, facilitating the assessment of the fuel cell's performance under standard and predictable conditions.

4.1.3 Solar Design Results

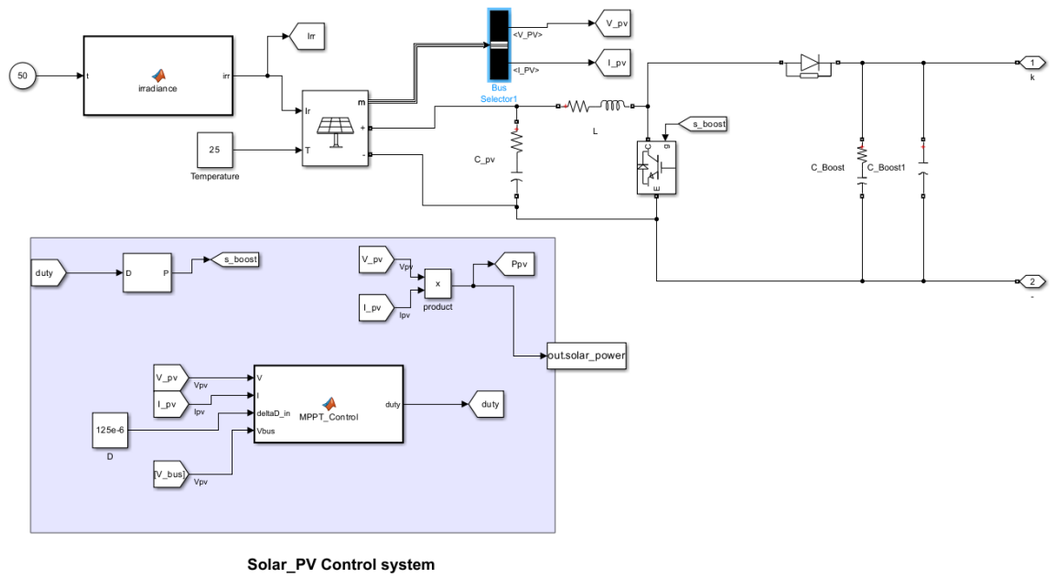

Figure 4.8: MATLAB/Simulink Solar PV Design

In this hybrid energy system, solar photovoltaic (PV) power functions as the primary energy source during daytime operations. The photovoltaic array transforms solar irradiance into electrical energy through the photoelectric effect, facilitating sustainable and renewable power generation. Due to the intermittent characteristics of solar energy, a charge controller and Maximum Power Point Tracking (MPPT) algorithm are employed to enhance energy acquisition and ensure stable power distribution to the system.

The figure below shows the equivalent circuit diagram of a solar cell, the load current output can be calculated as follows:

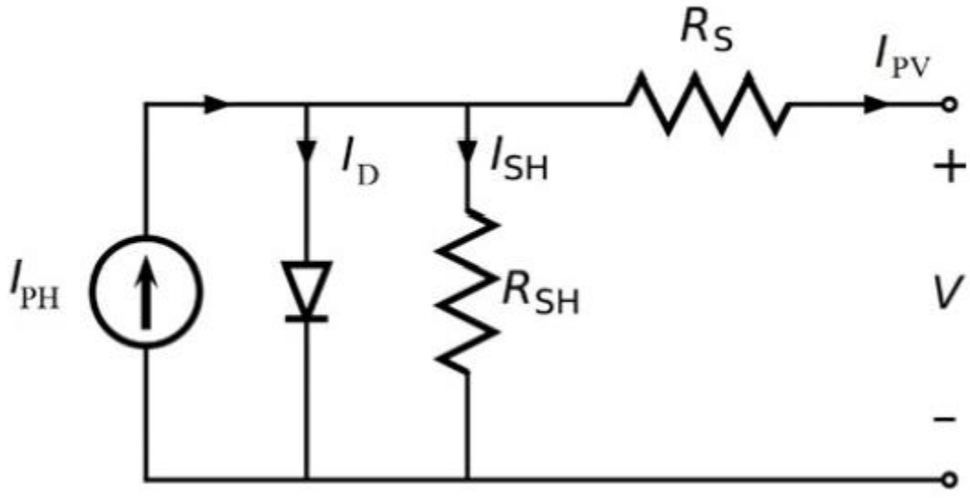

Figure 4.9: Equivalent Circuit of A Solar Cell.

$$I_{PV} = I_{PH} - I_0 \times \left(e^{\frac{V + I_{PV} R_S}{V_T}} \right) - I_{SH} \qquad 4.3$$

The above equation 4.3 represents the Output Load Current where:

I_{PV} = output PV current (A)

I_{PH} = photon-generated current (A)

I_O = saturation current (A)

V = output PV voltage (V)

V_T = thermal voltage (V)

I_{SH} = current through the shunt resistance (A)

R_S = series resistance (Ω)

R_{SH} = shunt resistance (Ω)

4.1.3.1 Solar I-V characteristics

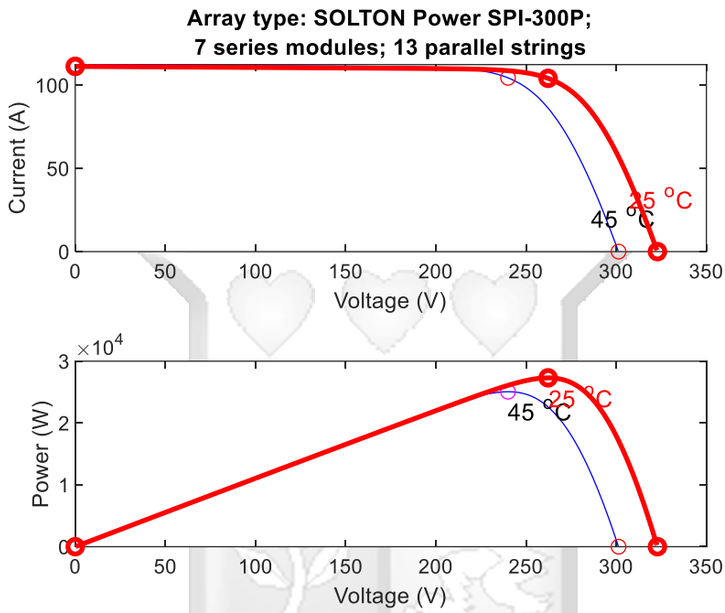

Figure 4.10: Solar PV I-V and P-V Characteristics At A Constant Temperature Of 25ºc.

The current-voltage (I-V) curve in the first graph indicates that the short-circuit current (Isc) remains comparatively constant throughout varying temperatures, whereas the open-circuit voltage (Voc) exhibits a marked decline with rising temperature. At 25°C, the photovoltaic array functions at a higher voltage; conversely, at 45°C, the voltage diminishes, resulting in a decreased power output. This decreases results from the negative temperature coefficient of voltage, leading to efficiency losses in elevated temperature circumstances.

The power-voltage (P-V) curve in the second graph illustrates the shift of the maximum power point (MPP) due to temperature fluctuations. At higher temperatures (45°C), the maximum power production is diminished relative to that at 25°C, validating that thermal factors decrease the overall efficiency of the photovoltaic system.

4.1.3.2 Irradiance Function in Solar Power Simulation

The function irradiance(t) represents the fluctuation of sun irradiance over a 4-day interval (96 hours) within a 50-second simulation. This function aims to replicate the daily variation in solar irradiance, which changes according to the time of day. It presumes that the solar panels function under standard test conditions (STC), with a temperature of 25°C and irradiance peaking at 1000 W/m² during optimal sunlight hours (noon).

4.1.3.3 Time Mapping and Conversion

The simulation lasts 50 seconds, equivalent to 4 days (96 hours). The function starts by transforming the input time t (in seconds) into hours for the four-day duration. The conversion is achieved by the equation 4.4 which represents conversion of time-seconds to hours:

$$t_{hours} = \frac{t}{50} \times 96 \tag{4.4}$$

This maps the time t from the range of [0, 50] seconds to the range of [0, 96] hours, which represents the full 4-day simulation period. The time is then reduced to the current hour of the day using the modulo operation:

$$t_{day} = mod(t_{hours}, 24) \tag{4.5}$$

The above equation 4.5 represents time modulo equation for daily cycle. This operation ensures that the time t_day is confined to a 24-hour cycle, which is necessary to simulate daily solar irradiance variations.

4.1.3.4 Modelling Solar Irradiance

The model assumes a normal daily pattern of solar irradiance which follows a trajectory of power generation starting at sunrise and ending at sunset, where sunrise begin at 6.00 AM and sunset ends at 6.00 PM. The irradiance is modelled with a sine wave function during daylight, as solar intensity exhibits a gradual increase and decrease throughout the day. The normalized time between sunrise and sunset is computed by:

$$norm\ time = \frac{t_{day\ -\ Sunrise}}{sunset - sunrise} \tag{4.6}$$

The above equation 4.6 represents the normalized time calculation for daylight hours. This normalises the time of day to a scale from 0 to 1, with 0 denoting sunrise and 1 denoting sunset. Equation 4.7 below calculates the solar irradiance calculation using sinewave function:

$$irr = 1000 \times \mathbf{sin}(\pi \times normtime) \tag{4.7}$$

At noon (t_{day} = 12), the sine function reaches the peak, achieving a maximum irradiance of 1000 W/m², which is the standard value that is used under standard test conditions (STC) for solar panels. As the sun moves across the sky, the irradiance decreases in accordance with the sine wave pattern, ultimately returning to zero at sunset.

4.1.3.5 Nighttime Condition

During the nighttime, that is from midnight to 6.00 AM in the morning and from 6.00 PM in the evening to midnight, the irradiance is set to zero depicting the absence of sunlight.

4.1.3.6 Assumptions in the Model

This model assumes that the solar panels are operating under standard conditions where the temperature is set at 25°C and a maximum irradiance of 1000 W/m2. The model does not consider

the fluctuations in the temperature, irradiance, weather and other weather variables which represents a real-world case scenario.

4.1.3.7 Sizing of The Solar PV Array

The selection of 7 series modules and 13 parallel strings is essential for the solar array to efficiently charge the battery and provide power to the load. The series connection of modules is necessary to attain a greater voltage, which corresponds with the battery's charging voltage needs and assists in mitigating voltage losses while charging. Conversely, the parallel strings enhance the total current capacity of the system, guaranteeing adequate power delivery to the load. The integration of 7 series modules and 13 parallel strings enables the system to satisfy the energy requirements of the load and the battery's charging needs, even amidst fluctuating climatic circumstances, while maximising power production.

4.1.3.8 Solar PV Control System

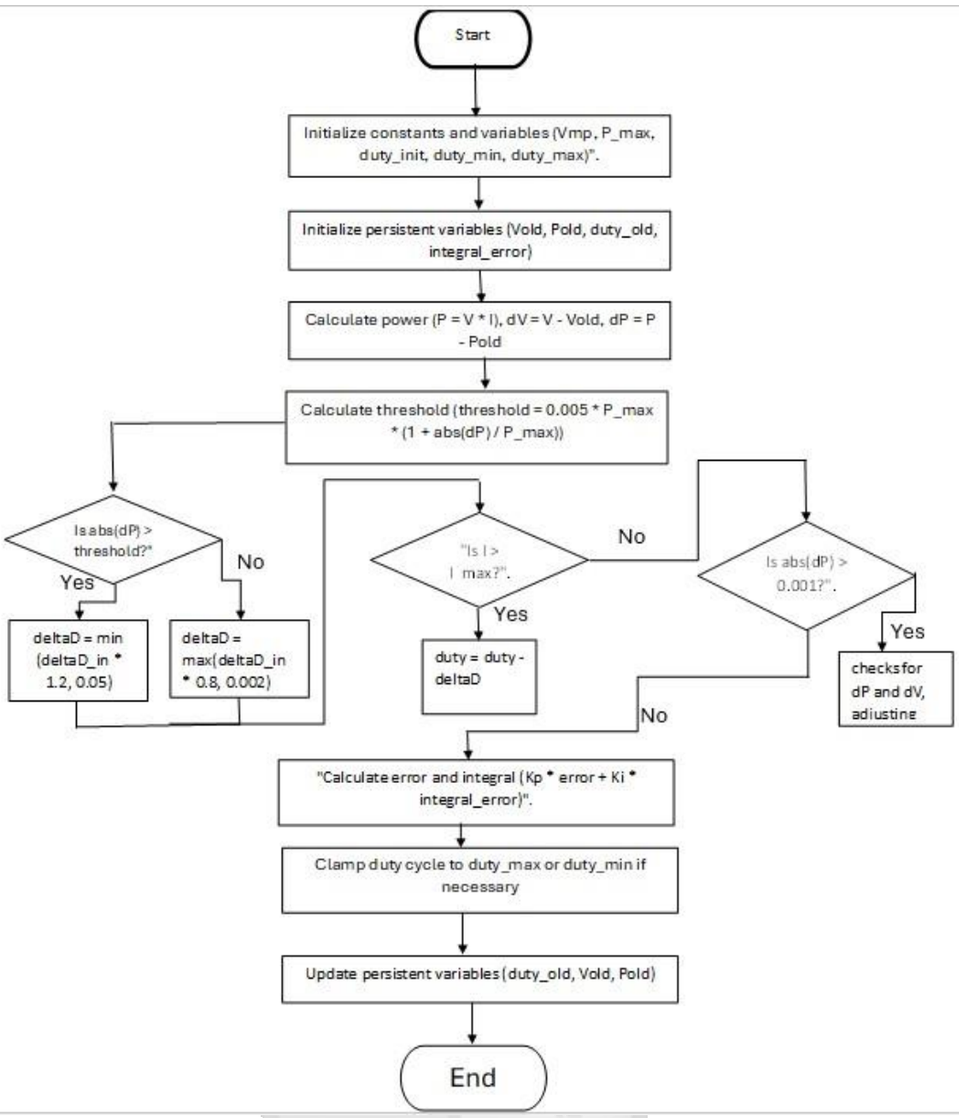

Figure 4.11: Simulation of flow logic of the Solar PV in MATLAB/Simulink

The Maximum Power Point Tracking (MPPT) control system is engineered to enhance the power output of a Solar Photovoltaic (PV) system. This technology continuously modifies the duty cycle of a DC-DC converter to ensure that the photovoltaic array functions at its maximum power point (MPP). The MPP is the voltage and current combination at which the solar panel generates its maximum power output.

To step down the output voltage of the PV panel to the DC bus voltage of 49.9V, a buck converter was designed using the following formulae. The inductance and capacitance calculated for the converter are given in Table 4.2

$$D = 1 - \frac{V_{in} \times \eta_c}{V_{out}} \quad 4.8$$

The above equation 4.8 represents the duty cycle calculation

$$\Delta i_L = 0.1 I_{in} \quad 4.9$$

The above equation 4.9 represents inductor current ripple calculation

$$L = \frac{DV_{out}}{f_s \Delta i_L} \qquad 4.10$$

The above equation 4.10 represents inductance calculation

$$C = \frac{DV_{out}}{f_s \Delta V_{out} R_{DC}} \qquad 4.11$$

The above equation 4.11 represents capacitance calculation

Table 4.1: Design Specifications for Solar PV

Parameters	Value
Switching Frequency(fs)	100 KHz
Input Voltage (Vin)	262.22V
Output Voltage (Vout)	49 V
Inductance (L)	36.22µH
Capacitance ©	28µF

4.1.4 Battery Design

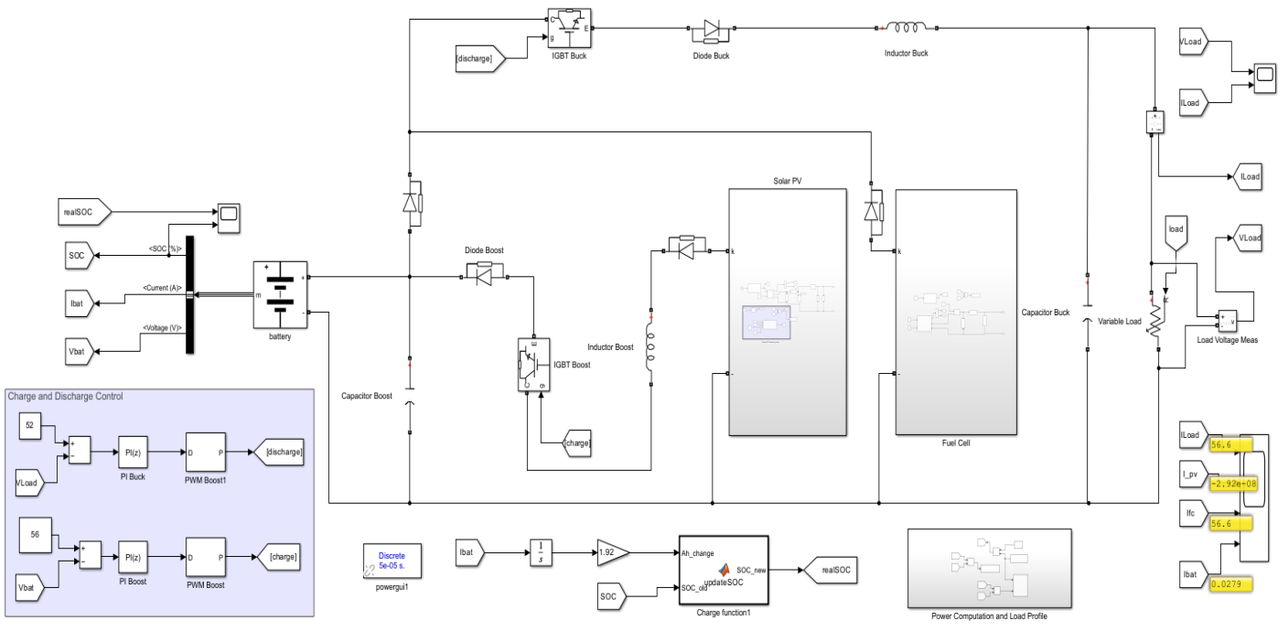

Figure 4.12: Battery Design in MATLAB/Simulink

The battery functions as an essential energy storage element in this hybrid energy system, providing a reliable power supply when solar PV or the fuel cell cannot fulfil the load demand. The control mechanism for charge and discharge meticulously manages the energy flow between the battery and the load, guaranteeing optimal performance while preventing issues such as overcharging or deep discharge. The system incorporates a buck-boost converter that dynamically modifies the battery voltage according to the requirements of the system.

4.1.4.1 Battery Characteristics

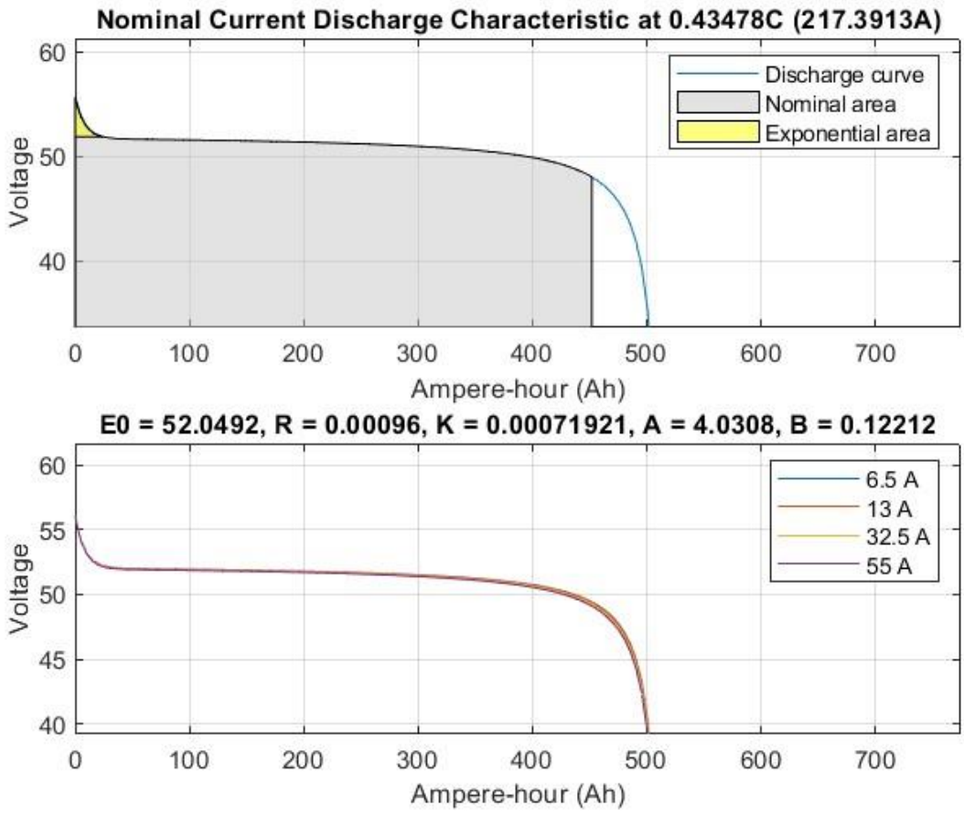

Figure 4.13: Voltage and Ampere-Hour Characteristics

4.1.4.2 Nominal Current Discharge Characteristics

The first graph illustrates the nominal current discharge curve at a rate of 0.43478C (217.3913A). The discharge process is comprised of three essential phases. At first, a significant voltage drop occurs as a result of electrode polarisation, which is then succeeded by a stable region where the voltage remains steady off, offering the majority of the battery's usable capacity. As the battery approaches depletion, a significant drop in voltage occurs, indicating the depletion of stored energy. The operational capacity is 500 Ah, after which voltage experiences a collapse, necessitating recharging.

4.1.4.3 Voltage Behaviour Under Different Discharge Currents

The second graph depicts the response of battery voltage across various discharge currents, specifically at 6.5A, 13A, 32.5A, and 55A. At low discharge rates, the voltage exhibits stability over a prolonged duration, thereby optimising battery lifespan. On the other hand, increased discharge rates lead to quicker depletion.

4.1.4.4 Buck-Boost Converter

A bi-directional buck-boost converter is utilised in the hybrid energy system to manage the bidirectional transfer of electrical energy between the battery and the DC load. The inductor accumulates energy when the switch is closed and discharges it when the switch is open. The capacitor facilitates voltage stabilisation.

The converter operates in buck mode during charging, stepping down the high DC bus voltage to an appropriate level for controlled battery charging. This ensures efficient energy transfer, preventing overvoltage and current surges that could damage the battery.

$$D_{buck} = \frac{V_{out}}{V_{in}}$$

4.12

The above equation 4.12 represents duty cycle for buck mode

$$L_{buck} = \frac{(V_{in} - V_{out})D_{buck}}{\Delta i_L f_s}$$

4.13

The above equation 4.13 represents inductance calculation for buck mode

$$C_{buck} = \frac{(1 - D_{buck})V_{in}}{8L_{buck}\Delta V_{in} f_s^2}$$

4.14

The above equation 4.14 represents capacitance calculation for buck mode

During discharging, the converter switches to boost mode, stepping up the battery's low voltage (48V) to match the DC bus voltage, ensuring a stable power supply to the load.

$$D_{boost} = 1 - \frac{V_{in}}{V_{out}}$$

4.15

The above equation 4.15 represents duty cycle for boost mode

$$L_{boost} = \frac{V_{in} D_{boost}}{\Delta i_L f_s}$$

4.16

The above equation 4.17 represents inductance calculation for boost mode

$$C_{boost} = \frac{V_{out} D_{boost}}{R_{DC}\Delta V_{out} f_s}$$

4.17

The above equation 4.17 represents capacitance calculation for boost mode

The final values of the inductor (L) and the capacitor (C) are chosen as follows and given in Table

$$L = max\ (L_{boost,} L_{buck}$$

$$C = max\ (C_{boost}, C_{buck}$$

Table 4.2: Design Specifications

Parameters	**Value**
Input voltage (Vin)	262.22V
Output voltage (Vout)	49V
Inductance (L) (boost)	36.22µH
Capacitance (boost)	28µF
Inductance (L) (buck)	36.22µH
Capacitance (buck)	28µF

4.1.4.5 Charge and Discharge control

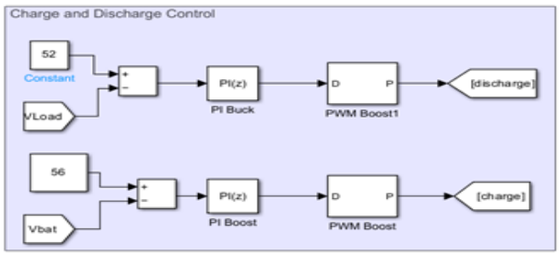

Figure 4.14: Design Block of The Battery Charge And Discharge Control

The charge and discharge control system optimises power management by precisely regulating the battery's operation in accordance with established voltage thresholds. The discharge control loop engages when the battery needs to provide power to the load. A reference voltage of 52V is set, and the system consistently tracks the load voltage (V_Load). When the load voltage dips beneath the set threshold, an error signal is triggered, which is then managed by the PI buck controller. The Pulse Width Modulation (PWM) control fine-tunes the buck converter to optimise power delivery. When required, the battery releases energy to maintain the load voltage, guaranteeing an uninterrupted power supply.

On the other hand, the charge control loop engages when there is surplus power generated from solar photovoltaic systems or alternative energy sources. A reference voltage of 56V was set, and the battery voltage (V_Bat) is under constant observation. When the battery voltage falls beneath this specified threshold, the PI boost controller modifies the power output to facilitate charging. The PWM control optimises the boost converter, elevating the voltage as required to facilitate effective charging. The system commences charging exclusively when the battery resides within a suitable state of charge range, effectively averting overcharging and promoting safe, sustainable battery longevity.

4.1.4.6 Battery State of Charge (SOC) Calculation Model for a 24-Hour Simulation

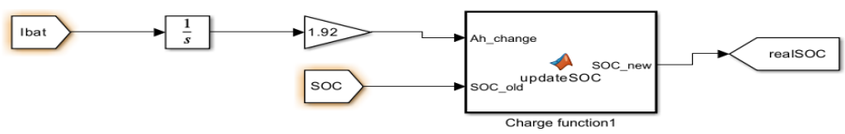

Figure 4.15: Design calculation for a 24-hour simulation

The SOC of the battery is computed over a simulated 24-hour period, with the simulation duration compressed to 12.5 seconds. This time-based scaling is achieved by equating 1 second of simulation time with 6912 seconds (or 1.92 hours) of actual time. This method aims to simulate the entire 24-hour cycle of a day within a feasible duration, optimising computational efficacy while preserving the system's behavioural accuracy. The model adds up the battery current which is then integrated to determine the area under the curve of which at this point is rated ampere-seconds (As). In order to convert the As into ampere-hours (Ah), the area under the curve is divided by 3600 seconds which represents the number of seconds in one hour. This results to a factor of 1.92 thus converting the ampere-seconds to ampere-hours. This will enable us to monitor the charging and discharging cycle of the battery for a whole day. The SOC update function uses this conversion to track the battery's charge level during the simulation, enabling precise modelling of energy consumption and battery performance throughout the day.

4.1.5 Modelling with Homer

The HOMER software, originally developed by the National Renewable Energy Laboratory (NREL) in the USA, is now licensed to HOMER Energy. This study will utilize HOMER software to conduct the investigated system's simulation, optimization, and sensitivity analysis. During the simulation, HOMER will model the system by simulating one year per hour and calculating the energy balance for each hour of the year. HOMER will assess the electric load and compare it to the system's energy capacity hourly throughout the year. HOMER will assess the viability of different configuration systems based on their ability to meet the specified electric demand. It will provide estimates of the installation and operating costs for the chosen system throughout the project's duration.

4.1.5.1 HOMER Input Data and Output Results

As mentioned, HOMER requires input data for simulation and optimization, resulting in feasible and infeasible output results. It is imperative to incorporate various significant input characteristics to conduct this Analysis. The parameters considered in this study are electric load, solar radiation, temperature, and several components of the system, including the PV array, electrolyzer, hydrogen tank, battery, and fuel cell generator. In addition, it is important to consider various factors, including CAPEX, replacement cost, O&M cost, project lifetime, inflation, and discount rate. The Figure below depicts the necessary input data for conducting simulation and optimization, as well as the expected output results for Analysis and discussion within the scope of this study.

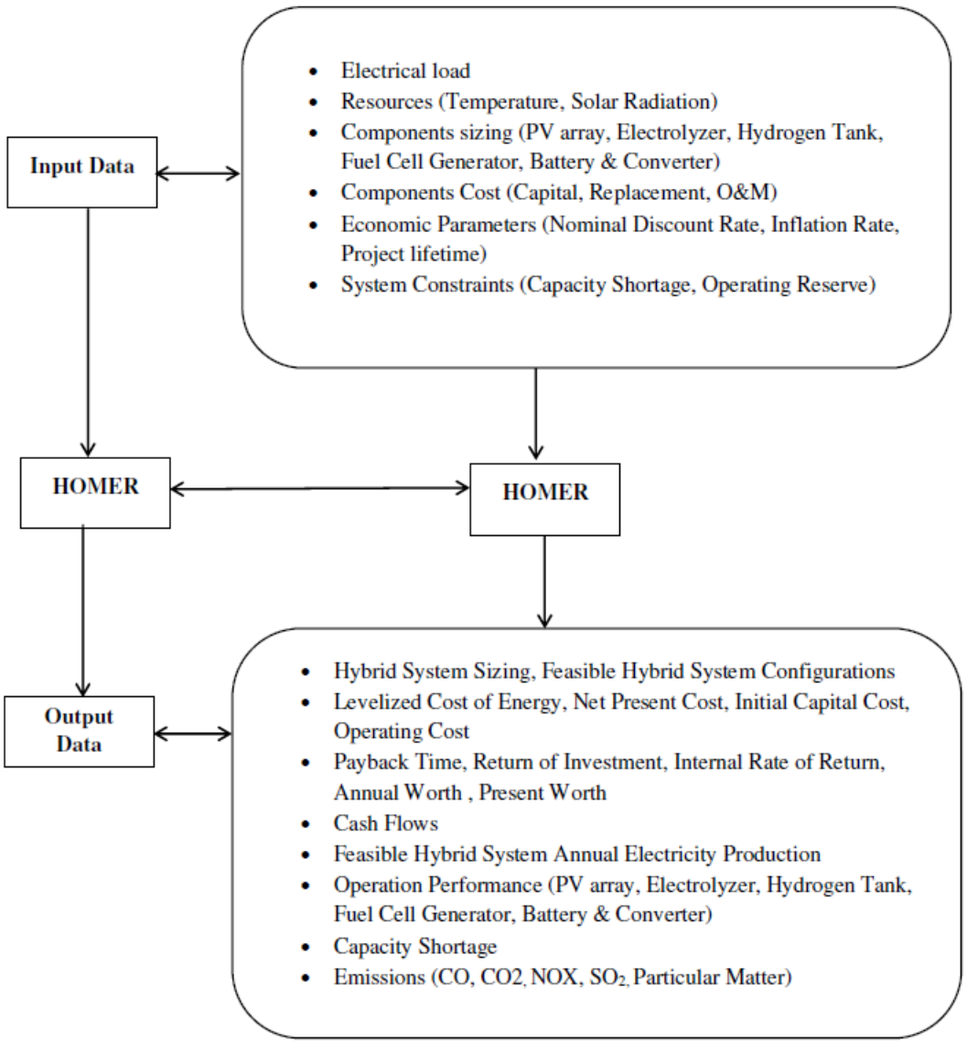

Figure 4.16: Key Parameters of Input Data and Output Results

4.1.5.2 Solar Resource Assessment

This study highlights the significance of solar radiation for charging batteries and producing hydrogen through electrolysis. Figure 4.15 from the HOMER software, utilizing data from the National Renewable Energy Laboratory Database, displays the global horizontal irradiation for the BTS Site at coordinates (-1.3080400, 36.6833950). The average daily solar insolation is 4.88 kilowatt-hours per square meter per Day.

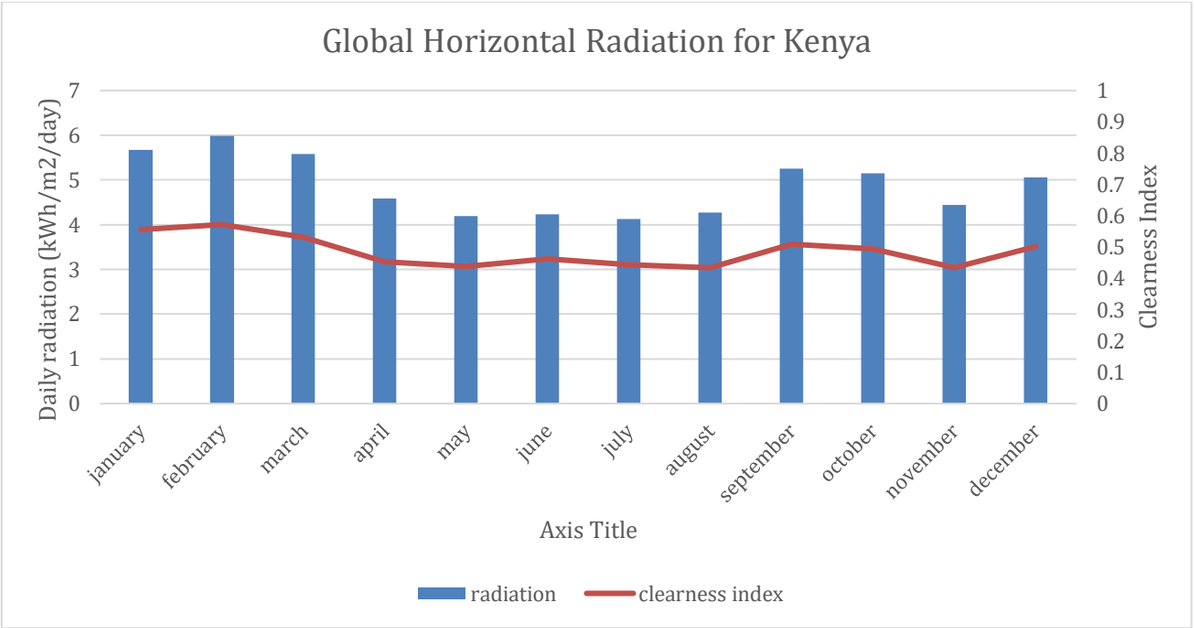

Figure 4.17: Global Horizontal Irradiation for Kenya

Source: National Solar Radiation Database.

Table 4.3: Monthly Average Clearness Index and Solar Global Horizontal Irradiation Data for the BTS.

Month	Daily Radiation (Kwh/m^2/Day)	clearness index
January	5.67	0.556
February	5.986	0.572
march	5.585	0.531
April	4.591	0.453
may	4.188	0.439
June	4.235	0.462
July	4.127	0.444
August	4.269	0.434
September	5.249	0.509
October	5.155	0.495
November	4.447	0.435
December	5.053	0.502
Annual Average Kwh/m^2/Day		**4.88**

4.1.5.3 Solar PV Module (Power Output)

$$P_{PV} = Y_{PV} f_{PV} \left(\frac{G_r}{G_{r,STC}}\right)[1 + \alpha_p(T_c - T_{c,STC})] \quad 4.18$$

The above equation 4.18 representing the power output of solar PV module will be utilized by Homer software to calculate the output of the PV array:

Where Y_{PV} is the rated capacity of the PV array, this means its power output at STC in kW. f_{PV} refers to the solar PV derating factor in [%]. G_r and $G_{r,STC}$ refer to the solar incident radiation at the present time step and at STC respectively in [kW/m^2]. α_p refer to the temperature coefficient

of power in [%/°C]. T_c *and* $T_{c,STC}$ refer to the PV cell temperature in the present time step and at STC respectively in [°C].

4.1.5.4 Fuel Cell System

The fuel cell produces electricity through a chemical reaction that oxidizes chemical fuel. The HOMER model represents a fuel cell system that operates as a generator, using stored hydrogen to generate direct current (DC) electricity. The electrolyzer is a device that uses electricity from a photovoltaic (PV) system to separate water into hydrogen and oxygen. The hydrogen is subsequently stored in a dedicated tank. Hydrogen fuel is utilized as an input in the fuel cell to generate electrical energy. The fuel cell generator (FCG) is essential for supplying electricity to the base station when solar radiation is low, such as during cloudy or rainy days. It is powered by stored hydrogen. The fuel slope indicates the fuel consumption rate of the generator for electricity generation. HOMER assumes a linear trajectory for the fuel slope.

The equation 4.19 provided below expresses the generator's fuel consumption in units per hour as a function of its electrical output.

$$F = F_0 . Y_{gen} + F_1 . P_{gen} \tag{4.19}$$

where F_0 represents the fuel curve intercept coefficient measured in units/hr/kW, F_1 denotes the fuel curve slope in units/hr/kW, Y_{gen} indicates the generator's maximum capacity in kW, and P_{gen} denotes the generator's electrical output in kW.

4.1.5.5 Battery System

The battery bank stores energy the solar PV/fuel cell hybrid power system generates. The energy is used to provide power to the base station when there are interruptions in the power supply or when the generating power systems, such as photovoltaic and fuel cell generators, are not operating efficiently. Battery bank autonomy and battery lifetime are important considerations in determining the suitable capacity for a battery bank. The equation used to determine the battery bank autonomy in HOMER is as follows.

$$A_{batt} = \frac{N_{batt} V_{norm} Q_{nom} \left(1 - {}^{q_{min}}/_{100}\right)(24h/d)}{L_{prim,ave}\ (1000Wh/kWh)} \tag{4.20}$$

The above equation 4.20 represents the battery bank autonomy where N_{batt} represents the number of batteries in the storage bank, V_{norm} is the nominal voltage of a single battery, Q_{nom} is the nominal capacity of a single battery in ampere-hours (Ah), q_{min} is the minimum state of charge of the storage bank as a percentage, and $L_{prim,ave}$ is the average daily primary load in kilowatt-hours per day (kWh/d). This equation ensures the storage bank is sized appropriately to meet the system's energy needs while accounting for the minimum state of charge and daily load.

HOMER calculates the lifespan of a storage bank, referred to as R_{batt} , by considering two key factors: throughput limitations and time-based limitations. The lifespan is determined by whichever factor is more restrictive, ensuring a realistic estimate of how long the storage bank will last.

First, if the lifespan is limited by throughput, it is calculated by dividing the total lifetime energy

throughput of all batteries in the bank ($N_{batt} \times Q_{lifetime}$) by the annual energy throughput of the system (Q_{thrpt}). Here, N_{batt} is the no. of batteries in the storage bank, $Q_{lifetime}$ is the total energy a single battery can handle over its lifetime in kilowatt-hours (kWh), and Q_{thrpt} is the annual energy throughput in Kwh per year (kWh/yr).

If the lifespan is limited by time, it is simply equal to the float life of the batteries, denoted as $R_{batt.f}$. This represents the expected lifespan of the batteries under ideal conditions, measured in years, regardless of how much energy they process.

$R_{batt} = \begin{cases} \frac{N_{batt} \cdot Q_{lifetime}}{Q_{thrpt}} \end{cases}$

if limited by the throughput

$R_{batt=}\{R_{batt.f}$ if limited by time

$R_{batt} = MIN\left(\frac{N_{batt} \cdot Q_{lifetime}}{Q_{thrpt}}, \{R_{batt.f}\right)$ if limited by throughput and time

4.21

The above equation 4.21 represents storage bank life.

4.1.5.6 Levelized Cost of Electricity (LCOE)

In HOMER, the Levelized Cost of Electricity (LCOE) or Cost of Energy (COE) shows how much the system costs on average per kilowatt-hour (kWh) of useful electricity it produces. It is one of the most important ways to measure how economically efficient the energy system is. Before figuring out the COE, HOMER finds the annualised cost of producing electricity, which is the system's total annualised cost minus the cost of meeting the thermal load. Then, this new cost is divided by the total amount of electricity the system handles in a year.

The formula for LCOE is shown by equation 4.22 below:

$$COE = \frac{C_{ann,tot} - c_{boiler} H_{served}}{E_{served}}$$

4.22

where:

$C_{ann,tot}$ is the total annualized cost of the system, measured in dollars per year ($/yr), C_{boiler} is the marginal cost of the boiler, representing the cost per kWh of thermal energy produced, measured in dollars per kWh ($/kWh). H_{served} is the total thermal load served by the system over the year, measured in kilowatt-hours per year (kWh/yr).Es_{erved} is the total electrical load served by the system over the year, also measured in kilowatt-hours per year (kWh/yr).

4.1.5.7 Net Present Cost

The Net Present Cost (NPC), which is also called the life-cycle cost, is the present value of all the costs that come with Installing and running a system or part for the whole project. Expenses like setting up, maintaining, and operation are included, but any revenue made by the components during the project's lifetime is subtracted. HOMER figures out the NPC for each part of the system as well as the whole system, which gives a full picture of the project's financial effects.

The equation 4.23 below is utilised to compute a project's Net Present Cost (NPC).

$$T_{NPC} = \frac{C_{a,t}}{CRF\left(i, P_{lifetime}\right)} \tag{4.23}$$

Where:

$C_{a,t}$ is the total annualized cost, which includes all yearly costs associated with the project, i is the annual real interest rate, derived from the discount rate, and reflects the time value of money, $P_{lifetime}$ is the project's lifetime, measured in years, CRF(i, N) is the Capital Recovery Factor, a factor used to convert annual costs into their present value equivalent.

The CRF(i,N) is given by the equation 4.24 below:

$$CRF(i, N) = \frac{i(1+i)^N}{(1+i)^N - 1} \tag{4.24}$$

Where:

i represents the annual real interest rate and

N is the total number of years, representing the project's lifetime.

4.1.5.8 Real Discount Rate

The real discount rate is an important part of financial analysis because it turns one-time costs into annualised costs. This makes it easier to see how expenditures and earnings change over time. The nominal discount rate and the projected inflation rate are used by HOMER to figure out the real discount rate, which is also called the real interest rate. The real discount rate is then used to find discount factors and turn net current costs into annualised costs. This gives a more accurate picture of how much a project will cost over its lifetime. The equation 4.25 below represents real discount formulae.

$$i = \frac{i' - f}{1 + f}$$

4.25

where:

i represents the real discount rate, which reflects the true cost of borrowing money after accounting for inflation, *i'* is the nominal discount rate, which is the rate at which you could borrow money without adjusting for inflation, f is the expected inflation rate, representing how much prices are expected to rise over time.

Table 4.4: Summary Cost Parameters Inputs for HOMER Simulation from Previous Research.

Electrolyzer

Capital Cost $/kW	Replacement Cost $/kW	O&M Cost $/yr
1000[a]	1000[a]	12[a]
2000[b]	2000[b]	80[b]
700[c]	700[c]	200[c]
1800[d]	1800[d]	100[d]
1100[e]	850[e]	10[e]

Fuel Cell Generator

Capital Cost $/kW	Replacement Cost $/kW	O&M Cost $/h/kw
2800[a]	2500[a]	0.04[a]
600[b]	600[b]	0.08[b]
2000[d]	2000[d]	0.01[d]
4000[e]	3000[e]	0.01[e]

VT OMNES VNVM SINT

Hydrogen Tank		
Capital Cost	Replacement Cost	O&M Cost
$/kg	$/kg	$/yr
1050[a]	1000[a]	18[a]
438[b]	438[b]	10[b]
100[c]	100[c]	10[c]
1000[d]	750[d]	0[d]
Solar PV panel		
Capital Cost	Replacement Cost	O&M Cost
$/kW	$/kW	$/yr
820[a]	0[a]	8[a]
1000[b]	1000[b]	10[b]
140[c]	140[c]	10[c]
1250[d]	1250[d]	12[d]
1000e	750[e]	55[e]
Battery Storage		
Capital Cost	Replacement Cost	O&M Cost
$/kW	$/kW	$/yr
220[a]	220[a]	5[a]
300[b]	300[b]	10[b]
400[d]	400[d]	10[d]
600[e]	300[e]	0[e]

[a](Odoi-Yorke & Woenagnon, 2021)

[b](Hossain et al., 2021)

[c](Hassan et al., 2023)

[d](Jansen et al., 2021)

[e](Luta & Raji, 2019)

4.1.5.9 System Architecture sizing and Input parameters

Table 4.5: Input sizing parameters

Component	Name	Size	Unit
Fuel cell Generator	Hydrogen Fuel Cell 1	0 – 6	kW
Solar PV	Generic flat plate PV	0 - 48	kW
Battery Storage	Polarium SLB48-250-146-2	1	strings
Electrolyzer	Generic Electrolyzer	0 - 50	kW
Hydrogen tank	Hydrogen Tank	0 – 30	kg

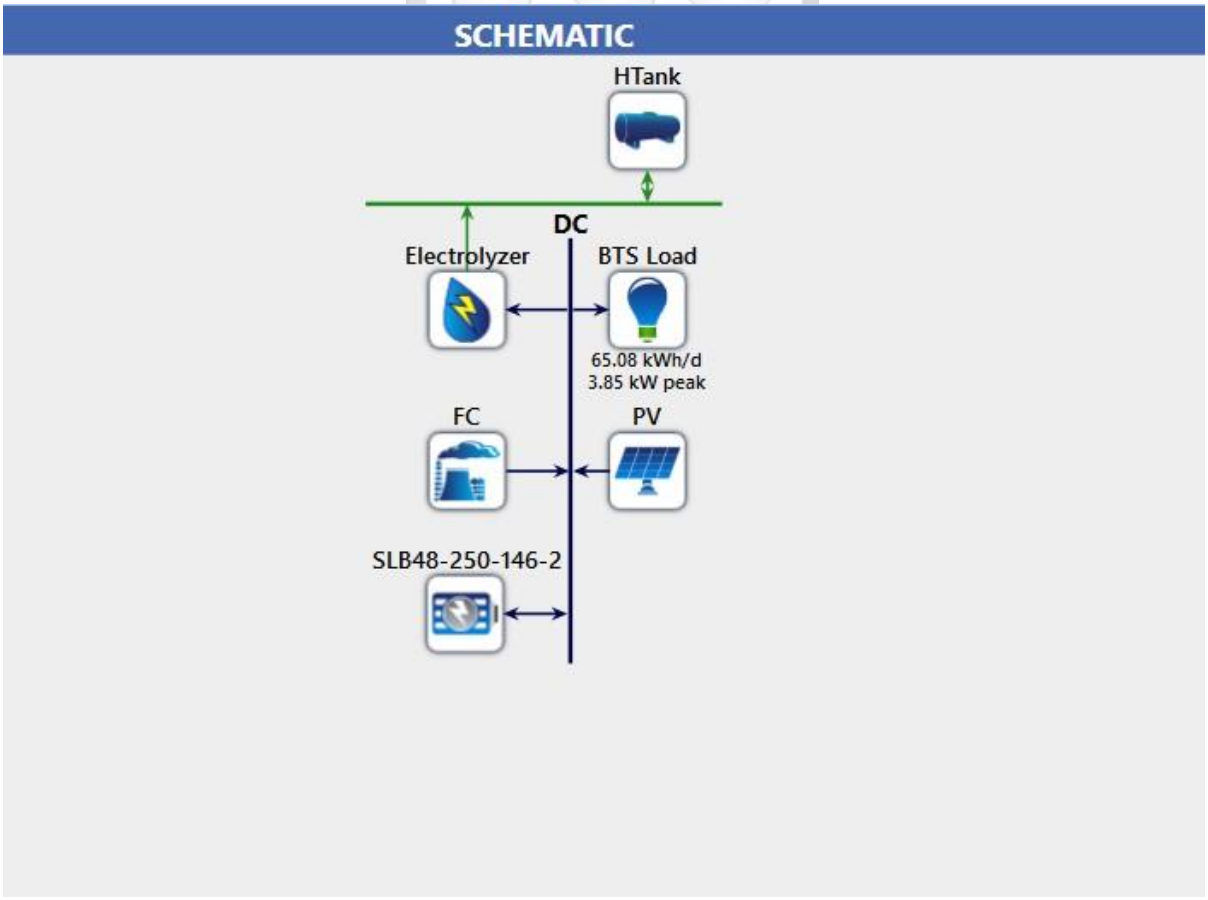

Figure 4.18: Power Hybrid System Architecture

Hydrogen fuel cells provide a substitute for traditional diesel generators in powering telecommunications infrastructure. Fuel cells exhibit extended operational durations, diminished pollutants, and decreased noise levels in comparison to diesel generators. This renders them a feasible and eco-friendly alternative for backup power in the

telecommunications industry. The energy usage of a Base Transceiver Station (BTS) fluctuates according on the number of users it serves. The implementation of hydrogen fuel cells seeks to address the growing carbon emissions associated with traditional energy sources, including diesel generators.

4.2 Discussion Of the Results

In this section an in-depth discussion of the results obtained from the models in Matlab/Simulink and HOMER are explained. The results are visually presented in graphical curves in Matlab and D-maps in HOMER, which provide a deeper comprehension of the hybrid system performance in various operational conditions. The analysis of the results gives insights in the behaviour, efficiciency and optimization of the renewable hybrid system.

4.2.1 MATLAB Simulation Results

4.2.1.1 Power Results

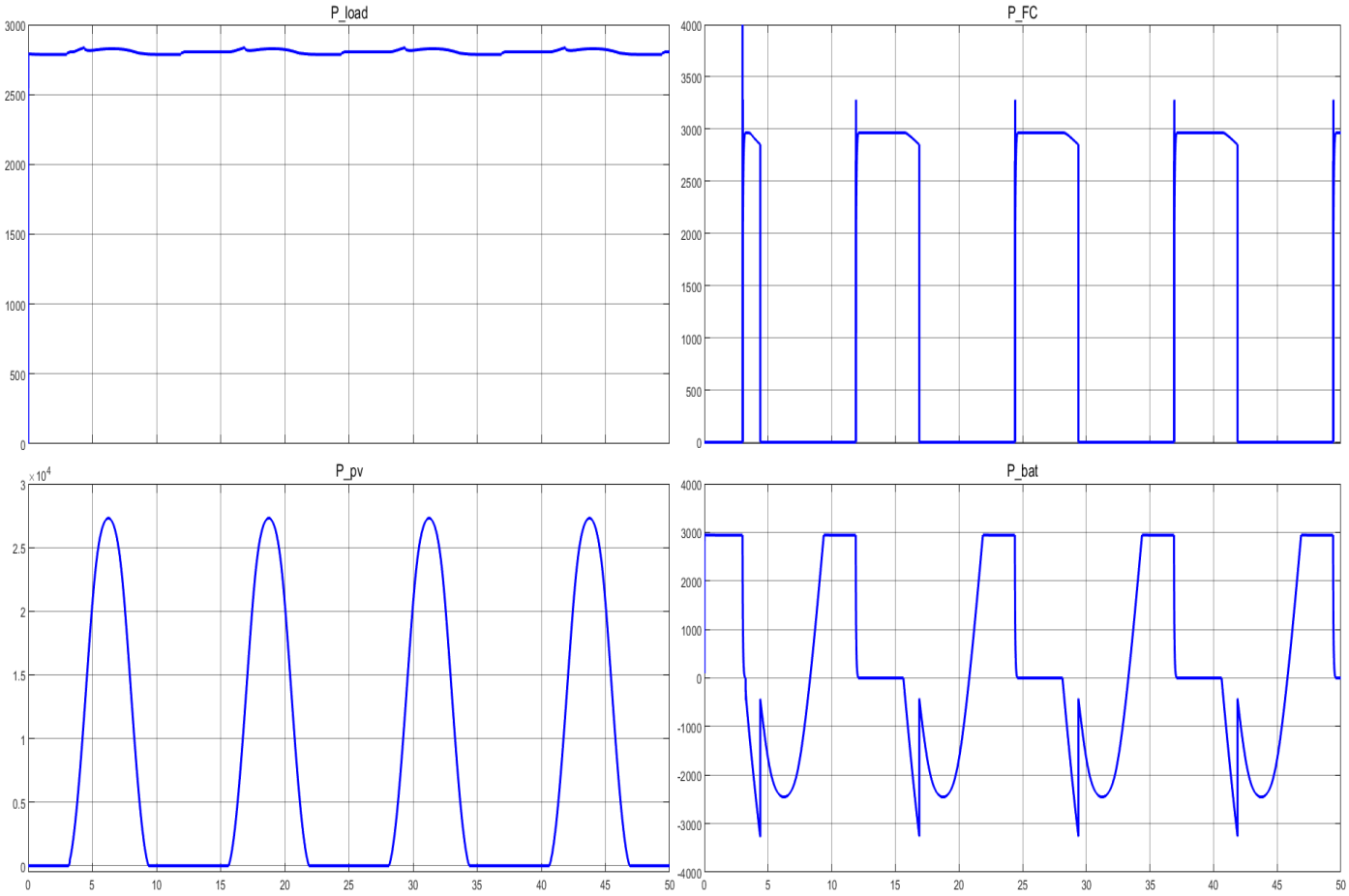

Figure 4.19: Power Results for Solar PV, Load, Battery and Fuel cell

4.2.1.2 Analysis of Power Distribution in a Hybrid Renewable Energy System

The MATLAB/Simulink simulation results illustrate the power dynamics of the designed hybrid renewable energy system over a 4-day period, with a simulation time of 50 seconds

representing four complete 24-hour cycles, based on the time scaling where 12.5 seconds equates to one full day. The findings provide an in-depth analysis of power generation, storage, and utilisation to meet the system's load demands. The four subplots illustrate Load Power, Battery Power, Solar PV Power, and Fuel Cell Power. All four are necessary to keep the energy flow steady.

4.2.1.3 Load Power Analysis

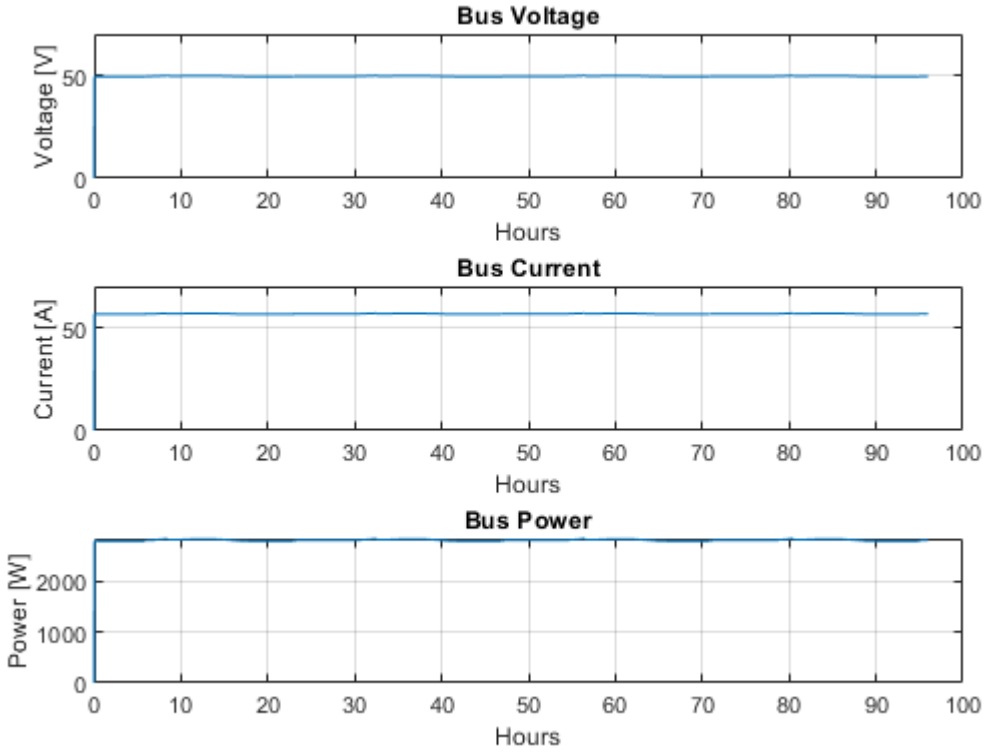

Figure 4.20: Load Voltage, Current and Power characteristics

From figure 4.20, it is evident that the bus voltage and the bus current graphs illustrate how stable the voltage and current is supplied to the load. The Load Power graph stays the same over the simulation, shows the energy consumption over time and its reference to the fluctuating load demand of approximately 3 kW. The continuous demand calls for the power generating and storage elements of the system to regularly supply energy to meet this need. The stable load profile underscores the system's ability to manage anticipated energy consumption without significant fluctuations in demand.

4.2.1.4 Solar PV Power Profile

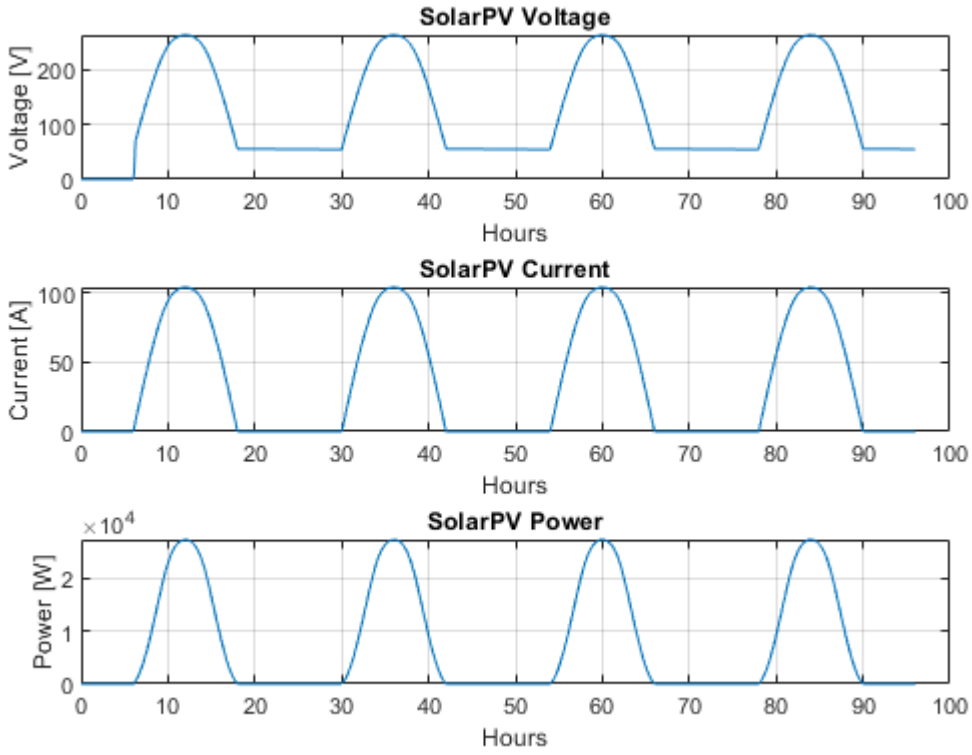

Figure 4.21: Solar PV Voltage, Current and Power Performance

The voltage and current graphs illustrate how the output from the solar PV varies with the sunlight availability. The Solar PV power curve exhibits a distinct cyclic pattern, reaching a maximum of approximately 27 kW during daylight hours (from 0600hrs - 1800hrs) and decreasing to zero at night. This trend is characteristic of solar power generation, wherein peak output transpires during daylight precisely around noon and halts at night.

The simulation indicates that the Solar PV Power system functions for approximately 12 hours daily during daylight, equivalent to 48 seconds of the simulation over four days. This operating duration is the aggregate of daylight hours during each day of the simulated 24-hour cycle. The generated solar energy is utilised to fulfil the load's demands and charge the battery. This yields roughly 48 hours of cumulative solar power operation during the simulated 4-day interval.

4.2.1.5 Battery Power Response

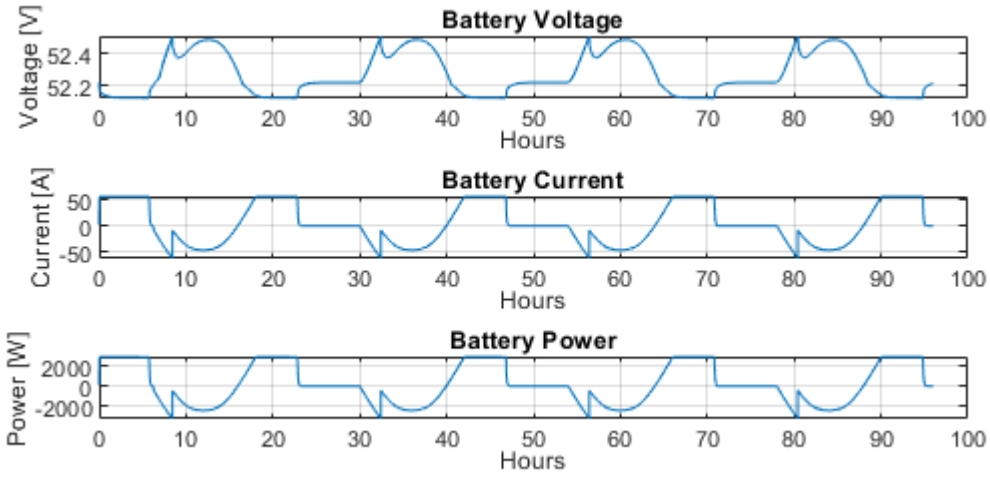

Figure 4.22: Battery voltage, current and power performance

The above figure 4.22, the battery voltage graph shows voltage fluctuations, while the current graph displays the charging and discharging patterns. Hence, the power graph illustrates energy storage and discharge. The Battery Power graph has a high dynamic response. The battery charges when solar energy exceeds load demand and discharges when solar power is inadequate. The battery functions almost throughout the day, charging with surplus energy from the solar photovoltaic system and discharging during periods of low sunlight. The Battery Power graph illustrates the battery's response to variations in solar power generation in order to meet the load's demand.

The battery functions for approximately 7 hours daily, discharging during nighttime or overcast conditions when solar output is unavailable, approximately for 9 hours daily the battery is charged by the excess solar power and for the remaining time the battery is off since it has reached its maximum threshold of 30% depth of discharge thus switching off. This equates to roughly 44 hours of battery operation supplying power to the load over a four-day period (24 hours per day). This underscores the battery's function in providing a reliable power supply during intervals when solar energy is unavailable, effectively addressing the intermittent nature of solar power.

4.2.1.6 Fuel Cell Power Contribution

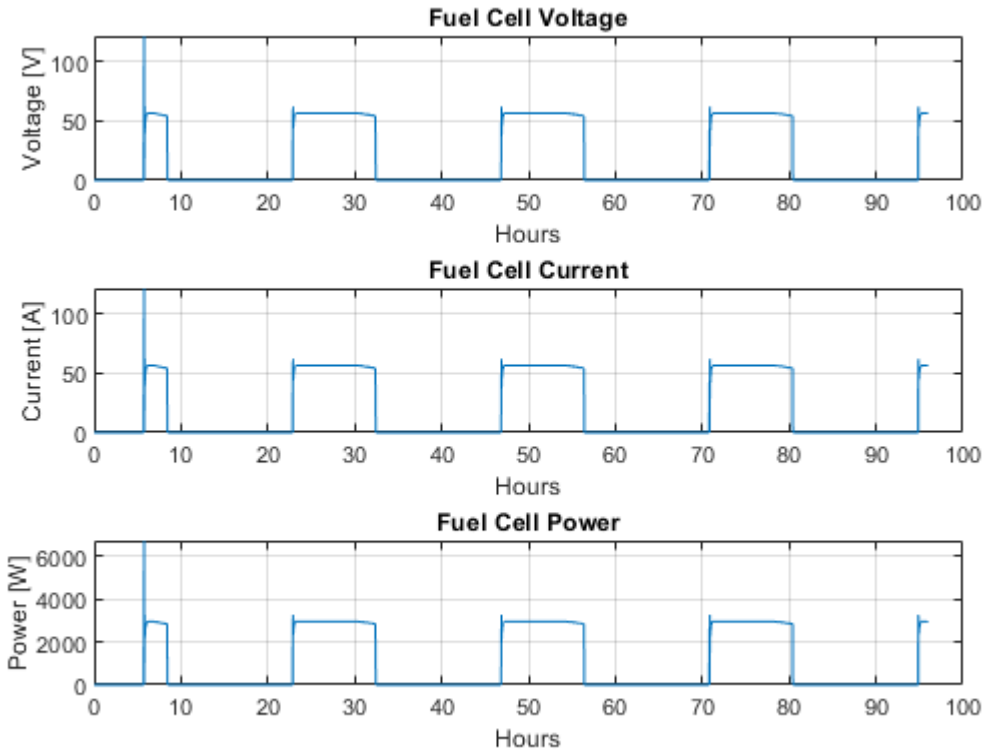

Figure 4.23: Fuel Cell Voltage, Current and Power Performance

From the above figure 4.23, the voltage and current graphs illustrate the current and voltage output contribution in meeting the energy demand of the system. The Fuel Cell Power graph illustrates the activation of the Proton Exchange Membrane Fuel Cell (PEMFC) in scenarios where solar energy and battery storage fall short, especially during nighttime or prolonged cloudy conditions. The fuel cell functions in a cyclical manner to maintain a steady power supply to the load. The fuel cell functions solely, when necessary, typically during periods of reduced solar energy generation, such as nighttime or cloudy days, when the battery's charge is inadequate.

The simulation reveals that the fuel cell operates for around to 8 to 9 hours per day, predominantly at night and during extended periods of reduced solar output. Within the four-day period, this equates to around 24 hours of fuel cell operation, functioning for six hours daily. The fuel cell functions as a crucial backup energy source, ensuring the system operates efficiently, even during extended periods of reduced solar energy availability.

4.2.1.7 Battery State of Charge results

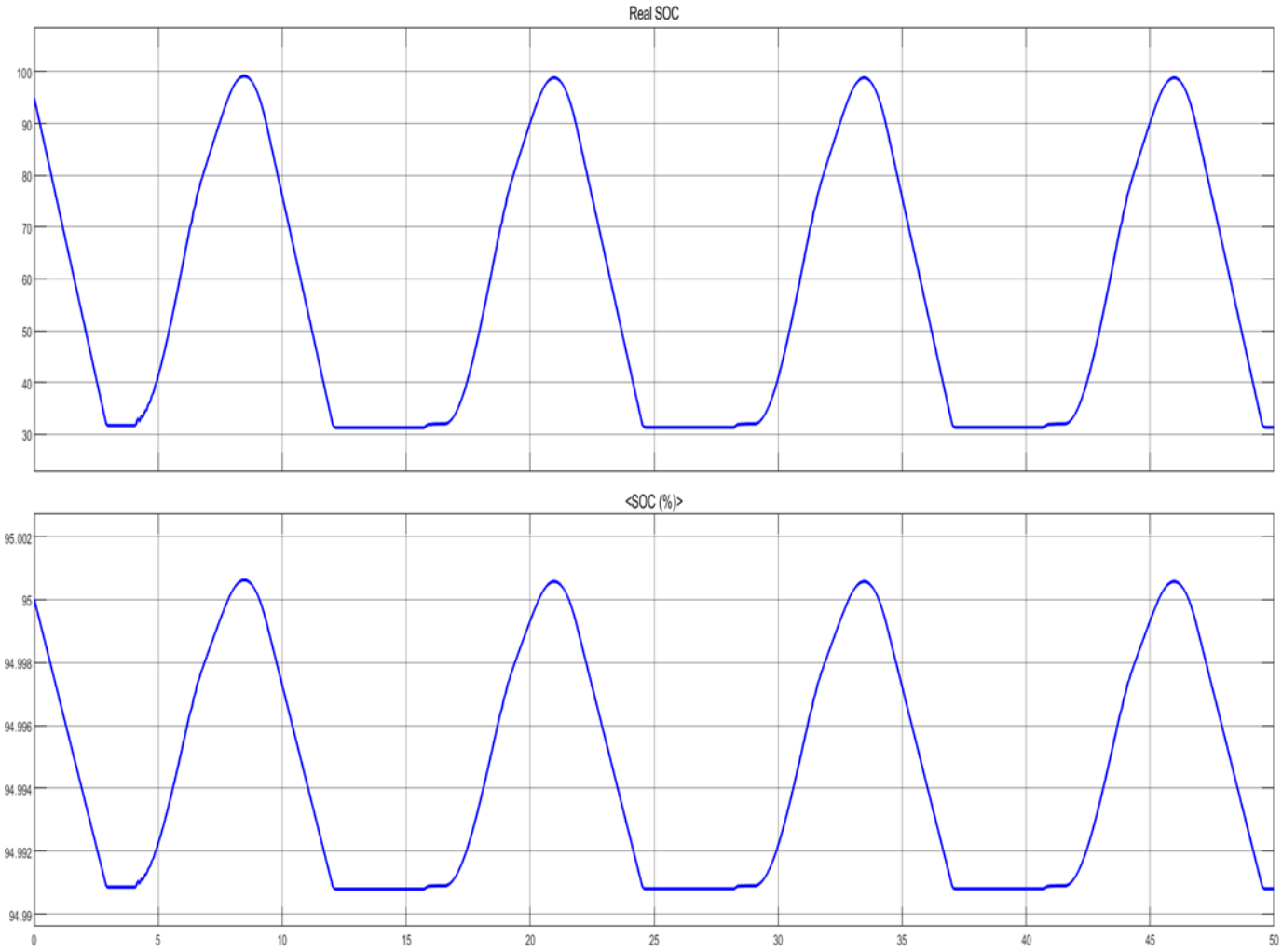

Figure 4.24: Battery SOC Results from The Scope

4.2.1.8 Analysis of Battery SOC Performance and Battery Management

During the 50-second, which represents 96 hours equivalent to 4 days simulation, the actual State of Charge (SOC) graph illustrates the optimal management of the battery, constantly preserving its stored energy while meeting load demands. The battery performance corresponds with the anticipated energy management approach, whereby surplus energy from solar generation is stored for future utilisation, guaranteeing a consistent power supply during periods of insufficient sunlight. The SOC range of 100% to about 31% implies a well-maintained system, since the battery's depth of discharge is maintained within safe parameters, hence preventing damage and safeguarding longevity. These periodic charging and discharging cycles signify a well-balanced hybrid energy system, where the battery plays a critical role in bridging the gaps between solar power generation and load consumption.

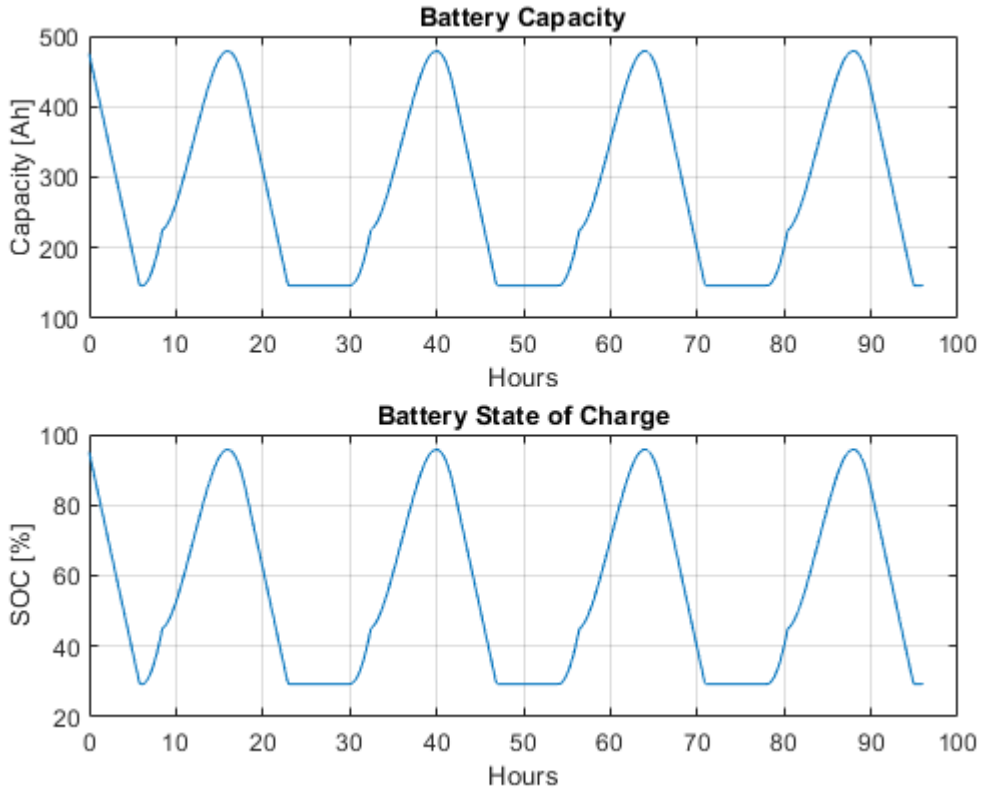

Figure 4.25: Battery SOC and Capacity Performance

In the above figure 4.25, the battery's capacity graph shows how the charge is used, while the SOC graph tracks the percentage of charge left in the battery, indicating the operational state of the battery over time.

4.2.2 HOMER Simulation Results

4.2.2.1 Electricity Production and Consumption

The hybrid system produces an annual electricity output of approximately 67.434MWh. Photovoltaic (PV) panels constitute 85.3% of the overall electricity generation, with fuel cells making up the remaining 14.7%. The Figure 4.26 depicts the monthly electricity production trend of a photovoltaic (PV) panel and a fuel cell system. The hybrid system produces electricity for DC loads and an electrolyzer. Electricity production is allocated to DC loads and an electrolyzer, with consumption rates of 23.744 MWh/yr and 28.202 MWh/yr, respectively.

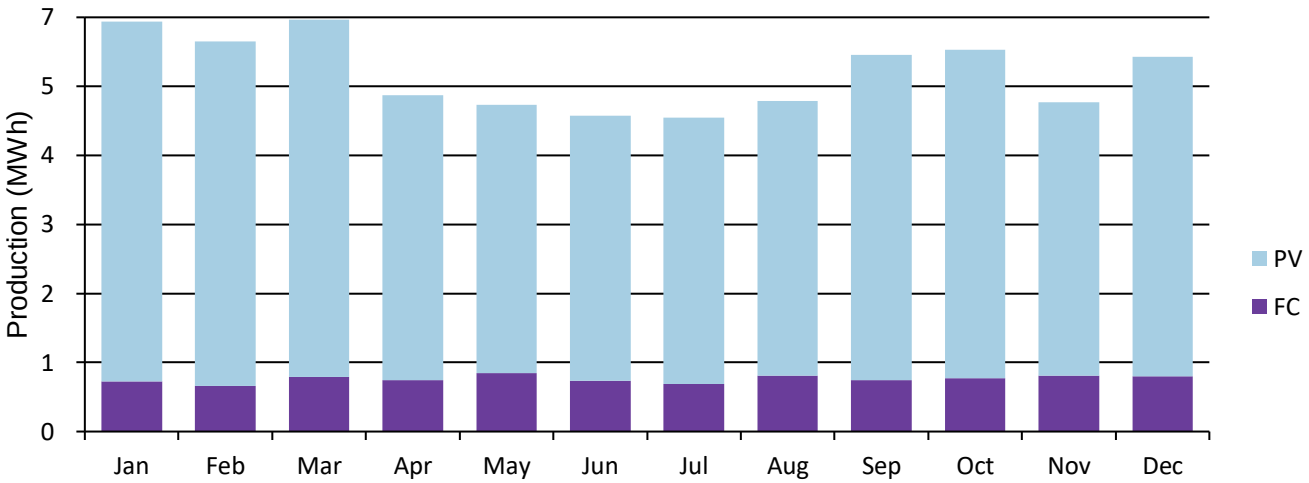

Figure 4.26: Monthly Electric Production.

4.2.3 Summary of the simulation results of the BTS.

Table 4.6 Summary of The Simulation Results Of The BTS.

Hydrogen Fuel cell

Quantity	Value	Units
Electrical Production	9,888	kWh/yr
Mean Electrical Output	2.38	kW
Minimum Electrical Output	0.0360	kW
Maximum Electrical Output	3.60	kW
Fuel Consumption	593	kg
Specific Fuel Consumption	0.0600	kg/kWh
Fuel Energy Input	19,776	kWh/yr
Mean Electrical Efficiency	50.0	%
Hours of Operation	4,146	hrs/yr
Number of Starts	420	starts/yr
Operational Life	9.65	yr
Capacity Factor	31.4	%

Solar PV

Quantity	Value	Units
Minimum Output	0	kW
Maximum Output	38.4	kW
Hours of Operation	4,345	hrs/yr
Levelized Cost	0.0459	$/kWh
Rated Capacity	36	kW
Mean Output	6.57	kW
Mean Output	158	kWh/d
Capacity Factor	18.2	%
Total Production	57,546	kWh/yr

Quantity	Value	Units
Batteries	**1**	**qty.**
String Size	1	batteries
Strings in Parallel	1	strings
Bus Voltage	50.8	V
Average Energy Cost	0	$/kWh
Energy In	3,135	kWh/yr
Energy Out	3,019	kWh/yr
Annual Throughput	3,081	kWh/yr
Autonomy	3.75	hr
Storage Wear Cost	0.0460	$/kWh
Nominal Capacity	12.7	kWh
Usable Nominal Capacity	10.2	kWh
Lifetime Throughput	30,810	kWh
Expected Life	10	yr

VNVM SINT

Electrolyzer

Quantity	Value	Units
Mean output	**0.0526**	**kg**/hr
Minimum Output	0	kg/hr
Maximum Output	0.323	kg/hr
Total production	608	kg/yr
Specific consumption	46.4	kWh/kg
Rated capacity	15	kW
Total input energy	28,202	kWh/yr
Capacity Factor	21.5	%
Hours of operation	2,932	hr/yr

Storage Tank

Quantity	Value	Units
Hydrogen storage capacity	**15**	**kg**
Energy storage capacity	500	kWh
Tank autonomy	184	hr

Stored Hydrogen

Quantity	Value	Units
Total fuel consumed	**593**	**kg**
Avg fuel per day	1.63	kg/day
Avg fuel per hour	0.0677	kg/hour

4.2.3.1 PV Panel Power Production and Performance

The photovoltaic panel has a rated capacity of 36 kilowatts peak (kWp). The photovoltaic (PV) system has an average power output of 6.57 kW and a capacity factor of 18.2%. The PV panel generates approximately 57.546 MWh/year of electricity, with a levelized cost of $0.0459/kWh. Approximately 49.0% of the electricity generated by photovoltaic (PV) panels is used specifically for operating the electrolyzer, which splits water into hydrogen and oxygen. The remaining 51.0% of the electricity generated is utilized to power DC loads during daylight hours. PV production is limited to sunrise at 6:00 and sunset at 18:00. The photovoltaic system operates for a total of 4,345 hours per year, accounting for approximately half of the total available operating hours of 8,670 hours per year. The Figure 4.27 displays a photovoltaic panel's annual power output profile (in kilowatts).

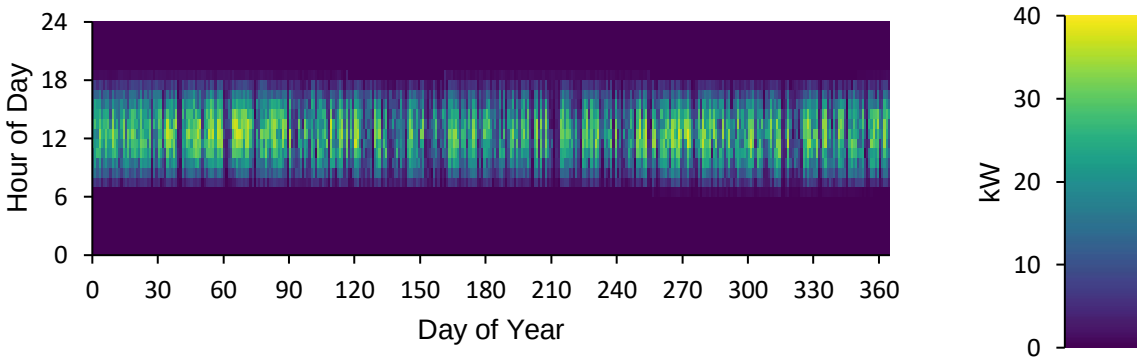

Figure 4.27: photovoltaic panel's annual power output profile (in kilowatts).

4.2.3.1 Fuel Cell Output and Performance

The rated capacity of the FCG is 3.6 kW. The FCG generates approximately 9.89 MWh per year of electricity to fulfil direct current (DC) power requirements. The FCG exhibits a mean power output of 2.38 kW and a minimum power output of 0.0360 kW. The capacity factor of the system is 31.4% with a fixed generation cost of $0.234 per hour. The Fuel Cell Generator (FCG) will require 593 kg of hydrogen, with a specific hydrogen consumption rate of 0.0600 kg/kWh. On average, it consumes 1.62 kg of hydrogen per Day, equivalent to approximately 0.068 kg of hydrogen per hour. The FCG has an annual operating time of approximately 4,146 hours.

HOMER states that the Fuel Cell is activated when the Solar power output falls below the peak load, and the battery has insufficient storage charge. When the FCG is activated, it provides electrical power to the designated load. The Figure illustrates that the FCG is activated from 2300hrs to 0700hrs, and this duration is subject to change based on the Solar PV power output and the state of charge (SOC) of the battery bank. Figure 4.28 displays the annual profile of power output for a fuel cell generator. Calculate the monthly average power output of a fuel cell generator.

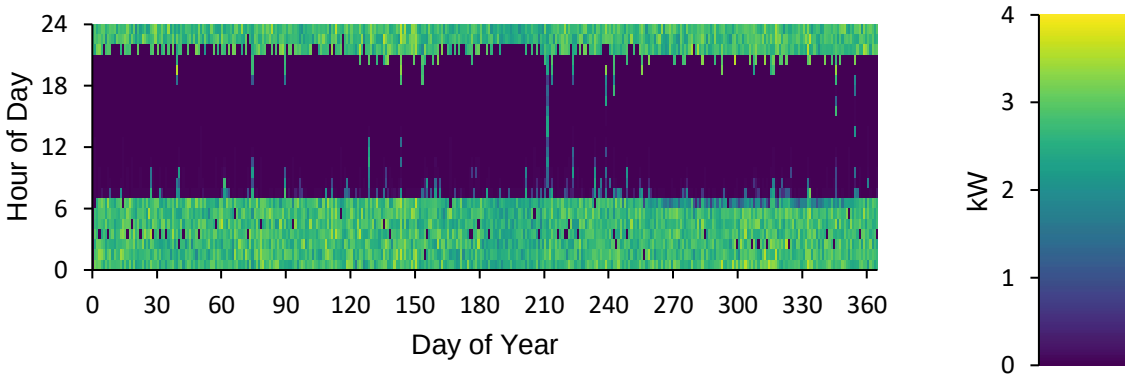

Figure 4.28: The annual profile of power output for a fuel cell generator

4.2.4 Electrolyser Output and Performance

The electrolyzer has a power rating of 15 kW. The annual electrical energy consumption of the electrolyzer is 28.202 MWh. The hydrogen production is 608 kg/yr, with a specific consumption rate of 46.4 kWh/kg. The electrolyzer is operational from 7:00 to 18:00, with the highest hydrogen production occurring between 12:00 and 15:00. In addition, the electrolyzer was unable to operate during the final week of July due to insufficient PV output, which resulted in the inability to produce hydrogen fuel. It is anticipated to operate for approximately 2,932 hours annually. The figure 4.29 shows the yearly profile for Electrolyser Input Power Profile (kW).

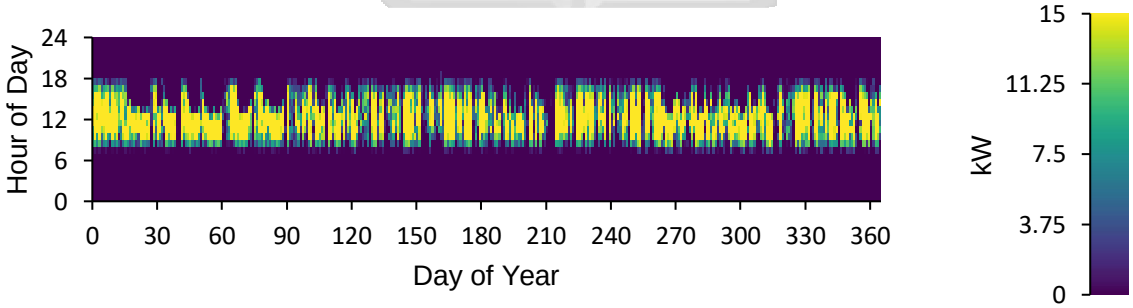

Figure 4.29: Electrolyser Output and Performance

4.2.5.1 Hydrogen Production and Storage Tank Output Performance

The electrolyzer generates approximately 608 kg of hydrogen annually. In this scenario, the FCG utilises approximately 593 kg of produced hydrogen, the remaining 15 kg is content in the hydrogen tank at the end of the year. The hydrogen tank has a maximum storage capacity of 15 kg, corresponding to an energy storage capacity of 500 kWh. It can provide hydrogen fuel for 184 hours. According to the Figure, the hydrogen storage capacity in January is relatively low, ranging from 0 to 5 kg. The hydrogen production from the electrolyzer is

insufficient during June, resulting in low hydrogen levels in the tank ranging between 2 – 5 kg. The figure 4.30 below illustrates the annual profile of the hydrogen tank level, measured in kilograms.

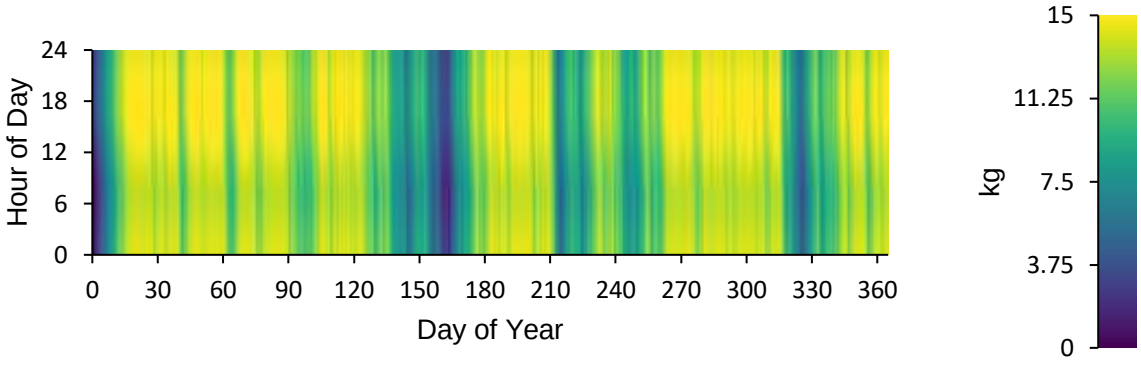

Figure 4.30: The Annual Profile of The Hydrogen Tank Level

Battery Storage Output and Performance

The hybrid system has a nominal capacity of 12.7 kWh, with a usable nominal capacity of 10.2 kWh. The battery's total energy output over its lifetime is approximately 30.810 MWh. The battery's energy input and output are 3.135 MWh/yr and 3.019 MWh/yr, respectively. The yearly throughput is 3.081 megawatt-hours. In addition, the battery storage system lasts 3.75 hours and will require replacement every decade. Figure 4.31 displays the annual profile of the state of charge (SOC) for battery storage, expressed as a percentage.

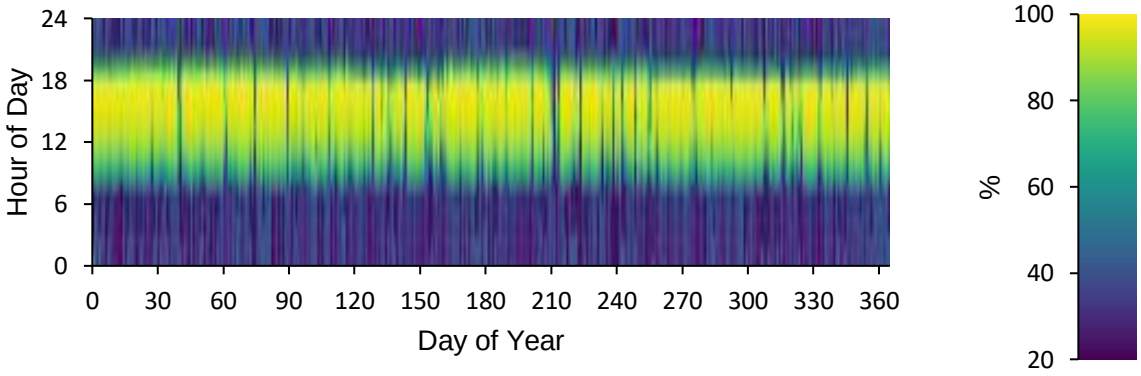

Figure 4.31: The Annual Profile Of The State Of Charge (SOC) For Battery Storage

According to Figure, except for the few weeks of the months of February, March and July, the battery's state of charge (SOC) is generally above 80% for the whole year during the period where there is solar irradiation. The low state of charge (SOC) of the battery can be attributed to its role in providing power to direct current (DC) loads, as the photovoltaic (PV) output is

insufficient to meet the loads during that specific period of the year. The Figure displays the monthly average state of charge (%) for battery storage.

4.2.5 Emissions

The absence of direct emissions characterizes a hydrogen fuel cell system for electricity generation. Hydrogen fuel cells generate electricity via a chemical reaction between hydrogen and oxygen, producing water as the sole byproduct. Hydrogen fuel cells possess a characteristic that renders them a clean and environmentally friendly technology, thereby facilitating a decrease in greenhouse gas emissions and air pollutants. The utilization of electrolysis for green hydrogen production methods guarantees a nearly emission-free process encompassing hydrogen generation and electricity production. In essence, a hydrogen fuel cell system offers an emission-free method of generating electricity.

4.2.6 Economic Input Parameters for Simulation

4.2.6.1 Solar PV/Battery/Fuel cell/Electrolyser

Table 4.7: Economic input parameters

QTY		Solar PV		
		Capital cost($/KW)	**Replacement cost($/KW)**	**O&M Cost($/yr)**
1	**Solar PV**	$820.00	$820.00	$10.00
		Battery		
		Capital cost($/KW)	**Replacement cost($/KW)**	**O&M Cost($/yr)**
1	**Polarium SLB 48-250-146**	$4,953.00	$4,953.00	$10.00
		Hydrogen Fuell		
		Capital cost($/KW)	**Replacement cost($/KW)**	**O&M Cost($/yr)**
1	**Hydrogen Fuel cell**	$2,000.00	$2,000.00	$10
		Electrolyser		
		Capital cost($/KW)	**Replacement cost($/KW)**	**O&M Cost($/yr)**
1	**Electrolyser**	$700.00	$700.00	$12.00
		Storage Tank		
		Capital cost($/Kg)	**Replacement cost($/Kg)**	**O&M Cost($/yr)**
1	**Storage tank**	$438.00	$438.00	$10.00

4.2.6 Economic Results

Table 4.8: Summary of the Economic Results

Economic Key Parameters	BTS Power configuration (Solar/Battery/Fuel cell/Electrolyser)
Net Present Cost	$87,404
CAPEX	$56,267
OPEX per year	$2,970
LCOE (per kWh)	$0.351
Inflation rate	3.50%
Nominal discount rate	12%
System fixed O&M cost per Year	$200
Project Lifetime (years)	25
CO2 Emitted (kg/yr)	0
Fuel Consumption (kg/yr)	593

The simulation outcomes for the Solar PV/Battery/Fuel Cell/Electrolyser power system indicate a Net Present Cost (NPC) of $87,404, which includes capital expenditure (CAPEX), operational expenditure (OPEX), and replacement expenses. The capital expenditure of $56,267 denotes the initial investment necessary for the installation of solar panels, battery storage, a fuel cell, and an electrolyser. The initial expenditure, although considerable, is mitigated by the low annual operating expenses of $2,970, which encompass minimum maintenance and operational costs.

The study assumed an annual fixed Operation and Maintenance (O&M) cost of $200 to cover emergency maintenance of the hybrid system at any time. This annual budget of $200 enable us to quickly sort out unexpected problems or performance issues, like small component failures and control logic errors. The model gives the LCOE of the hybrid system as $0.351 per kWh, which shows the cost of electricity of producing one unit of electricity over the lifetime of the hybrid renewable energy system. Since there is no fossil fuel involved, the LCOE of the hybrid system is competitive with no CO_2 emissions, thus showing how clean and environmentally friendly of the system. In this study the LCOE of $0.351 per kWh serves as an important point of focus for comparison with other similar studies in the field of renewable energy specifically on hybrid systems that concentrate on hybrid systems for off-grid BTS.

Odoi-Yorke and Woenagnon (2021) examined a solar PV/fuel cell hybrid system as an alternative to the BTS power configuration of solar PV/battery/diesel generator. In their study, they achieved a much lower LCOE of $0.222 per kWh. The lower LCOE was because of lack of a battery system in their proposed solar PV/Fuel cell power configuration. The solar PV/ fuel cell system would make it harder for the system to deal with the intermittency from the solar irradiation, thus ending using more fuel for the Fuel cell to continuously supply power to the load. This makes the system to lack reliability as compared to the hybrid system using battery storage examined in this study.

Conversely, a study conducted by Bartolucci et al. (2019) examined three BTS sites in Italy which had the power configuration of solar photovoltaic systems, battery storage, and fuel cells. In their study, they achieved an average LCOE of $0.50 per kWh, which is higher than the LCOE of $0.351 per kWh found in this study. The high LCOE in their study could be attributed to the economic input variables for CAPEX that included the electrolyser, fuel cells, and batteries. Even though Bartolucci et al.'s configuration has a higher LCOE, it is much more reliable and resilient in terms of power availability. When fuel cells and battery storage are combined, power can be managed well, and there is a steady flow of energy even when solar generation is low, thus less hydrogen fuel for the fuel cell will be utilized. The battery storage reduces intermittent power outages by storing extra energy made during sunlight hours. The fuel cell, on the other hand, provides reliable backup power during long times of low solar irradiance or high demand.

The LCOE of $0.351 per kWh in this study is situated between the lower figure obtained by Odoi-Yorke & Woenagnon (2021) and the higher figure attained by Bartolucci et al. (2019), underscoring the trade-offs among system configuration, capital expenditures, and reliability.

4.2.6.2 Comparison with the Existing Diesel Generator System

For this particular BTS site, it constitutes an AC diesel generator which is rated 20 KVA, from figure, displays the daily average utilization of the DG for the period of 6 months. The generator loading is normally at 64% in order ensure efficiency of the DG and achievement of the consumption rate of 2.84 L/Hr.

Table 4.9: Parameters of the Existing Diesel Generator at the BTS site

DG Key Parameters	Value
Capacity (KW)	16
Fuel consumption (L/Hr)	2.84
Daily Average operation (Hrs)	6.28
Price of diesel	$1.3

The current BTS site utilises a diesel generator that functions for an average of 6.28 hours daily as evident in figure 4.2, burning 2.84 litres of fuel per hour. This yields an estimated daily fuel usage of 17.83 litres, culminating in an annual consumption of 6,507.95 litres. The annual fuel expenditure totals $8,460.34 at a diesel price of $1.30 per litre. This is significantly higher than the operational expenditure of the hybrid system.

In the research done by (Spyrou et al., 2020), the DG properties for a BTS case study in Greece were as follows:

Table 4.10: DG key parameters of a BTS case study in Greece.

DG Key Parameters	Value
Capacity (KW)	13.2
Fuel consumption (L/Hr) @50% loading	2.6
Operation and Maintenance cost ($/Hr)	0.24
Capital cost ($/KW)	870
Replacement cost ($/KW)	870
Mean Time Between Failure (Hrs)	20,000

4.2.6.3 Calculation comparison of the hybrid system and the existing Diesel Generator on Site

This study adopts a 12% discount rate, which aligns with the findings of Burgess & Zerbe (2011). Their research highlights that discount rates in the 10-12% range appropriately reflect the social opportunity cost of capital for private-sector investments. This rate accounts for both risk and alternative returns that are pertinent to investments in energy projects.

The study also includes an inflation rate of 3.5%, as reported by the KNBS (2025) document. The inflation rate serves to modify future costs and revenues, guaranteeing that the financial analysis accurately represents the anticipated rise in prices throughout the lifetime of the

project. At the time of conducting this study, the cost of diesel fuel was $1.3 per liter, as referenced in the (*Maximum Retail Petroleum Prices in Kenya for the Period 15th January to 14th February 2025_4.Pdf*, n.d.) ensuring that the analysis reflects the prevailing market conditions during the study period.

In calculating the Net Present Cost (NPC) of the Diesel Generator, one of the key assumptions is that the Operational Expenditure (OPEX) of the DG are consistent with those in the case study of Greece's BTS (Spyrou et al., 2020). According to ATC Kenya the price of a single generator of 20 KVA from Jubaili Bros company is 1,000,000 Kenya shillings, which is approximately $7,694, which is the cost that was used in computing the net present cost. The fuel consumption rate, capacity of the Diesel Generator, and hours of operation are adopted as outlined in Table 4.9.

$$\text{Capital cost} = \text{Capacity} \times \text{capital cost per KW}$$

$$= 16 \times \$870$$

$$= \$13{,}920$$

$$real\ discount = \{\frac{1 + nominal\ discount}{1 + inflation\ rate}\} - 1$$

$$= \frac{1 + 0.12}{1 + 0.035} - 1$$

$$= 8.2\%$$

$$\text{Annual fuel cost} = \text{Annual Fuel Consumption} \times \text{Fuel Price}$$

$$= 6{,}507.95 \times \$1.3$$

$$= \$8{,}460$$

$$\text{Annual O\&M cost} = \text{O\&M per hour} \times \text{operation hours of DG} \times 365 \text{ days a year}$$

$$= \$0.24 \times 6.28 \times 365$$

$$= \$550$$

$$\text{NPC} = \$7{,}694 + \{\frac{9{,}010}{(1+0.082)\text{^}1} + \frac{9{,}010}{(1+0.082)\text{^}2} + \frac{9{,}010}{(1+0.082)\text{^}3} + \frac{9{,}010}{(1+0.082)\text{^}4} + \text{-------} + \frac{9{,}010}{(1+0.082)\text{^}25}\}$$

$$= \$102{,}253$$

The annual fuel cost and the O&M costs of the DG are much higher as compared to those of the renewable hybrid power system by more than twofold. The above calculation illustrates that the annual fuel and the O&M costs of the DG are $9,010 as compared to the O&M cost of the renewable hybrid power system of $2,970. This shows that the operational costs of a DG are much higher than those of the renewable hybrid system. Additionally, the Net present cost (NPC) of the DG, which is approximately $102,253, is much higher than the NPC of the renewable power system which is $87,404. This difference is brought about by the substantial

DG's fuel and maintenance costs which accumulate over the lifetime of the DG, thus resulting in financial inefficiency in the reliance on the DG for long-term operations.

Chapter 5: Conclusion and Recommendation

5.1 Conclusion

This study aimed to evaluate the feasibility, performance, and economic viability of a hybrid renewable energy system comprising of a solar PV, battery and a PEMFC system for an off-grid BTS in Kenya. MATLAB/Simulink and HOMER were utilized where MATLAB/Simulink was used to model and monitor the energy management performance of the components of the system, that is, voltage, current, and power to ensure effective stability of the system. On the other hand, HOMER was used to design and optimize the renewable hybrid system to give a view of the financial implication of deploying the hybrid system in Kenya. The results show that the hybrid power solution increases the energy reliability, have lower operational costs and have no carbon emissions.

The findings from MATLAB/Simulink, the solar PV met the energy demand by the load during the sunlight hours, hence the excess power was used to charge the batteries. The batteries were used to increase the reliability of the system by mitigating the intermittency of the solar PV during times of low or no sunlight. The fuel cell served as an auxiliary power source, providing energy when there is low solar output and the battery has reached its threshold of 30%, thus maintaining the system stability. The battery SOC remained within safe operational zone preventing over discharge.

The HOMER simulation results showed that the proposed hybrid system reduces reliance on fossil fuels. The system generated an annual electrical production of roughly 67.434 MWh, with 85.3% derived from solar photovoltaic sources and 14.7% from the fuel cell. The hybrid power solution is more environmentally friendly as compared to the DGs since it has no greenhouse gas emissions. The system's carbon footprint was reduced, aiding Kenya's goal of decreasing greenhouse gas emissions by 32% by 2030, as specified in the Nationally Determined Contributions (NDC) report.

The economic assessment revealed that the hybrid system is more cost-effective, exhibiting a lower levelized cost of electricity (LCOE) and net present cost (NPC) compared to traditional diesel-based power generation. The LCOE for the hybrid system was determined to be $0.351 per kWh, and the NPC was $87,404. This is much lower than the NPC of a diesel generator, recorded at $102,253. During a predicted 25-year operational lifetime, the proposed system demonstrated a significantly higher return on investment, due to the low OPEX by more than double the expenses of the diesel-based system, which faced high fuel and maintenance costs.

5.2 Recommendation

The following are the recommendations for areas related to this study that need further investigation:

I. Hydrogen fuel cells should be incorporated into off-grid BTS infrastructure as a backup power solution. This study has shown that PEM fuel cells provide a reliable energy source during periods of low solar irradiance, ensuring uninterrupted power supply. Further pilot projects should be conducted to validate the operational efficiency and performance of hydrogen fuel cells in real-world telecom applications.

II. A detailed life-cycle environmental impact assessment of the hybrid system should be conducted, considering all stages from component production to system decommissioning. This would ensure that the adoption of hybrid energy systems not only addresses operational costs but also aligns with environmental sustainability goals.

III. More research needs to be done on how to include electrolysers in MATLAB/Simulink models that combine battery systems, fuel cells, and photovoltaic (PV) systems. The research should concentrate on how to integrate the electrolyser and the storage tank where the hydrogen generated by the electrolyser is from the surplus solar energy of the hybrid power system.

IV. The Levelized cost of hydrogen in this system is $16.7 per kilogramme, this shows a high price point of the hydrogen fuel. The cause of this high result is due to the energy consumption that take place in the electrolyser during generation of hydrogen, along with the initial capital investment costs of the electrolyser, hydrogen storage tanks, and the solar PV system. For hydrogen-based systems to be financially viable, more research should be done in the transportation and storage of hydrogen to lower the cost of producing the hydrogen onsite via the electrolyser.

References

Ayang, A., Ngohe-Ekam, P. S., Videme, B., & Temga, J. (2016). Power consumption: base stations of telecommunication in sahel zone of cameroon: typology based on the power consumption—model and energy savings. *Journal of Energy*, *2016*.

Bartolucci, L., Cordiner, S., Mulone, V., & Pasquale, S. (2019). Fuel cell based hybrid renewable energy systems for off-grid telecom stations: Data analysis and system optimization. *Applied Energy*, *252*, 113386. https://doi.org/10.1016/j.apenergy.2019.113386

Bezmalinović, D., Barbir, F., & Tolj, I. (2013). Techno-economic Analysis of PEM fuel cells role in photovoltaic-based systems for the remote base stations. *International journal of hydrogen energy*, *38*(1), 417-425. https://doi.org/10.1016/j.ijhydene.2012.09.123

Bruni, G., Cordiner, S., Mulone, V., Giordani, A., Savino, M., Tomarchio, G., ... & Picciotti, G. (2014). Fuel cell based power systems to supply power to Telecom Stations. *International journal of hydrogen energy*, *39*(36), 21767-21777.https://doi.org/10.1016/j.ijhydene.2014.07.078

Hoffmann, P. (2006). Tomorrow's Energy: Hydrogen, Fuel Cells, and the Prospects for a Cleaner Planet. https://www.tandfonline.com/doi/pdf/10.1080/15453660609509095

Hossain, M. S., Jahid, A., Islam, K. Z., & Rahman, M. F. (2020). Solar PV and biomass resources-based sustainable energy supply for off-grid cellular base stations. *IEEE access*, *8*, 53817-53840. https://ieeexplore.ieee.org/abstract/document/9022971

Ike, D. U., Adoghe, A. U., & Abdulkareem, A. (2014). Analysis of telecom base stations powered by solar energy. *Int. J. Sci. Technol. Res*, *3*(4), 369-374. https://core.ac.uk/download/pdf/32225442.pdf

Lorincz, J., & Bule, I. (2013). Renewable energy sources for power supply of base station sites. *International Journal of Business Data Communications and Networking (IJBDCN)*, *9*(3), 53-74. https://www.igi-global.com/article/renewable-energy-sources-for-power-supply-of-base-station-sites/95723

Maurice R. Greenberg Center for Geoeconomic Studies. (2015). *Reducing Deforestation to Fight Climate Change*. Council on Foreign Relations. http://www.jstor.org/stable/resrep16756

McCusker, P. (2014, Jun 18). Climate change 'the most climate change 'the most crucial issue of our time': Climate change and policies to reduce carbon dioxide emissions were put under the spotlight at a lively debate in durham city. panellist and journal energy writer PETER MCCUSKER reports. *Journal* Retrieved

from https://eznvcc.vccs.edu/login?url=https://www.proquest.com/newspapers/climate-change-most-crucial-issue-our-time/docview/1536525501/se-2

Mohamad Aris, A., & Shabani, B. (2015). Sustainable power supply solutions for off-grid base stations. *Energies*, *8*(10), 10904-10941.

Odoi-Yorke, F., & Woenagnon, A. (2021). Techno-economic assessment of solar PV/fuel cell hybrid power system for telecom base stations in Ghana. *Cogent Engineering*, *8*(1), 1911285. https://doi.org/10.1080/23311916.2021.1911285

Radonjič, G., & Tompa, S. (2018). Carbon footprint calculation in telecommunications companies–The importance and relevance of scope 3 greenhouse gases emissions. *Renewable and Sustainable Energy Reviews*, *98*, 361-375.

Revankar, S. T., & Majumdar, P. (2014). *Fuel cells: principles, design, and Analysis*. CRC press. https://books.google.co.ke/books?hl=en&lr=&id=LkChAwAAQBAJ&oi=fnd&pg=PP1&dq=Revankar,+S.+T.,+Majumdar,+P.+(2016).+Fuel+Cells:+Principles,+Design,+and+Analysis.+United+States:+CRC+Press.&ots=sSvq8RUZuA&sig=lF5fLI1LQVqvAGEDvb2wIDeqvxA&redir_esc=y#v=onepage&q&f=false

Spagnuolo, A., Petraglia, A., Vetromile, C., Formosi, R., & Lubritto, C. (2015). Monitoring and optimization of energy consumption of base transceiver stations. *Energy*, *81*, 286-293.

Tătaru, I. M., Fleacă, E., & Fleacă, B. (2020). Insights on the impact of telecommunication companies on the environment. In *Proceedings of the International Conference on Business Excellence* (Vol. 14, No. 1, pp. 202-213).

Vereecken, W., Van Heddeghem, W., Deruyck, M., Puype, B., Lannoo, B., Joseph, W., ... & Demeester, P. (2011). Power consumption in telecommunication networks: overview and reduction strategies. *IEEE Communications Magazine*, *49*(6), 62-69.

Verma, S., & Gustafsson, A. (2020). Investigating the emerging COVID-19 research trends in the field of business and management: A bibliometric analysis approach. *Journal of Business Research*, *118*, 253-261.

Wang, J., Jiang, Q., Dong, X., & Dong, K. (2021). Decoupling and decomposition analysis of investments and CO2 emissions in information and communication technology sector. *Applied Energy*, *302*, 117618.

Deevela, N. R., Kandpal, T. C., & Singh, B. (2024). A review of renewable energy based power supply options for telecom towers. *Environment, Development and Sustainability*, *26*(2), 2897-2964.

Bartolucci, L., Cordiner, S., Mulone, V., & Pasquale, S. (2019). Fuel cell based hybrid renewable energy systems for off-grid telecom stations: Data analysis and system optimization. *Applied Energy*, *252*, 113386. https://doi.org/10.1016/j.apenergy.2019.113386

Crompton, T. R. (2000). *Battery reference book* (3rd ed). Newnes.

Deevela, N. R., Kandpal, T. C., & Singh, B. (2023). A review of renewable energy based power supply options for telecom towers. *Environment, Development and Sustainability*, *26*(2), 2897–2964. https://doi.org/10.1007/s10668-023-02917-7

Dicks, A., & Rand, D. A. J. (2018). *Fuel cell systems explained* (Third edition). Wiley.

Gupta, P., Toksha, B., & Rahaman, M. (2024). A Critical Review on Hydrogen Based Fuel Cell Technology and Applications. *The Chemical Record*, *24*(1), e202300295. https://doi.org/10.1002/tcr.202300295

Hossain, E. (2022). *MATLAB and Simulink Crash Course for Engineers*. Springer International Publishing. https://doi.org/10.1007/978-3-030-89762-8

Jansen, G., Dehouche, Z., & Corrigan, H. (2021). Cost-effective sizing of a hybrid Regenerative Hydrogen Fuel Cell energy storage system for remote & off-grid telecom towers. *International Journal of Hydrogen Energy*, *46*(35), 18153–18166.

Larminie, J., & Dicks, A. (2003). *Fuel cell systems explained* (2nd ed). J. Wiley.

Luque, A., & Hegedus, S. (Eds.). (2003). *Handbook of photovoltaic science and engineering*. Wiley.

Millet, P., & Grigoriev, S. (2013). Water Electrolysis Technologies. In *Renewable Hydrogen Technologies* (pp. 19–41). Elsevier. https://doi.org/10.1016/B978-0-444-56352-1.00002-7

Whittingham, M. S., Savinell, R. F., & Zawodzinski, T. (2004). Introduction: Batteries and Fuel Cells. *Chemical Reviews*, *104*(10), 4243–4244. https://doi.org/10.1021/cr020705e

Zohuri, B. (2018). *Hybrid Energy Systems*. Springer International Publishing. https://doi.org/10.1007/978-3-319-70721-1Ayodele, T. R., Ogunjuyigbe, A. S. O., Ehinlaiye, P. A., Mosetlhe, T. C., & Yusuff, A. A. (2023). Hybrid Solar/Hydro Renewable Energy System with Hydrogen Storage for Powering a Typical Remote Base Transceiver Station. *2023 IEEE PES/IAS PowerAfrica*, 1–5. https://doi.org/10.1109/PowerAfrica57932.2023.10363311

Bartolucci, L., Cordiner, S., Mulone, V., & Pasquale, S. (2019). Fuel cell based hybrid renewable energy systems for off-grid telecom stations: Data analysis and system optimization. *Applied Energy*, *252*, 113386. https://doi.org/10.1016/j.apenergy.2019.113386

Bowmans-guide-EA-Data-Infrastructure_21.04.2022.pdf. (n.d.).

Deevela, N. R., Kandpal, T. C., & Singh, B. (2023). A review of renewable energy based power supply options for telecom towers. *Environment, Development and Sustainability*, *26*(2), 2897–2964. https://doi.org/10.1007/s10668-023-02917-7

Dicks, A., & Rand, D. A. J. (2018). *Fuel cell systems explained* (Third edition). Wiley.

Gupta, P., Toksha, B., & Rahaman, M. (2024). A Critical Review on Hydrogen Based Fuel Cell Technology and Applications. *The Chemical Record*, *24*(1), e202300295. https://doi.org/10.1002/tcr.202300295

Hassan, Q., Abdulrahman, I. S., Salman, H. M., Olapade, O. T., & Jaszczur, M. (2023). Techno-Economic Assessment of Green Hydrogen Production by an Off-Grid Photovoltaic Energy System. *Energies*, *16*(2), 744. https://doi.org/10.3390/en16020744

Hossain, Md. S., Alharbi, A. G., Islam, K. Z., & Islam, Md. R. (2021). Techno-Economic Analysis of the Hybrid Solar PV/H/Fuel Cell Based Supply Scheme for Green Mobile Communication. *Sustainability*, *13*(22), 12508. https://doi.org/10.3390/su132212508

Jansen, G., Dehouche, Z., & Corrigan, H. (2021). Cost-effective sizing of a hybrid Regenerative Hydrogen Fuel Cell energy storage system for remote & off-grid telecom towers. *International Journal of Hydrogen Energy*, *46*(35), 18153–18166.

KEN210108.pdf. (n.d.).

Larminie, J., & Dicks, A. (2003). *Fuel cell systems explained* (2nd ed). J. Wiley.

Luque, A., & Hegedus, S. (Eds.). (2003). *Handbook of photovoltaic science and engineering*. Wiley.

Luta, D. N., & Raji, A. K. (2019). Renewable Hydrogen-Based Energy System for Supplying Power to Telecoms Base Station. *International Journal of Engineering Research in Africa*, *43*, 112–126. https://doi.org/10.4028/www.scientific.net/JERA.43.112

Ma, Z., Eichman, J., & Kurtz, J. (2019). Fuel Cell Backup Power System for Grid Service and Microgrid in Telecommunication Applications. *Journal of Energy Resources Technology*, *141*(6), 062002. https://doi.org/10.1115/1.4042402

Martinho, D. L., Simon Araya, S., Sahlin, S. L., Liso, V., Li, N., & Berg, T. L. (2022). Modeling a Hybrid Reformed Methanol Fuel Cell–Battery System for Telecom Backup Applications. *Energies*, *15*(9), 3218. https://doi.org/10.3390/en15093218

Millet, P., & Grigoriev, S. (2013). Water Electrolysis Technologies. In *Renewable Hydrogen Technologies* (pp. 19–41). Elsevier. https://doi.org/10.1016/B978-0-444-56352-1.00002-7

Moseley, P. T., & Garche, J. (2015). *Electrochemical energy storage for renewable sources and grid balancing*. Elsevier.

Odoi-Yorke, F., & Woenagnon, A. (2021). Techno-economic assessment of solar PV/fuel cell hybrid power system for telecom base stations in Ghana. *Cogent Engineering*, *8*(1), 1911285. https://doi.org/10.1080/23311916.2021.1911285

Shah, A. (Ed.). (2020). *Solar Cells and Modules* (Vol. 301). Springer International Publishing. https://doi.org/10.1007/978-3-030-46487-5

UNDP-Kenya-Annual-Report-2021.pdf. (n.d.).

Whittingham, M. S., Savinell, R. F., & Zawodzinski, T. (2004). Introduction: Batteries and Fuel Cells. *Chemical Reviews*, *104*(10), 4243–4244. https://doi.org/10.1021/cr020705e

Zohuri, B. (2018). *Hybrid Energy Systems*. Springer International Publishing. https://doi.org/10.1007/978-3-319-70721-1

Appendices

Appendix A: Strathmore University energy research Approval

Strathmore UNIVERSITY

15th July 2024

Mr Nganga Andrew,
andrew.nganga@strathmore.edu

Dear Mr Nganga,

RE: Renewable Energy-Based Hybrid Power Systems for Off-grid Base Transceiver Stations

This is to inform you that SU-ISERC has reviewed and **approved** your above **SU-masters** proposal. Your application reference number is **SU-ISERC2330/24.** The approval period is from **15th July 2024 to 14th July 2025.**

This approval is subject to compliance with the following requirements:

i. Only approved documents including (informed consents, study instruments, MTA) will be used.
ii. All changes including (amendments, deviations, and violations) are submitted for review and approval by SU-ISERC.
iii. Death and life-threatening problems and serious adverse events or unexpected adverse events whether related or unrelated to the study must be reported to SU-ISERC within 72 hours of notification.
iv. Any changes anticipated or otherwise that may increase the risks or affected safety or welfare of study participants and others or affect the integrity of the research must be reported to SU-ISERC within 72 hours.
v. Clearance for the export of biological specimens must be obtained from relevant institutions.
vi. Submission of a request for renewal of approval at least 60 days prior to the expiry of the approval period. Attach a comprehensive progress report to support the renewal.
vii. Submission of an executive summary report within 90 days of completion of the study to SU-ISERC.

Before commencing your study, you will be expected to obtain a research license from National Commission for Science, Technology, and Innovation (NACOSTI) https://research-portal.nacosti.go.ke/ and obtain other clearances needed.

Yours sincerely,

Mr Ambrose Rachier,
Chairperson; SU-ISERC

Ole Sangale Rd, Madaraka Estate. PO Box 59857-00200, Nairobi, Kenya. Tel +254 (0)703 034000
Email admissions@strathmore.edu www.strathmore.edu

Appendix B: NACOSTI research permit

REPUBLIC OF KENYA

NATIONAL COMMISSION FOR SCIENCE,TECHNOLOGY & INNOVATION

Ref No: **974727**

Date of Issue: **22/July/2024**

RESEARCH LICENSE

This is to Certify that Mr.. Andrew Benson Kiarie of Strathmore University, has been licensed to conduct research as per the provision of the Science, Technology and Innovation Act, 2013 (Rev.2014) in Kajiado, Nairobi on the topic: Renewable Energy-Based Hybrid Power Systems for Off-grid Base Transceiver Stations for the period ending : 22/July/2025.

License No: **NACOSTI/P/24/38193**

974727

Applicant Identification Number

Director General
NATIONAL COMMISSION FOR SCIENCE,TECHNOLOGY & INNOVATION

Verification QR Code

NOTE: This is a computer generated License. To verify the authenticity of this document, Scan the QR Code using QR scanner application.

See overleaf for conditions

THE SCIENCE, TECHNOLOGY AND INNOVATION ACT, 2013 (Rev. 2014)

Legal Notice No. 108: The Science, Technology and Innovation (Research Licensing) Regulations, 2014

The National Commission for Science, Technology and Innovation, hereafter referred to as the Commission, was the established under the Science, Technology and Innovation Act 2013 (Revised 2014) herein after referred to as the Act. The objective of the Commission shall be to regulate and assure quality in the science, technology and innovation sector and advise the Government in matters related thereto.

CONDITIONS OF THE RESEARCH LICENSE

1. The License is granted subject to provisions of the Constitution of Kenya, the Science, Technology and Innovation Act, and other relevant laws, policies and regulations. Accordingly, the licensee shall adhere to such procedures, standards, code of ethics and guidelines as may be prescribed by regulations made under the Act, or prescribed by provisions of International treaties of which Kenya is a signatory to
2. The research and its related activities as well as outcomes shall be beneficial to the country and shall not in any way;
    i. Endanger national security
    ii. Adversely affect the lives of Kenyans
    iii. Be in contravention of Kenya's international obligations including Biological Weapons Convention (BWC), Comprehensive Nuclear-Test-Ban Treaty Organization (CTBTO), Chemical, Biological, Radiological and Nuclear (CBRN).
    iv. Result in exploitation of intellectual property rights of communities in Kenya
    v. Adversely affect the environment
    vi. Adversely affect the rights of communities
    vii. Endanger public safety and national cohesion
    viii. Plagiarize someone else's work
3. The License is valid for the proposed research, location and specified period.
4. The license any rights thereunder are non-transferable
5. The Commission reserves the right to cancel the research at any time during the research period if in the opinion of the Commission the research is not implemented in conformity with the provisions of the Act or any other written law.
6. The Licensee shall inform the relevant County Director of Education, County Commissioner and County Governor before commencement of the research.
7. Excavation, filming, movement, and collection of specimens are subject to further necessary clearance from relevant Government Agencies.
8. The License does not give authority to transfer research materials.
9. The Commission may monitor and evaluate the licensed research project for the purpose of assessing and evaluating compliance with the conditions of the License.
10. The Licensee shall submit one hard copy, and upload a soft copy of their final report (thesis) onto a platform designated by the Commission within one year of completion of the research.
11. The Commission reserves the right to modify the conditions of the License including cancellation without prior notice.
12. Research, findings and information regarding research systems shall be stored or disseminated, utilized or applied in such a manner as may be prescribed by the Commission from time to time.
13. The Licensee shall disclose to the Commission, the relevant Institutional Scientific and Ethical Review Committee, and the relevant national agencies any inventions and discoveries that are of National strategic importance.
14. The Commission shall have powers to acquire from any person the right in, or to, any scientific innovation, invention or patent of strategic importance to the country.
15. Relevant Institutional Scientific and Ethical Review Committee shall monitor and evaluate the research periodically, and make a report of its findings to the Commission for necessary action.

National Commission for Science, Technology and Innovation(NACOSTI),
Off Waiyaki Way, Upper Kabete,
P. O. Box 30623 - 00100 Nairobi, KENYA
Telephone: 020 4007000, 0713788787, 0735404245
E-mail: dg@nacosti.go.ke
Website: www.nacosti.go.ke

Appendix C: Similarity Index

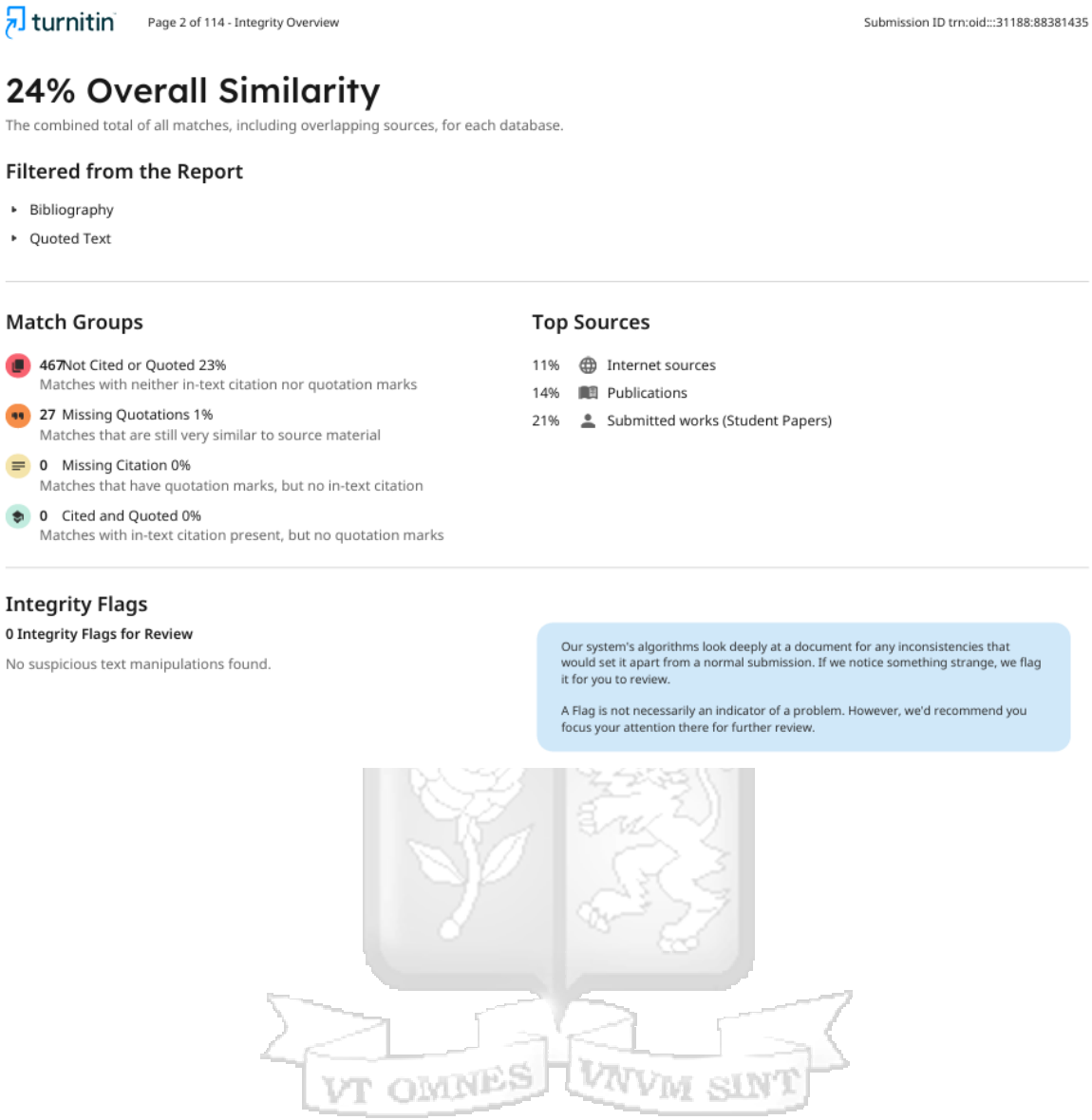

turnitin Page 2 of 114 - Integrity Overview Submission ID trn:oid:::31188:88381435

24% Overall Similarity

The combined total of all matches, including overlapping sources, for each database.

Filtered from the Report

- Bibliography
- Quoted Text

Match Groups

467 Not Cited or Quoted 23%
Matches with neither in-text citation nor quotation marks

27 Missing Quotations 1%
Matches that are still very similar to source material

0 Missing Citation 0%
Matches that have quotation marks, but no in-text citation

0 Cited and Quoted 0%
Matches with in-text citation present, but no quotation marks

Top Sources

11% Internet sources
14% Publications
21% Submitted works (Student Papers)

Integrity Flags

0 Integrity Flags for Review

No suspicious text manipulations found.

Our system's algorithms look deeply at a document for any inconsistencies that would set it apart from a normal submission. If we notice something strange, we flag it for you to review.

A Flag is not necessarily an indicator of a problem. However, we'd recommend you focus your attention there for further review.

Match Groups

- **467** Not Cited or Quoted 23%
  Matches with neither in-text citation nor quotation marks
- **27** Missing Quotations 1%
  Matches that are still very similar to source material
- **0** Missing Citation 0%
  Matches that have quotation marks, but no in-text citation
- **0** Cited and Quoted 0%
  Matches with in-text citation present, but no quotation marks

Top Sources

11% Internet sources
14% Publications
21% Submitted works (Student Papers)

Top Sources

The sources with the highest number of matches within the submission. Overlapping sources will not be displayed.

1	Internet	
www.tandfonline.com		<1%
2	Internet	
www.mdpi.com		<1%
3	Submitted works	
Malaviya National Institute of Technology on 2015-08-22		<1%
4	Submitted works	
Institute of Technology, Sligo on 2021-05-07		<1%
5	Submitted works	
University of Edinburgh on 2020-04-09		<1%
6	Internet	
pureportal.coventry.ac.uk		<1%
7	Submitted works	
University of New South Wales on 2018-10-22		<1%
8	Internet	
etd.cput.ac.za		<1%
9	Internet	
cs.overleaf.com		<1%
10	Submitted works	
Universiti Malaysia Sarawak on 2025-03-15		<1%

Appendix D: January Load data for BTS site

Total Days	Group Name	Rectifier 1 Initial [KWH]	Rectifier 1 Final [KWH]	ATS - kWH Init [KWH]	ATS - kWH Final [KWH]	ATS consumption (kwh)	Rectifier consumption (kwh)	ATS Load KW
1	BTF 2020	38273	38340	30556.47	30600.3	43.83	67	
1	BTF 2020	38340	38408	30600.3	30656.74	56.44	68	
1	BTF 2020	38408	38476.18	30656.74	30699.58	42.84	68.18	
1	BTF 2020	38476.18	38546	30699.58	30743.36	43.78	69.82	
1	BTF 2020	38546	38614	30743.36	30784.85	41.49	68	
1	BTF 2020	38614	38680	30784.85	30837.75	52.9	66	
1	BTF 2020	38680	38748	30837.75	30887.89	50.14	68	
1	BTF 2020	38748	38817	30887.89	30933.72	45.83	69	
1	BTF 2020	38817	38883	30933.72	30980.11	46.39	66	
1	BTF 2020	38883	38951	30980.11	31028.29	48.18	68	
1	BTF 2020	38951	39019	31028.29	31077.9	49.61	68	
1	BTF 2020	39019	39088	31077.9	31124.79	46.89	69	
1	BTF 2020	39088	39157	31124.79	31177.88	53.09	69	
1	BTF 2020	39157	39226	31177.88	31225.92	48.04	69	
1	BTF 2020	39226	39295	31225.92	31268.67	42.75	69	
1	BTF 2020	39295	39361.48	31268.67	31314.06	45.39	66.48	
1	BTF 2020	39361.48	39424	31314.06	31358.89	44.83	62.52	
1	BTF 2020	39424	39486	31358.89	31403.72	44.83	62	
1	BTF 2020	39486	39550	31403.72	31450.33	46.61	64	
1	BTF 2020	39550	39613	31450.33	31504.59	54.26	63	
1	BTF 2020	39613	39675	31504.59	31540.33	35.74	62	
1	BTF 2020	39675	39737.61	31540.33	31585.06	44.73	62.61	
1	BTF 2020	39737.61	39800	31585.06	31628.5	43.44	62.39	
1	BTF 2020	39800	39864	31628.5	31673.22	44.72	64	
1	BTF 2020	39864	39927	31673.22	31713.44	40.22	63	
1	BTF 2020	39927	39991	31713.44	31758.89	45.45	64	
1	BTF 2020	39991	40055	31758.89	31802.61	43.72	64	
1	BTF 2020	40055	40118	31802.61	31846.89	44.28	63	
1	BTF 2020	40118	40182	31846.89	31890.78	43.89	64	
1	BTF 2020	40182	40246	31890.78	31935	44.22	64	
1	BTF 2020	40246	40310	31935	31978	43	64	

Appendix E: Fuel cell control block function

Name	Script

fuel cell on-off function	`function fuelCell_enable = fuelCell_control(SOC, fuelCell_state)`
	`  % fuelCell_state: 1 if fuel cell is currently ON, 0 if OFF`
	
	`  % Define hysteresis thresholds`
	`  SOC_on_threshold = 30;  % SOC below which fuel cell turns ON`
	`  SOC_off_threshold = 45; % SOC above which fuel cell turns OFF`
	
	`  if fuelCell_state == 1 % Fuel cell is currently ON`
	`  if SOC > SOC_off_threshold`
	`  fuelCell_enable = 0; % Turn OFF if SOC is above the OFF threshold`
	`  else`
	`  fuelCell_enable = 1; % Keep ON`
	`  end`
	`  else % fuelCell_state == 0 (Fuel cell is currently OFF)`
	`  if SOC < SOC_on_threshold`
	`  fuelCell_enable = 1; % Turn ON if SOC is below the ON threshold`
	`  else`
	`  fuelCell_enable = 0; % Keep OFF`
	`  end`
	`  end`
	`end`
	
	`% function fuelCell_enable = fuelCell_control(SOC)`
	`%  if SOC < 31`
	`%  fuelCell_enable = 1;`
	`%  else`
	`%  if SOC < 40`
	`%  fuelCell_enable = 1;`
	`%  else`
	`%  fuelCell_enable = 0;`
	`%  end`
	`%  end`
	`% end`

Appendix F: Solar MPPT Tracking

Name	Script

MATLAB Function1	`function duty = MPPT_Control(V, I, deltaD_in, Vbus)`
	`  % Initialize constants and variables`
	`  Vmp = 29.8; % Maximum power point voltage`
	`  P_max = 214.858*5; % Maximum solar PV power in Watts`
	`  duty_init = 1 - Vmp/Vbus;`
	`  duty_min = 0;`
	`  duty_max = 0.75;`
	
	`  % Declare persistent variables`
	`  persistent Vold Pold duty_old integral_error;`
	
	`  % Initialize persistent variables if they are empty`
	`  if isempty(Vold)`
	`  Vold = 0;`
	`  Pold = 0;`
	`  duty_old = duty_init;`
	`  integral_error = 0;`
	`  end`
	
	`  % Calculate power and its changes`
	`  P = V * I;`
	`  dV = V - Vold;`
	`  dP = P - Pold;`
	
	`  % Dynamic threshold based on rate of change of power`
	`  threshold = 0.005 * P_max * (1 + abs(dP) / P_max);`
	
	`  if abs(dP) > threshold`
	`  deltaD = min(deltaD_in * 1.2, 0.05); % Increase but limit max step size`
	`  else`
	`  deltaD = max(deltaD_in * 0.8, 0.002); % Decrease but limit min step size`
	`  end`
	
	`  % Initialize duty cycle`
	`  duty = duty_old;`
	
	`  % Overcurrent protection`
	`  I_max = P_max / Vmp; % Max expected current at MPP`
	`  if I > I_max`
	`  duty = duty - deltaD; % Reduce duty cycle if overcurrent`
	`  end`
	
	`  % MPPT algorithm with PI controller`
	`  if abs(dP) > 0.001`
	`  if dP ~= 0`
	`  if dP < 0`
	`  if dV < 0`
	`  duty = duty_old - deltaD;`
	`  else`
	`  duty = duty_old + deltaD;`
	`  end`
	`  else`
	`  if dV < 0`
	`  duty = duty_old + deltaD;`
	`  else`
	`  duty = duty_old - deltaD;`
	`  end`
	`  end`
	`  end`
	`  end`
	
	`  % PI Controller`
	`  Kp = 0.1; % Proportional gain`
	`  Ki = 0.01; % Integral gain`
	`  error = Vmp - V;`
	`  integral_error = integral_error + error;`
	`  duty = duty + Kp * error + Ki * integral_error;`
	
	`  % Clamp duty cycle to its limits`
	`  if duty >= duty_max`
	`  duty = duty_max;`
	`  elseif duty < duty_min`
	`  duty = duty_min;`
	`  end`
	
	`  % Update persistent variables`
	`  duty_old = duty;`
	`  Vold = V;`
	`  Pold = P;`
	`end`

Appendix G: Solar Irradiance Function

Name	Script

MATLAB Function2	`function irr = irradiance(t)`
	`  % We want 4 days (96 hours) in 50 seconds:`
	`  % Each "day" = 12.5 seconds --> 4 days = 12.5*4 = 50 seconds total simulation.`
	`  %`
	`  % Map t in [0, 50] seconds to 0-96 hours:`
	`  %   t_hours = (t / 50) * 96`
	`  % Then figure out which hour of the current day we are in:`
	`  %   t_day = mod(t_hours, 24)`
	
	`  % Define total simulation time for 4 days`
	`  T_sim_total = 50;    % 4 days × 12.5s/day`
	
	`  % Convert current time t (s) -> hours in the 4-day span`
	`  t_hours = (t / T_sim_total) * 96;  % 96 hours in 4 days`
	
	`  % Extract "hour of the day" by mod 24`
	`  t_day = mod(t_hours, 24);`
	
	`  % Define sunrise and sunset times (hours)`
	`  sunrise = 6;`
	`  sunset  = 18;`
	
	`  % Compute irradiance`
	`  if t_day < sunrise || t_day > sunset`
	`  % Night`
	`  irr = 0;`
	`  else`
	`  % Daytime: use a sine wave from sunrise to sunset`
	`  normTime = (t_day - sunrise) / (sunset - sunrise);`
	`  irr = 1000 * sin(pi * normTime);  % peak ~1000 W/m^2 at noon`
	`  end`
	`end`

Appendix H: January Time Utilization Data For Energy Sources at the BTS

Unit Id	Unit Name	Start date	End date	Duration (Days)	Usage Time Grid	Usage Time Generator 1	Usage Time Solar	Usage Time
8007965	Negist, 621450	01/01/2024	01/01/2024	1	0	5.43	7.63	10.94
8007965	Negist, 621450	02/01/2024	02/01/2024	1	0	6.98	6.61	10.4
8007965	Negist, 621450	03/01/2024	03/01/2024	1	0	5.34	7.45	11.2
8007965	Negist, 621450	04/01/2024	04/01/2024	1	0	5.42	7.72	10.84
8007965	Negist, 621450	05/01/2024	05/01/2024	1	0	5.17	7.51	11.31
8007965	Negist, 621450	06/01/2024	06/01/2024	1	0	6.59	7.41	10
8007965	Negist, 621450	07/01/2024	07/01/2024	1	0	6.67	5.47	11.86
8007965	Negist, 621450	08/01/2024	08/01/2024	1	0	5.83	7.65	10.49
8007965	Negist, 621450	09/01/2024	09/01/2024	1	0	5.74	8.75	9.5
8007965	Negist, 621450	10/01/2024	10/01/2024	1	0	6.42	6.18	11.4
8007965	Negist, 621450	11/01/2024	11/01/2024	1	0	6.16	7.76	10.06
8007965	Negist, 621450	12/01/2024	12/01/2024	1	0	5.85	7.88	10.26
8007965	Negist, 621450	13/01/2024	13/01/2024	1	0	6.97	5.46	11.57
8007965	Negist, 621450	14/01/2024	14/01/2024	1	0	5.98	7.43	10.58
8007965	Negist, 621450	15/01/2024	15/01/2024	1	0	5.3	7.96	10.73
8007965	Negist, 621450	16/01/2024	16/01/2024	1	0	5.8	6.97	11.18
8007965	Negist, 621450	17/01/2024	17/01/2024	1	0	5.71	8.11	10.18
8007965	Negist, 621450	18/01/2024	18/01/2024	1	0	5.68	7.46	10.85
8007965	Negist, 621450	19/01/2024	19/01/2024	1	0	6.29	6.54	11.16
8007965	Negist, 621450	20/01/2024	20/01/2024	1	0	6.92	4.85	12.23
8007965	Negist, 621450	21/01/2024	21/01/2024	1	0	4.54	7.29	12.17
8007965	Negist, 621450	22/01/2024	22/01/2024	1	0	5.76	7.6	10.57
8007965	Negist, 621450	23/01/2024	23/01/2024	1	0	5.83	7.41	10.74
8007965	Negist, 621450	24/01/2024	24/01/2024	1	0	5.71	8.54	9.75
8007965	Negist, 621450	25/01/2024	25/01/2024	1	0	5.43	7.22	11.35
8007965	Negist, 621450	26/01/2024	26/01/2024	1	0	5.82	7.64	10.51
8007965	Negist, 621450	27/01/2024	27/01/2024	1	0	5.76	7.69	10.48
8007965	Negist, 621450	28/01/2024	28/01/2024	1	0	5.76	7.74	10.44
8007965	Negist, 621450	29/01/2024	29/01/2024	1	0	5.75	7.06	11.16
8007965	Negist, 621450	30/01/2024	30/01/2024	1	0	5.75	7.85	10.38
8007965	Negist, 621450	31/01/2024	31/01/2024	1	0	5.75	7.46	10.76